OAR Box 1933

Prepped by Ollie Stewart

Document Number:

100) IV-A-98

Docket Number:

A-2000-01

AN INVESTIGATION OF DRIVER EXPOSURE TO CARBON MONOXIDE WHILE TRAVELING IN THE WAKE OF A SNOWMOBILE

A Dissertation

Presented for the

Doctor of Philosophy

Degree

The University of Tennessee, Knoxville

Lori Marie Snook

August, 1996

AN INVESTIGATION OF

DRIVER EXPOSURE TO CARBON MONOXIDE

WHILE TRAVELING

IN THE WAKE OF A SNOWMOBILE

A Dissertation

Presented for the

Doctor of Philosophy

Degree

The University of Tennessee, Knoxville

Lori Marie Snook

August, 1996

ACKNOWLEDGMENTS

This dissertation would not have been possible without support and assistance from many individuals. I would like to formally thank and acknowledge those who have generously helped me in my efforts.

Dr. Wayne Davis has served as my advisor at the University for the past three years. Words can not fully express my appreciation for the knowledge that he has shared with me, the freedom that he has allowed me, and the dedication that he has shown to my research. Without his guidance, this research would not have been possible.

I would also like to thank the other members of my committee, Dr. J. W. Hodgson. Dr. T. L. Miller, and Dr. J. L. Smoot for their interest in and assistance with this dissertation. Their comments, concerns, and particularly their questions served to strengthen this research and aid in my professional growth.

I am grateful to the National Science Foundation (NSF) for funding my education for the past three years. The NSF's support allowed me the freedom to pursue non-traditional research away from the university environment. I truly believe that this unique situation has allowed me to strengthen my opportunities to pursue future research on snowmobile emissions. I am also grateful to Dr. Linda Painter (from the University of Tennessee Graduate School) for serving as the administrator of this fellowship.

Many companies were generous enough to donate equipment for use in this dissertation. I am indebted to them for their willingness to support my research. Air Liquide supplied all of my calibration gases as well as a regulator free of charge. SKC

Inc. provided their 224-PCXR8 sampling pump and kit for use free of charge. Thermo Environmental Instruments allowed me to use one of their Model 48 carbon monoxide analyzers free of charge. And finally, the Environmental Supply Company, supplied sixty air sampling bags to me at a greatly reduced rate. Without the support of these companies, it would have been impossible to obtain the quality present in this research on such a small budget.

I must also thank the Air and Waste Management Association (A&WMA) for providing the forum (the 1995 Annual Meeting and Exhibition) to approach these companies to ask for support. It would have been difficult to solicit equipment for use in this study if it weren't for the A&WMA's Exhibition.

Bob Schiller of Grand Teton National Park allowed me to use two of the park's snowmobiles for this research as well as made it possible for me to collect data on park property. I am grateful to him for his enthusiastic support of my research. Additionally, I would like to thank Mason Reid of Grand Teton National Park. Mason was responsible for teaching me how to drive a snowmobile as well as taking care of all administrative details with respect to utilizing park snowmobiles for research purposes.

My father, Sidney Eastwood Snook, is an engineer with many years of experience writing and reviewing technical reports. He has spent many hours reviewing and editing draft copies of my dissertation. This was truly an act of love and I am grateful for his help and support.

I am grateful to my friend and colleague, Scott Sluder. In addition to providing many useful insights, Scott helped me with the calibration of my laminar air flow element.

My mother, Joan G. Moffitt, has been a source of love and support throughout my college career (which has been a very long time). I am grateful to her.

Many individuals supported my efforts indirectly. Thanks go to Mary Hecktner of Yellowstone National Park, Ron Heavner of the National Park Service, Tom Watson of the National Oceanographic and Atmospheric Administration, Wendy and Scott Ross, Jim Carrol of Southwest Research Institute, and Howard Haines of the Montana Department of Environmental Quality. Their ideas, support, and interest helped to shape this research into what it is today.

Finally, I would like to thank all of my fellow students at the University of Tennessee. Their standard of excellence forced me to work harder to meet them at their level.

ABSTRACT

A dramatic increase in the popularity of snowmobiling across the nation raises new concerns regarding exposure to pollution from snowmobiles. Because many tourists choose to snowmobile in large groups along fixed trails, this study investigates exposure to carbon monoxide (CO) while traveling in the wake of a snowmobile. Steady-state measurements of engine-out CO concentrations were taken at four different speeds while traveling on level ground. Values ranged from 9.9 grams per mile (g/mile) at 10 miles per hour (mph) to 19.9 g/mile at 40 mph. At these same speeds, bag samples were taken on a second snowmobile while traveling at fixed distances behind the first snowmobile. A maximum centerline exposure of 25.7 parts per million (ppm) occurred at 10 mph and 25 ft behind the lead snowmobile. Off-centerline exposure data as well as exposure data without the lead snowmobile were also taken at the same speeds and distances. This information was then used to develop a model to predict exposure to CO while traveling behind another snowmobile as a function of both the vehicle speed and the distance between the snowmobiles. This model can also be used to predict exposure to pollutants other than CO (if emission factors are known). The results are of interest to snowmobilers, snowmobile manufacturers, environmentalists, park managers, and regulatory agencies. Recommendations for further study are made.

TABLE OF CONTENTS

LIST OF FIGURES

LIST OF TABLES

LIST OF SYMBOLS AND ABBREVIATIONS

A&WMA	Air and Waste Management Association
A	Variable used in wake theory defined by Equation 3.6
A	Number of moles of CO_2
ASME	American Society of Mechanical Engineers
A_f	Frontal area of the vehicle (snowmobile)
A_w	Cross-sectional area of the wake
B	The chemical species in Equation 3.9
B	Number of moles of H_2O
C	Concentration
C	Number of moles of N_2
CARB	California Air Resources Board
cc	Cubic centimeters
C_D	Coefficient of drag
$CH_{1.85}$	Approximation for chemical formula of fuel used
CO	Carbon Monoxide
CO_2	Carbon Dioxide
D	Number of moles of CO
E	Emission source term in Equation 3.9
E	Number of moles of H_2
ft	Feet

g bhp-hr	Grams brakehorsepower-hour
GFC	Gas Filtration Correlation
g mile	Grams mile
H	Source height (in Gaussian modeling)
H_2	Hydrogen
H_2O	Water
H_V	Height of the vehicle (snowmobile)
H_W	Height of the wake
ISIA	International Snowmobile Industry Association
k	Equilibrium constant of water-gas shift reaction
K	Diffusivity in Equation 3.10
K^S	Diffusivity of the standard atmosphere
K^W	Diffusivity of the wake
LAFE	Laminar Air Flow Element
l min	Liters minute
ml min	Milliliters minute
mph	Miles per hour
MS	Master of Science
m s	Meters Second
MW_X	Molecular weight of chemical species X
N_2	Nitrogen
NO_X	Oxides of Nitrogen

NSF	National Science Foundation
O_3	Ozone
P, P_T	Pressure total pressure of system
Ph.D.	Doctor of Philosophy
ppm	Parts per million (volume)
P_X	Partial pressure of chemical species X
Q	Source emission rate
rpm	Revolutions per minute
R_u	Universal gas constant
R_W	Radius of a semi-circular wake
T	Absolute temperature
t	Time
u	Wind speed
UHC	Unburned Hydrocarbons
USEPA	United States Environmental Protection Agency
VOC	Volatile Organic Compounds
V_s	Velocity of the vehicle (snowmobile)
V_W	Velocity of the wake
x	Distance behind the moving snowmobile
y	Distance off-centerline
YNP	Yellowstone National Park
z	Distance in the vertical direction

α_{ent}	Entrainment factor, a constant of proportionality in Equation 3.3
λ_1	Constant used in Equations 3.5 and 3.6 (approximately 4.13)
$\phi_{F/A}$	Fuel Air equivalence ratio
	Constant used in Equations 3.6, 3.7, and 3.8 (approximately 0.4)
	Variable defined by Equation 3.8
π	Pi
ρ	Density of air
σ_y	Standard deviation of concentration in the horizontal direction (in Gaussian modeling)
σ_z	Standard deviation of concentration in the vertical direction (in Gaussian modeling)
	Variable defined by Equation 3.7
$\vec{\nabla}_{xz}$	Divergence operator in x and z coordinates

CHAPTER 1

INTRODUCTION

Thirty years ago, snowmobiling as a recreational activity was in its developmental years. It was a sport in which very few people participated. In 1964, fewer than a dozen snowmobiles entered the center of Yellowstone National Park (Wilkinson, 1995).

Today, snowmobiling has grown into a booming business. During the 1993-94 winter, snowmobilers spent an estimated $127 million in the state of Wyoming alone (Associated Press, 1995). During this same winter, over 143,000 tourists snowmobiled through West Yellowstone, Montana and into Yellowstone National Park (Wilkinson, 1995).

This large increase in the snowmobile's popularity is raising new concerns about air quality. Rangers staffing the entrance to Yellowstone complain of headaches and nausea which they believe to be caused by fumes and noise from snowmobiles. Additionally, John Sacklin, Supervisory Outdoor Recreation Planner for Yellowstone, reports that "Every year we receive more and more letters from visitors. They're not all saying necessarily that they are having a bad experience, but they are seriously questioning the direction that winter recreation in the park is going." (Wilkinson, 1995)

At the present time, there are no federal laws regulating the exhaust from snowmobile engines. The typical snowmobile utilizes a small, two-stroke engine. The two-stroke engine is less expensive than it's four-stroke counterpart and is able to provide

a high power/weight ratio. However, it also has the potential to produce relatively high exhaust emissions. The two-stroke is typically calibrated to run rich to provide smooth engine response, resulting in high CO and unburned hydrocarbon (UHC) emissions. Additionally, UHC and particulate emissions are high due to the crankcase scavenging process. "A certain fraction of the intake charge is untrapped in the combustion chamber and passes directly through the engine and out the exhaust port." (White et. al., 1993) Data obtained from snowmobile manufacturers circa 1980 have been used to estimate that one snowmobile may emit as much carbon monoxide as 225 automobiles and as many UHCs as 3,000 automobiles (Heavner, 1994).

The International Snowmobile Industry Association (ISIA) correctly responds that "since snowmobiles are operated only during the winter, they do not contribute to the ozone problem." (ISIA, 1995) However, their assertion that "snowmobile exhaust emissions do not pose a health or safety risk" is based on the assumptions that large numbers of snowmobiles located at the same site are unusual and that twenty-five snowmobiles on a trail are considered to be a large group. These assumptions may be true in many locations across the country; but in Yellowstone National Park (YNP), this is not the case. At the west entrance to YNP it is a common site to see over fifty snowmobiles in line, waiting to enter the park. Additionally, with over 1000 snowmobiles traveling to Old Faithful on one particular day (most between the hours of 8 and 11 in the morning), a steady stream of traffic exists on the trail. At Flagg Ranch, WY (the south entrance to YNP) outfitters unload hundreds of snowmobiles daily, preparing them to make the trip to Old Faithful (see Figure 1).

Because of the increase in popularity of the snowmobile, and its inherently "dirty" exhaust emissions, it seems timely to re-evaluate the potential for the snowmobile to cause excessive pollution. Except in cases where snowmobiles operate in towns or must wait in lines to pay fees, the public at large is not at risk...snowmobile trails are generally placed in relatively remote locations.. However, the potential does exist for the snowmobiler to be exposed to a significant amount of exhaust fumes, either from the snowmobile being ridden or from other snowmobiles in the immediate vicinity. This dissertation focuses on modeling the dispersion of pollutants from snowmobiles and determining the exposure of a driver to snowmobile exhaust while traveling on a trail, behind other snowmobiles.

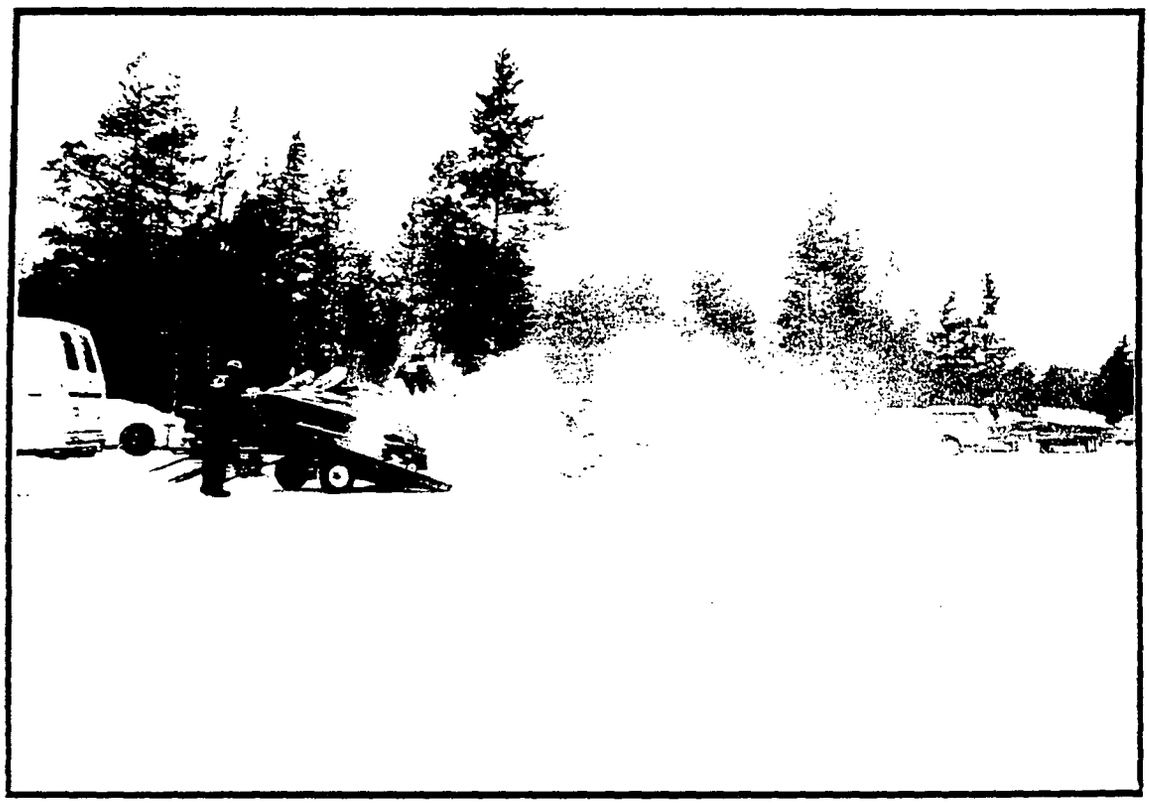

Figure 1 *Picture of Snowmobile Staging Area at Flagg Ranch*

CHAPTER 2

THE PROBLEM

2.1 Significance

As discussed in the Introduction, the snowmobiling industry has seen tremendous growth in the past few years. This growth has resulted in locations which experience a high density of snowmobile traffic unseen in previous years. Many environmentalists, park rangers, and snowmobilers are becoming concerned about air pollution emanating from snowmobiles.

As will be seen in the Literature Review, very little quantitative information is available on the actual emissions from snowmobiles. All of the available data on snowmobile emissions were obtained in a laboratory with the snowmobile engine on a dynamometer. Therefore, it most likely does not represent the behavior of a snowmobile operating in a very cold climate and at high altitude. Additionally, most of these data are over ten to twenty years old and, as such, may appear to be out of date.

Even if appropriate emission factors could be found, an appropriate method of modeling the driver's exposure to pollution from other snowmobiles is not immediately obvious. Most models that deal with mobile sources focus on determining concentrations of pollutants beside a roadway which originated from automobile emissions. In order to determine exposure to a snowmobile driver, concentrations on the trail itself are necessary. Additionally, the model must address the fact that the snowmobile may not

create the same turbulent mixing cell as is typically assumed when larger vehicles are modeled.

Therefore, this dissertation focuses on presenting more information to help clarify both of these issues. Field measurements of snowmobile emissions significantly add to the state of knowledge regarding the exhaust characteristics of a snowmobile as it is actually driven (at high altitude in very cold weather). Field measurements of pollutant concentrations (at various distances and speeds behind a moving snowmobile) provide an estimate of the concentrations to which someone riding behind that snowmobile is exposed. These data, along with photographic measurements, facilitate the investigation of a technique to model exposure to a receptor which is moving on the road. This "moving-receptor" issue has not yet been addressed in air pollution models.

2.2 Statement of the Problem

The purpose of this dissertation is to quantify the amount of CO emitted from a snowmobile under steady-state conditions, to quantify the amount of CO an individual is exposed to while driving behind another snowmobile as a function of speed and distance behind that snowmobile, and to use this information to develop a model to predict exposure to CO while traveling in the wake of the snowmobile.

2.3 Technical Approach

The investigation was divided into three different tasks. The first task of the research was to determine the steady-state mass emission rate of CO (the source term) at

four different snowmobile speeds. Additionally, the snowmobile's CO emissions were measured both for the case of idling and also for the case of power enrichment.

The second task of the research was to determine the CO concentration behind the moving snowmobile as a function of its speed and distance behind it. As in Task 1, only steady-state conditions were investigated. Five different distances and four different speeds were considered. Concentrations were measured both along the wake centerline and fifteen feet off-centerline. In order to determine the amount of self-exposure, measurements were also taken at each speed without the lead snowmobile.

Task 3 of the research was to use the data from Tasks 1 and 2 (source term and exposure) to develop a suitable method to predict exposure to CO while traveling in the wake of a snowmobile.

2.4 Delimitations

CO emission rates were determined for one snowmobile only. Therefore, the obtained data are not necessarily representative of all snowmobiles, but are used to satisfy the need for emission values in model development.

A test cycle (such as would be used in federal test procedures) was not used to determine the rate of CO emission from the snowmobile. Therefore, the resulting emission rates can not be compared to emission rates measured using test cycles. CO emission measurements were taken only for the cases of: the snowmobile moving under steady-state conditions at four different speeds, the snowmobile idling, and the snowmobile under acceleration.

Only steady-state conditions were considered for exposure measurements and modeling. No exposure data were taken during acceleration, deceleration, under power, or while idling. Therefore, caution should be exercised if the model is used to predict exposure under such conditions.

CO is the only exhaust component which was measured. It is assumed that the results of this research may be extrapolated to other pollutants if appropriate emission factors are known.

The manufacturer's specifications determined oil type, and the oil/fuel ratio used in the snowmobile. Different oils and ratios would most likely produce different levels of emissions, but will not affect the modeling algorithms that were developed as the same snowmobile was used to measure emissions and exposure.

2.4 Limitations

The most difficult variable to control was the wind. All tests were run during morning hours and every effort was made to test only during calm conditions. However, the wind speed did vary between tests. This variable was recorded and analyzed as needed.

The wind direction also varied between tests. During any given test, every effort was made to keep the wind direction parallel to the direction of snowmobile travel. This yielded the highest concentration, or worst case condition. There were times, however, during which a slight cross-wind was present.

2.5 Summary

This research on driver exposure to snowmobile exhaust is undertaken at a time in which much interest is focused on pollution from snowmobiles, but relatively little information is available. It is anticipated that the results of this research will be of great interest to all involved with snowmobiling. By measuring both exhaust and air concentrations in the field, it was possible to develop a model to determine exposure to pollution while traveling in the wake of a snowmobile This model will not only be useful to snowmobilers, environmentalists, regulators and snowmobile manufacturers to determine exposure from snowmobiles, but it may also prove useful for modeling exposure from other types of vehicles of similar structure.

CHAPTER 3

LITERATURE REVIEW

3.1 Snowmobile Emissions

The first reported study undertaken to characterize the exhaust emissions from snowmobile engines was completed by Charles Hare and Karl Springer of the Southwest Research Institute in 1974 (Hare and Springer, 1974), (Hare et. al., 1974). In that study, four different snowmobile engines (of varying displacements and power ratings) were selected to obtain exhaust emissions data. The data were then used in conjunction with available information on snowmobile population and usage to determine emissions factors and national impact. Their work is the basis for the emission factors for snowmobiles which are published in AP-42 (USEPA, 1985).

Because there was no standard testing procedure for small utility engines in the early seventies, Hare and Springer designed their own test for the snowmobile engines. In their procedure, snowmobile emissions were determined by placing the engine on a dynamometer and then measuring emissions at idle, plus approximately seven loads by four engine speeds for a uniform "map" of conditions. In order to better simulate field conditions, inlet air was maintained at approximately 20 degrees Fahrenheit.

In the early eighties, the California Air Resources Board (CARB) requested that snowmobile manufacturers provide them with emission measurements from their snowmobiles. The data that the manufacturers supplied were made available by Charles

Emmet, an engineer with CARB. The data were from tests performed in 1980. It is unclear what test procedure was used by the manufacturers.

The only other published information available on snowmobile emissions was part of a larger study performed by both the Southwest Research Institute and the California Air Resources Board in 1993 (White et. al., 1993). In that study, one snowmobile engine was tested according to the Society of Automotive Engineers Test Procedure ISO 8178-G1.

The data from each of those tests are listed in Table 1. It should be noted that each study used a different test procedure and averaging method. Therefore, the data should not be compared directly to determine trends in emissions. However, the data most likely represent a range of emissions which may be seen in the snowmobile population. It is expected that these data are representative of present-day snowmobiles due to the fact that snowmobile emissions have never been regulated by federal or state agencies. Additionally, the improvements in combustion technology made in the past 30 years (which also improve emissions) are most likely offset by the larger snowmobiles in use today.

3.2 Driver Exposure Studies

A variety of experimental studies have been conducted which focus on the measurement of automobile in-cabin pollutant concentrations. In general, the studies used a fleet of test vehicles which either drive a standard route or record traffic conditions and road type while measuring CO, volatile organic compounds (VOCs), ozone (O_3),

Table 1 *Summary of Snowmobile Emission Studies*

Study	*Snowmobile Type*	*CO g/bhp-hr* *	*UHC g/bhp-hr*	*NOx g/bhp-hr*
Hare & Springer 1974	436 cc Air Cooled	142.0	88.6	1.43
	436 cc Air Cooled, RICH	270.0	110.0	0.97
	335 cc Air Cooled	235.0	118.0	1.81
	247 cc Air Cooled	63.0	196.0	3.36
	528 cc Rotary Engine**	356.0	20.6	3.01
Manufacturer's Data 1980	Composite Estimate	564	216***	
White et. al 1993	497 cc Fan Cooled	347	96.7	0.328

* Grams/brake horsepower-hour

** All other engines studied were two stroke engines

*** Manufacturers supplied combined UHC+NOx data

oxides of nitrogen (NO_X), or a combination of these pollutants. The purpose of the studies was to obtain general information to aid in population exposure assessment studies. Trends in in-cabin concentrations were determined based on traffic density, road-type, and vehicle speed. However, specific modeling scenarios of driver and passenger exposure based on vehicle emissions, speed, distance from vehicles, etc. were not investigated. Some of the major studies are summarized below.

In 1966, Robert Brice and Joseph Roesler measured CO and UHC inside vehicles moving in moderate to heavy traffic in six different cities (Brice and Roesler, 1966). In all of the cities, integrated half-hour CO concentrations exceeded 30 ppm in at least 10% of the samples. The range of city averages was 21-39 ppm CO. The data indicated an increase in cabin concentration with an increase in traffic density, little dependence on ambient air temperature, and an inverse relationship between the wind speed and the cabin concentration.

A 1976 study by Lewis Mayron and John Winterhalter measured CO concentrations inside idling automobiles (with no other vehicles around) and CO concentrations in ventilating air entering automobiles while they were driven in different traffic conditions (Mayron and Winterhalter, 1976). It was determined that for the case of idling, there was no correlation between the interior CO levels and the CO concentration in the vehicle's exhaust. CO levels for the ventilating air ranged from 2 to 36 ppm. Additionally, the prime factor that appeared to result in higher levels of CO was traffic delays.

D. Colwill and A. Hickman performed a study in 1980 which measured CO concentrations in vehicles traveling around a 35 kilometer route comprising heavily trafficked roads in and around London (Colwill and Hickman, 1980). The average CO levels measured inside the vehicles varied between 12 and 60 ppm, the major influence on CO levels being the traffic density. While in dense traffic, maximum CO levels were in excess of 200 ppm outside of the vehicles, and 50 ppm inside of the vehicles.

A fairly extensive study was conducted by William Petersen and Rodney Allen in 1982 (Petersen and Allen, 1982). This study measured CO exposure to commuters in three different vehicles as they traveled typical commuter routes in the Los Angeles Area. Additionally, meteorological conditions and hourly averaged CO measurements were taken from eight fixed-site monitoring stations and six vans in the proximity of the commuter routes. Based on collected data, the researchers concluded that fixed site monitors are not a good measure of exposure to commuters. With respect to internal CO concentrations, the researchers concluded that traffic flow and congestion were the most influential parameters. Additionally, meteorological conditions (wind speed and direction) affected ambient CO levels but appeared to have little influence on in-cabin concentrations.

In 1987, a study was completed which found that Washington area commuters were exposed to average CO concentrations that typically ranged from 9 to 14 ppm over trips that typically took between 40 and 60 minutes (Flachsbart et. al., 1987). The researchers concluded that the most important factors influencing CO concentrations inside the automobiles were traffic density, vehicle mix, road type, meteorological

conditions, and the ambient CO concentration. In addition, the study noted that by increasing the automobile's speed from 10 to 60 miles per hour one could reduce the average CO exposure by 35 percent regardless of travel period.

During the summer of 1988, the concentrations of 24 VOCs, O_3, CO, and NO_2 were measured inside of two vehicles under different driving conditions (Chan et al., 1991). Additionally, fixed site measurements were taken in the area. Results indicated that in-vehicle VOC and CO concentrations were highest for the urban roadway, second highest for the interstate highway, and lowest for the rural road. Additionally, CO and VOC concentrations were approximately the same in the morning as in the afternoon, while O_3 and NO_X were higher during afternoon driving. Of the VOCs, isopentane was the most abundant aliphatic hydrocarbon and toluene was the most abundant aromatic VOC measured inside the vehicles.

Although all of the experimental commuter exposure studies vary in design, purpose, and results, they do indicate general trends. All of the studies indicated that in-cabin concentrations increased with an increase in traffic density and decreased with an increase in vehicle speed. Results conflicted as to the relative importance of meteorological conditions on interior concentrations, although increasing wind speed appeared to decrease concentrations in two of the studies.

Additionally, all studies indicated that drivers may be exposed to significant amounts of CO while driving in a car (depending upon the time spent driving and the conditions). The 1-hour National Ambient Air Quality Standard for CO is 35 ppm and the 8-hour National Ambient Air Quality Standard for CO is 8 ppm.

3.3 Gaussian Highway Modeling

The modeling of human exposure to vehicular pollutants has received considerable attention and many models exist which can predict concentrations along roadways. Although different modeling techniques are used, the models must all consider several factors: the vehicle emission rate, the wind speed and direction relative to the axis of the roadway, the atmospheric turbulence, and the mixing induced by vehicle motion. Of these factors, the vehicle induced mixing is the most difficult to characterize and, until recently, has been relatively ignored or over-simplified by many highway models (Samson, 1988).

The most common method used to model highway emissions is to approximate the highway as a continuous line source. In this case, the following Gaussian equation is used for situations in which the wind is normal to the roadway:

$$C = \frac{Q}{\sqrt{2\pi}u\sigma_z}\left\{\exp\left[\frac{-(z-H)^2}{2\sigma_z^2}\right] + \exp\left[\frac{-(z+H)^2}{2\sigma_z^2}\right]\right\} \qquad (3.1)$$

In this equation, C is the concentration in g/m^3, Q is the emission rate in g/m-sec, u is the wind speed in m/s, z is the receptor height in m, H is the source height in m, and σ_Z is the standard deviation of concentration expected in the vertical direction as a function of travel distance downwind (Turner, 1970). Figure 2 contains a schematic of the coordinate system for a line source emission.

It is easily seen that the only term which can be used by this modeling method to incorporate the vehicle induced mixing is σ_Z. However, published values of σ_Z (Turner, 1970) are dependent only upon atmospheric conditions and downwind distance.

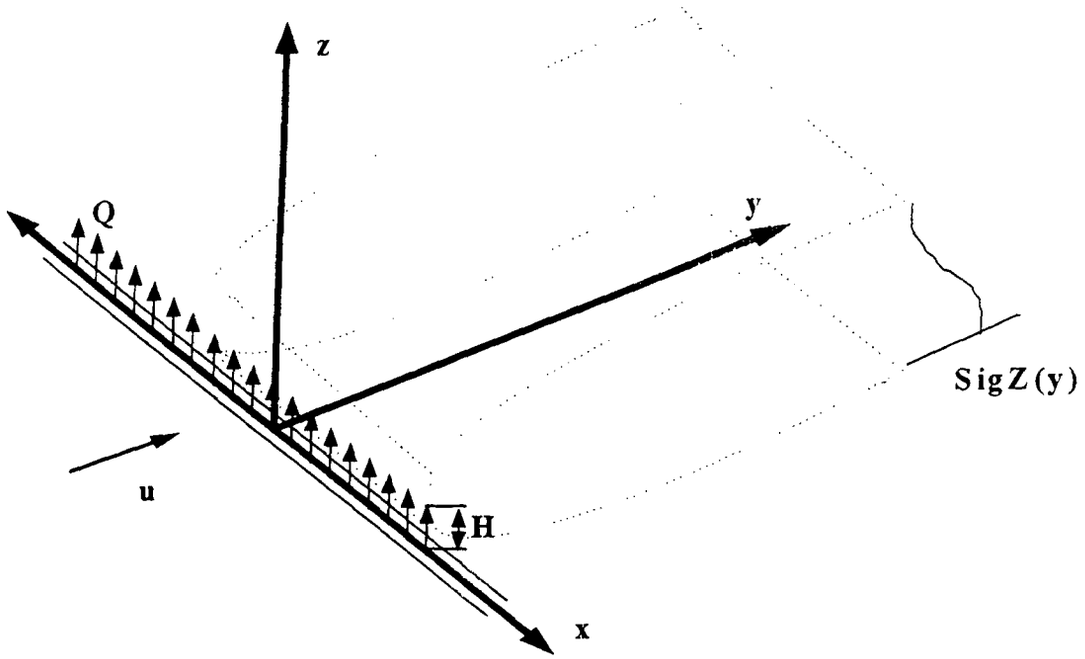

Figure 2 *Schematic of a Line Source Emission*

Additionally, they were derived for passive ground level releases and smooth terrain. In 1974 Pasquill (Pasquill, 1974) published modifications to these original standard deviations to account for surface roughness and thermal stratification using power law relations. However, highway models still needed to incorporate modifications to in order to better account for vehicular turbulence.

Several researchers have conducted empirical studies on the dynamic release of pollutants along roadways in order to derive actual σ_z values. In 1972, smoke releases behind a single vehicle were conducted which lead the researchers to conclude that an initial value of 4 meters should be used for σ_z under all stability and traffic conditions (Beaton et al, 1972). The original EPA HIWAY model used the results of a 1973 study (Calder 1973) which assumed neutral stability near the roadway and a modified power

curve for σ_Z with an initial value of 1.5 meters. In 1974 the results of tracer releases from a two lane highway indicated that vertical dispersion near the roadway was independent of atmospheric stability and considerably greater than predicted by the standard curves (Johnson, 1974). In 1981, Bensen used four independent dispersion studies to estimate σ_Z. His analysis of the databases indicated that the initial value of σ_Z near the roadway edge is relatively insensitive to surface layer stability, but significantly increases with decreasing wind speed. Additionally, a method of combining a residence time model for initial σ_Z and established vertical dispersion curves was developed.

The current United States' regulatory model for highways, CALINE3 (Bensen, 1979), uses this residence time/dispersion curve technique. It accounts for vehicle induced turbulence by treating the region directly over the highway as a zone of uniform emissions and turbulence. This concept is shown schematically in Figure 3. In this model, the initial horizontal dispersion imparted to pollutants by the vehicle's wake is

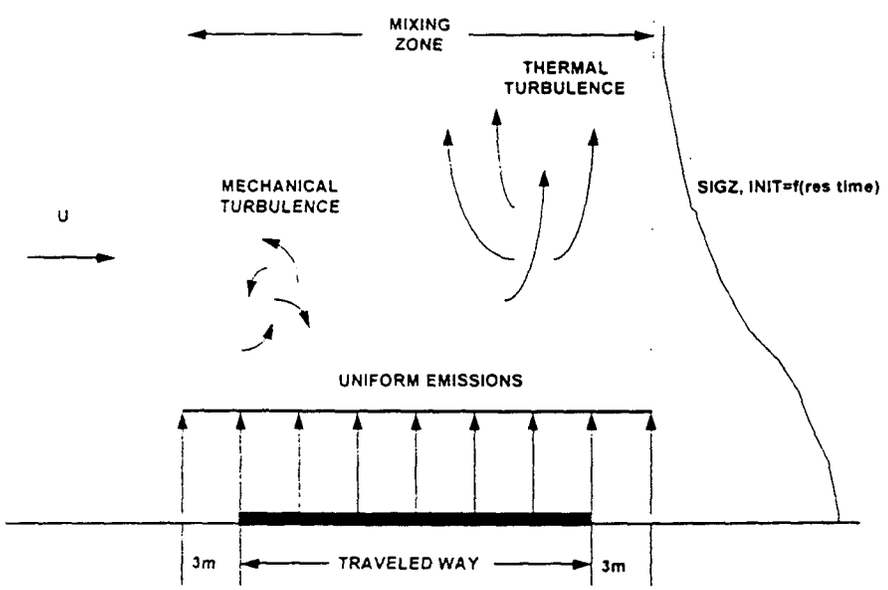

Figure 3 *Schematic of the Mixing Zone Model Used by CALINE3 (Bensen, 1979)*

accounted for by increasing the width of the road by 3 meters on either side. The initial vertical dispersion is accounted for with an empirically derived value for σ_Z in the mixed zone.

CALINE3 assumes that the turbulence within the mixing zone is constant (for 4,000 to 8,000 vehicles per hour and 30 to 60 miles per hour) due to the offsetting effects of traffic speed and volume. Empirical relationships are used by CALINE3 to calculate an initial value for σ_Z based upon the pollutant's residence time within the mixing zone, and the averaging time. In order to calculate σ_Z values downwind from the line source, CALINE3 uses the initial σ_Z value from the mixing zone model, and the value of σ_Z at 10 kilometers (a function of the surface roughness, the stability class, and the averaging time) as defined by Pasquill (Pasquill, 1976). Essentially, the power curve approximation suggested by Pasquill is elevated near the highway by the intense mixing zone turbulence (Bensen, 1979).

Other researchers have developed methods to account for vehicle induced mixing with the Gaussian line source approximation. Bullin and Maldonado (Bullin and Maldonado, 1977) used an empirical equation near the highway and the Gaussian dispersion equation downwind. Chock and Rao et. al. suggested improvements to the Gaussian line source model through redefinition of $\sigma_Z(x)$ near the highway (Chock, 1977 and Rao et. al., 1980). All of these methods improve the performance of the Gaussian line source model near the highway, but they are only valid for certain ranges of speeds. Additionally, concentrations can not be determined on the roadway itself.

3.4 Characterization of Vehicle Wakes

Due to the limitations of the Gaussian line source model near a highway (described above) much research has been conducted to better characterize the wake of a moving vehicle and its effect on the transport and dispersion of pollutants. This research is summarized below.

When a vehicle moves along a highway, it imparts momentum to the air passing by it, leaving a wake of fluid moving in the direction of travel of the vehicle (Fay, 1994). This causes considerable mixing that influences pollutant concentrations within about 100 m of a highway (Samson, 1988). In the field of fluid mechanics, this wake is sometimes modeled as having a semicircular cross-section with radius R_w and wake speed V_w relative to the ground (Fay, 1994). Figure 4 shows a schematic of the wake behind a moving vehicle. In this model, R_w increases and V_w decreases with time $t=x/V_v$ (the elapsed time since the passage of the vehicle).

An approximation for V_W can be obtained by performing a momentum balance and making the assumptions that x is large compared to the wake radius close behind the vehicle and that the velocity of the wake is much less than the velocity of the vehicle

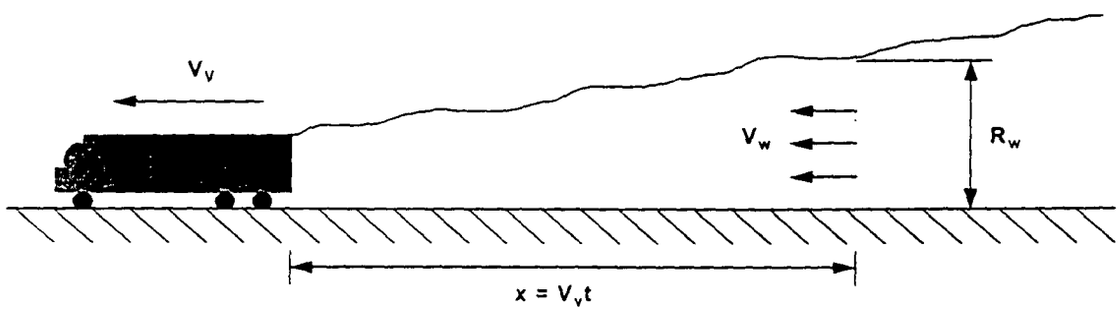

Figure 4 *Schematic Representation of a Vehicle's Wake (Fay, 1994)*

($V_W << V_V$). This yields the following equation:

$$V_w = V_v \left[\frac{C_D A_v}{2 A_W} \right] \tag{3.2}$$

where C_D is the coefficient of drag, A_v is the frontal area of the vehicle, and A_W is the cross-sectional area of the wake ($A_W = \pi R_W^2/2$) (Fay, 1994).

This equation is only useful if one knows the radius of the wake, R_W, as a function of distance behind the vehicle. A crude approximation of this function is expressed in the following manner:

$$R_w = 2\alpha_W x \tag{3.3}$$

where α_W is an empirical constant of order unity determined experimentally.

A more complex model of a vehicle's wake was derived by Eskridge and Hunt in 1979. Eskridge and Hunt used the continuity equation, appropriate boundary conditions, and many simplifying assumptions to derive complex equations describing the structure and turbulence of the wake behind a single vehicle when there is no wind. As a result of their analysis, they concluded that the height of the wake (H_W) behind a vehicle is proportional to the distance behind the vehicle (x) to the 1/4 power. This can be expressed in the following equation:

$$H_W \propto x^{1/4} \tag{3.4}$$

where H_W and x are as defined above. Note that if the cross-section of the wake is semicircular, $H_w = R_w$.

The velocity of the wake determined by Eskridge and Hunt is as follows:

$$V_W = V_V (x / H_V)^{-3/4} A^4 \Lambda_1 \zeta \exp\left[-\frac{(\zeta^2 + \eta^2)}{8}\right] \quad (3.5)$$

where V_w, V_v, and x are as previously defined, Λ_1 is a constant approximately equal to 4.13, and A, ζ, and η are as calculated below:

$$A = \left[\frac{\rho\, C_D A_V}{2\,(32\pi)^{1/2}\gamma^3 H_V^2 \Lambda_1}\right]^{1/4} \quad (3.6)$$

$$\zeta = \frac{(z / H_V)}{(x / H_V)^{1/4}\gamma\ A} \quad (3.7)$$

$$\eta = \frac{(y / H_V)}{(x / H_V)^{1/4}\gamma\ A} \quad (3.8)$$

where all variables are as defined previously and y is the distance off-centerline, z is the distance above ground, ρ is the density of the air, and γ is a constant (approximately 0.4).

3.5 Mixing Caused by Vehicle Wakes

Experimental research on vehicle induced mixing has determined that under certain conditions, traffic wake induced turbulence can dominate ambient turbulence. In 1979, Green et. al. noted that ground-level pollutant concentrations near a highway did not increase as rapidly with decreasing wind speed as predicted by most Gaussian line-source models. In 1980, Rao et. al. compared calculated values of σ_Z (determined using the GM database) to σ_Z values suggested by Briggs in 1975. The calculated σ_Z values did not vary according to stability class as did the Brigg σ_Z's, but rather fell in the region bounded by stability classes A and C of the Brigg σ_Z's. In 1984 Petersen et. al. reported that pollutant concentrations generally decrease with increasing vehicle speed regardless

of ambient atmospheric stability, suggesting that vehicle induced turbulence dominates ambient turbulence. In 1987 Gronskei reported that when the atmospheric wind is perpendicular to the road, the vertical dispersion is linearly dependent on the estimated scale of a vehicle's wake. However, his results were valid only when the scales of turbulence in the atmospheric surface layer are smaller than the scale of the wake. Additionally, Eskridge et. al. (1991) theorized that under stable conditions the effect of vehicle speed on pollutant concentrations is significant. Data taken along the Long Island Expressway indicated that the influence of vehicle speed on the ambient pollutant concentrations is not significant during unstable and neutral conditions (there was not enough data to evaluate stable conditions).

In 1977 and 1978, Chock used data from the General Motors sulfate dispersion experiment to investigate the possibility of high temperature automotive exhaust causing buoyancy induced dispersion. He determined that under light wind speeds (u<1 m/s) the plume rise was significant at locations not very near the road. However, at larger wind speed and very close to the road, the mechanical mixing from moving vehicles dominated the buoyancy induced turbulence from hot exhaust gases

With respect to modeling, a finite-difference model for calculating pollutant concentrations on and near a highway that incorporates a vehicle wake theory and surface-layer similarity theory was developed by Eskridge and Hunt in 1979. This model was then validated by Eskridge et. al. in 1979. The model functions by determining the atmospheric structure along a roadway using both surface layer similarity theory and a

vehicle wake theory. A conservation of species equation is then solved to determine pollutant concentrations.

The general form of the conservation of species equation (neglecting chemical reactions) is:

$$\frac{\partial B}{\partial t} + \bar{\nabla}_2 \bullet B\bar{V} = \bar{\nabla}_2 \bullet K\bar{\nabla}_2 B + E(x,t) \tag{3.9}$$

where $\bar{\nabla}_2$ is the divergence operator in x and z coordinates, $E(x,t)$ is an emission source term, B is the chemical species, $\nabla 2 \bullet V$ is assumed to be zero, and K is the eddy diffusivity. The model functions by determining an effective diffusivity K simply by adding calculated diffusivities from both the standard atmosphere and the vehicle's wake:

$$K = K^S(z) + K^W(x,z) \tag{3.10}$$

where K^S is the diffusivity of the standard atmosphere determined through similarity theory and K^W is the diffusivity of the wake determined through wake theory. The wake theory used by Eskridge et. al. calculates the wake diffusivity as being approximately the product of the turbulence fluctuations in the wake and the wake thickness.

The results showed that although the model did overpredict concentration, the predictions made using the wake effect were closer to actual observations than those of the EPA HIWAY model. They also found that if the wake effect was ignored when the wind was nearly parallel to the axis of the highway, overpredictions in concentrations were made. In 1982, Eskridge and Thompson modified this wake theory and validated it in a wind tunnel. However, their results are limited to cases where the vehicle speed is much greater than the wind speed.

In conclusion, several researchers have advanced the state of knowledge of pollutant dispersion in vehicle wakes. It is possible to approximate the speed and size of a vehicle's wake using theoretical relationships and empirical data. Vehicle turbulence can dominate atmospheric turbulence at high vehicle speeds or under calm atmospheric conditions. At low wind speeds, the exhaust may rise over highways with high traffic density. Additionally, a finite-difference model has been developed which incorporates vehicle wake theory and yields accurate predictions when the vehicle speed is much greater than the wind speed.

3.6 Summary of State of Knowledge

The state of knowledge of driver exposure to carbon monoxide is fairly extensive if one is concerned with pollution from automobiles. However, there is little or no information which is specific to snowmobiles. The data on emissions from snowmobiles are relatively old and are limited to a few snowmobiles under uncertain conditions. No published information is available on exposure to pollutants while riding on a snowmobile. And although modeling methods exist which can predict pollutant concentrations from automobiles, they do not all incorporate the vehicle wake theory which is necessary to predict concentrations on a roadway. In stagnant conditions (no wind), the mechanical turbulence dominates ambient turbulence and these models are of little or no use. Additionally, those models which do incorporate wake theory have been developed for automobiles. The turbulence associated with a snowmobile may differ to the extent that the road vehicle models may not be applicable to snowmobiles.

CHAPTER 4

TASK 1: PURPOSE AND DESIGN

4.1 Purpose of Task 1

The purpose of Task 1 was to measure the steady-state mass emission rate of CO from the test snowmobile as a function of the snowmobile's speed. Therefore, measurements of CO exhaust concentrations were taken at four different speeds while a snowmobile was traveling over flat terrain. The speeds ranged from 10 mph to 40 mph in order to cover the range of speeds usually witnessed on park snowmobile trails. Additionally, CO exhaust concentrations were measured both while the snowmobile was idling and also while the snowmobile was under power. In order to convert the exhaust CO concentrations to a mass emission rate, the air flow into the engine was also measured under each condition.

4.2 Task 1 Site Selection

Many criteria were taken into consideration when selecting a test location. First and foremost, the site needed to have convenient snowmobile access with 2-3 mile of straight trail over level terrain. The trail needed to be straight in order to allow the second snowmobile to travel precisely along the centerline of the lead snowmobile for at least two consecutive minutes. Level terrain was desired for two reasons. First, flat terrain would allow the snowmobile to be more easily operated under steady-state conditions.

Second, complex topography might influence the dispersion of the snowmobile's exhaust. In order to prevent interference from other snowmobiles, the trail needed to be relatively unpopular (ruling out any trails in YNP). It was also desired for the site to be within 3 hours of the researcher's residence (although this was negotiable). And finally, it was desired to find a location where the trail was parallel to the prevailing wind directions.

A site which met all of the above criteria was located in Grand Teton National Park (near Moose, WY). A map of the site is located in Figure 5, with the selected testing location indicated by an arrow. This section of trail was ideal for testing. It runs along the valley floor and is relatively flat and straight (predominately north-south). Additionally, there is very little snowmobile traffic on this trail (most tourists in the area choose to snowmobile in Yellowstone). As an added bonus, the valley in which this site is located is known for its strong winter inversions. This was important for taking exposure measurements in calm conditions.

4.3 Task 1 Sample Collection Equipment

Task 1 involved the collection of engine-out exhaust samples from a moving snowmobile. Therefore, the exhaust sampling train was designed to allow the researcher to collect exhaust samples while riding the snowmobile. This was accomplished by inserting a piece of copper tubing (1/4" inner diameter) into the snowmobile's exhaust pipe, securing it under the snowmobile and routing it out along the right side of the driver. Copper tubing was selected both to permit the exhaust gases to cool and also to

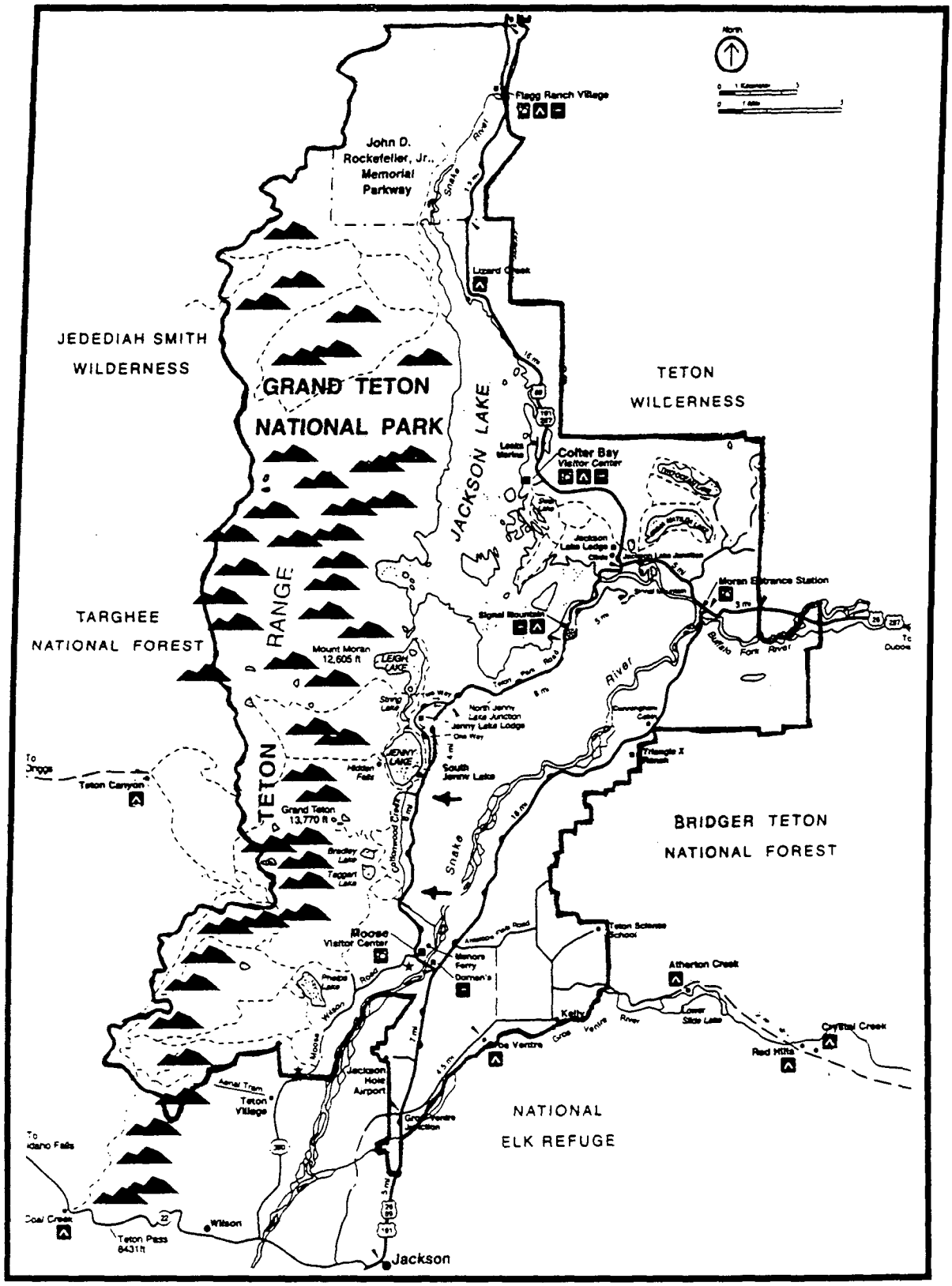

Figure 5 *Map of Test Site*

encourage water to condense out of the exhaust. The copper tubing was able to transfer enough heat out of the exhaust to allow the use of tygon tubing for the rest of the sample line.

Therefore, a hose barb was connected to the copper tubing with the use of a compression fitting to allow the connection of tygon tubing. The exhaust sample was then fed through a tube filled with indicating Drierite®. The purpose of the Drierite® was to remove any remaining water from the exhaust. It indicated saturation with a color change, notifying the researcher of the need to change the tube. After passing through the Drierite®, the sample flowed through a personal sampling pump.

The pump used in this research was an SKC universal flow sample pump (number 224-PCXR8). This pump is a constant air flow sampler. It allows a flow rate of 5-5000 ml/min, operates up to 8 hours on battery power, operates in temperatures ranging from -4 °F to 113 °F (very important for this study), and is extremely durable. During testing, the pump was secured to the researcher with the use of a special carrying case.

The sample then exited the pump and was fed into a 2 liter Tedlar® sampling bag. The sampling bag was fitted with a Roberts® valve, allowing the exhaust to be sealed in the bag until it was ready for analysis. A picture of the entire sample train is located in Figure 6. As mentioned above, The pump (and sampling bag) were worn by the researcher during testing.

In addition to collecting exhaust samples, Task 1 required the measurement of the air flow rate into the engine. For this purpose, a piece of rubber tubing was fitted and sealed over the inlet port of the snowmobile. The "new" air inlet was then routed around

AN INVESTIGATION OF

DRIVER EXPOSURE TO CARBON MONOXIDE

WHILE TRAVELING

IN THE WAKE OF A SNOWMOBILE

A Dissertation

Presented for the

Doctor of Philosophy

Degree

The University of Tennessee, Knoxville

Lori Marie Snook

August, 1996

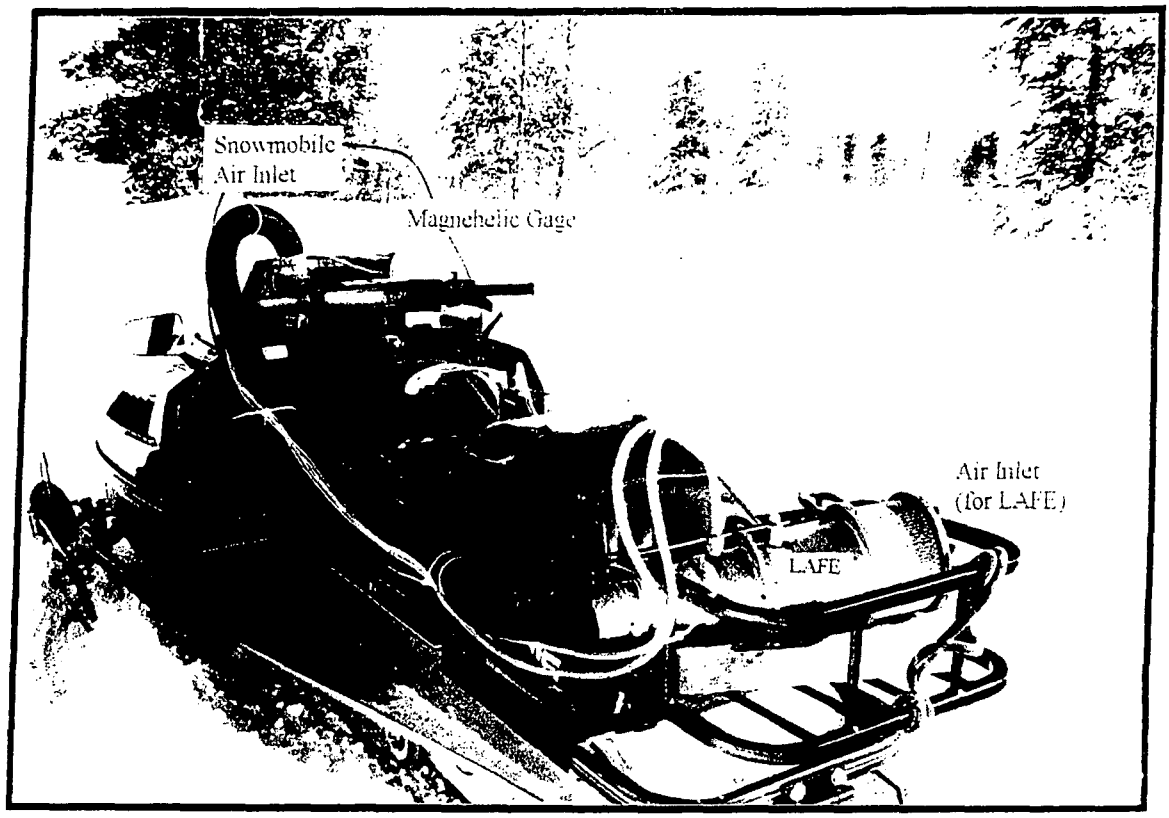

Figure 6 *Picture of Exhaust Sampling Train*

to the back of the snowmobile where a Meriam 60 AC O2 Laminar Air Flow Element (LAFE) was mounted. The LAFE operates on the principles of laminar flow and measures flow rate by creating a slight differential pressure with the insertion of a matrix resistance element. The element is designed to create a differential pressure which follows a linear flow relationship. This allows the system to be used on pulsating flow applications. The pressure drop across the element was measured using a magnehelic gage mounted in view of the snowmobile driver. Figure 7 shows the air flow measurement system installed on the snowmobile.

All connections on the ducting from the LAFE to the air intake of the engine were sealed with duct tape and/or caulking and secured with hose clamps if appropriate. A test

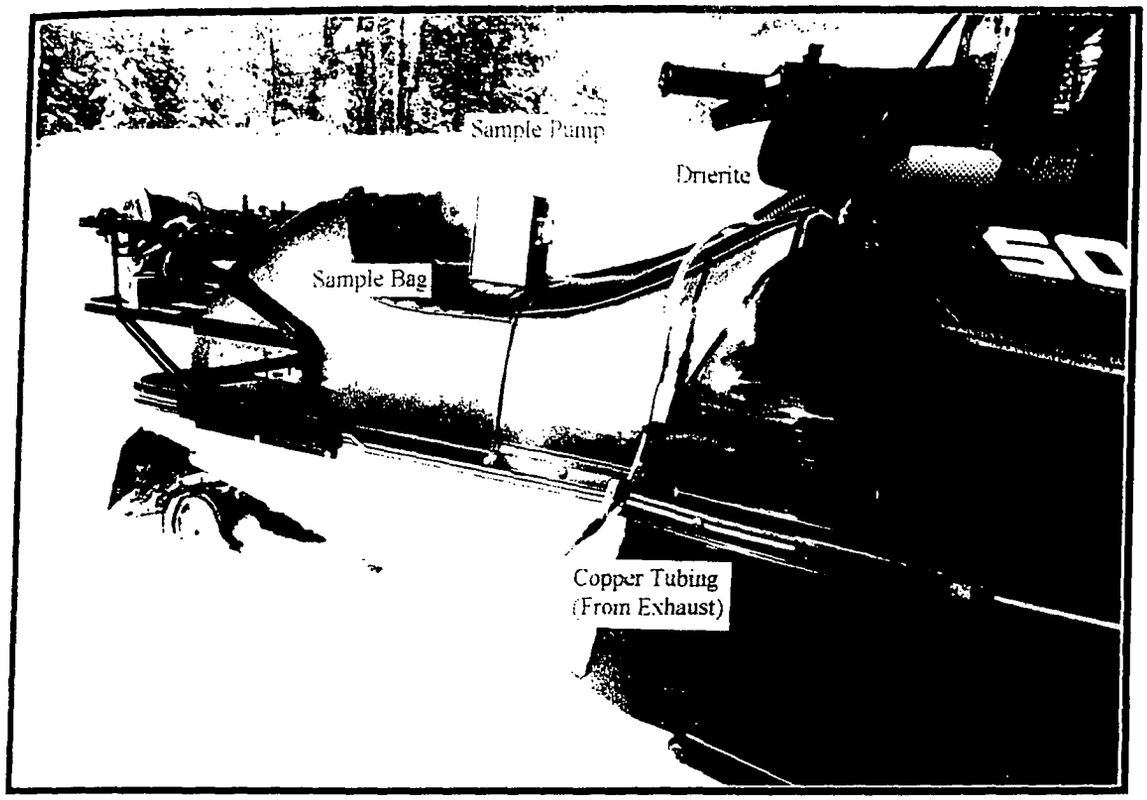

Figure 7 *Picture of Air Flow Measurement Equipment*

was run to verify that there were no air leaks between the air intake and the engine itself. In this test, a hand was placed over the air intake of the snowmobile. When this was done the engine stalled, verifying that no air leaks were present.

The snowmobile used for all exhaust testing was a 1992 Polaris Indy 500. This snowmobile is equipped with a 488 cc two-stroke engine, electronic fuel injection, and is water/snow cooled. It represents a "typical" snowmobile in use today.

Meteorological conditions were also measured during Task 1. Air temperature was measured with a standard thermometer. Wind direction was determined with a light piece of landscape tape and a compass. The wind speed was measured with a Davis Turbometer. The Davis Turbometer is a small, hand-held, vane-axial anemometer with

and accuracy of ±3%. Note: A detailed list and description of all equipment used in this dissertation is located in Appendix A.

4.4 Task 1 Sample Collection Equipment Calibration

The only two pieces of Task 1 sample collection equipment requiring calibration were the LAFE and the magnehelic gage. The LAFE was calibrated in the engine lab at the University of Tennessee with the use of a second (factory calibrated) LAFE. Details on the procedure and results are located in Appendix B. The magnehelic gage was calibrated with a U-tube manometer. Its calibration resulted in: inches of H_20 measured = actual inches of H_20.

4.5 Task 1 Sample Collection Procedure

Each day that exhaust samples were taken, a specific procedure was followed to ensure consistent results. Upon arrival at the test site, meteorological conditions were recorded. These included temperature, wind speed, wind direction, snow (trail) condition and whether or not an inversion was present (determined from the air temperature at the valley floor and the air temperature 4,000 feet above the valley floor). After the weather conditions were recorded, all equipment was double checked and the magnehelic gage was zeroed. If everything was satisfactory, the snowmobile was started and driven for a minimum of 10 minutes. This was done to allow enough time for the snowmobile to warm-up and reach standard operating conditions.

Samples of exhaust were taken at 10, 20, 30, and 40 mph. The following procedure was used:

1. A new sample bag was prepared for collection by attaching it to the researcher and opening its valve.
2. The bag number and test speed were recorded.
3. The pump was activated (flow rate = 1 l/min).
4. The snowmobile was accelerated to the appropriate speed.
5. The speed was held constant for a minimum of one minute.
6. The pressure drop across the LAFE, the engine rpm, and the snowmobile's speed were recorded.
7. The pump outlet tubing was attached to the sample bag.
8. The bag was allowed to fill (approximately 2 minutes).
9. The roberts valve on the bag was closed.
10. The snowmobile was brought safely to a stop.
11. The sample bag was removed and strapped to the researcher's backpack.

The same procedure was used to take the idle exhaust sample. When taking the acceleration exhaust sample, this procedure was used with the following exceptions. It was impossible to accelerate for one minute (to flush the lines) before sampling started. Therefore, the pump flow rate was set on maximum flow (5 l/min) and the lines were flushed for a few seconds before sampling began. Sampling occurred only while the snowmobile was accelerating. The actual acceleration rate was not recorded but was estimated to be approximately 0 to 60 mph in 30 seconds. The pump was disconnected from the sample when the snowmobile reached approximately 60 mph.

4.6 Task 1 Sample Analysis Equipment

Analysis of the exhaust samples involved dilution of the raw exhaust by a factor of approximately 70:1 and measurement of the diluted sample with a CO analyzer. Dilution was accomplished with the same SKC universal sampling pump that was used to collect the exhaust samples. This pump has two separate controls to regulate flow. The main flow control is a part of the main pump assembly and controls flow from 0.5 to 5.0 l/min. The other flow control device is part of a separate low flow adapter which attaches to the pump inlet. It controls flow from 5 ml/min to 0.5 l/min. Therefore, it was possible to set the high flow rate with the main flow control screw and a separate low flow rate with the low flow adapter control screw. This allowed the researcher to use one of two flow rates without any adjustment of flow other than removal of the low flow assembly. In this way, repeatable dilutions were possible with the SKC pump. Dilutions were made into clean 2 liter Tedlar® sampling bags.

The diluted samples were measured with a Thermo Environmental Model 48 CO analyzer. This analyzer uses the Gas Filtration Correlation (GFC) method of analysis which (among other advantages) is highly specific to CO. GFC spectroscopy is based upon detailed comparison of the structure of the infrared absorption spectrum of the measured gas to that of other gases also present in the sample being analyzed. The technique is implemented using a high concentration sample of CO as a filter for the infrared radiation transmitted through the analyzer. This particular analyzer can measure CO concentrations from 0.1-1000 ppm with a precision of ±0.1 ppm.

Because the exhaust gas analysis took place in a tightly sealed room, several safety precautions were taken to prevent and detect CO build-up. To prevent CO build-up, all gases were exhausted from the room through a trap in a sink. This was considered a better method to remove exhaust gases than venting out a window due to Wyoming's extreme winter conditions. To detect CO build-up in the lab, two different CO detectors (one with an alarm) were placed in the laboratory.

4.7 Task 1 Sample Analysis Equipment Preparation and Calibration

To ensure accurate analysis of the exhaust gas samples, a standard procedure was followed to guarantee that the CO analyzer was started, calibrated, and operated properly. This involved turning the instrument on, allowing it to stabilize, and calibrating both the zero and span settings on the analyzer. For Task 1 analysis, the span gas was a 700 ppm CO standard. The analyzer was calibrated every day before use and every four hours thereafter (drift was insignificant).

All bags to be used for making dilutions were cleaned before use. This involved purging each bag three times with room air. Room air was deemed adequate for this purpose as the CO concentration in the room air measured less than 0.5 ppm.

The final preparatory step involved setting the low flow adapter screw on the air pump to obtain a satisfactory dilution ratio. As mentioned earlier, the pump flow rate could be controlled by adjusting both a main screw (0.5 to 5.0 l/min) which is located on the main pump assembly and a low flow screw (5 ml/min to 0.5 l/min) which is located on a separate adapter. The pump also has a small flowmeter which indicates flow in the

range of 0.5 to 5.0 l/m. Therefore this flowmeter was used to set the main screw at 1.5 l/min.. Then, trial and error was used to set the low flow adapter screw to obtain an appropriate dilution ratio. Trial and error was necessary as the sampling pump does not have a flow measurement device capable of measuring flow in the range of 5 ml/min to 0.5 l/min.

The low flow screw setting was determined in the following manner. The low flow screw was adjusted and the pump outlet was connected to an empty sample bag. Air was then pumped into the bag for 30 minutes. The air in the bag was measured using an inverted graduated cylinder and a bucket of water. This allowed an approximate flow rate to be calculated. This process was repeated until the low flow rate was approximately 15 ml/min (1/100 of the high flow setting). The low flow screw was then taped in such a way as to prevent further adjustment. It is important that this process was only used to set the approximate desired dilution ratio. The actual dilution ratio obtained was calculated each day before analysis and is described in detail in the next section.

4.8 Task 1 Sample Analysis Procedure

As mentioned in the previous section, the first step in analyzing the exhaust gas samples involved preparing the analyzer, the sample bags, and the dilution pump. The next step in this procedure was measuring the actual dilution ratio that would be used for the particular day's worth of analysis. This procedure was as follows:

1. Turn on the CO analyzer.
2. Place the analyzer's exhaust down the p-trap of the sink.
3. Allow the analyzer to stabilize.

4. Zero the analyzer with zero gas.
5. Calibrate the span of the analyzer using 20 ppm standard.
6. Set the high flow screw on the air pump at 1.5 l/min.
7. If low flow adapter is attached, remove it from the pump inlet.
8. Run pump for approximately 1 minute to flush all lines with room air.
9. Turn off the pump.
10. Attach clean sample bag to the outlet of the pump.
11. Run the pump for exactly 1 minute (filling the sample bag with room air).
12. Close the valve on the sample bag.
13. Attach the low flow adapter (with permanently set low flow screw) to the inlet of pump.
14. Attach the 700 ppm standard to the inlet of the low flow adapter (pump inlet).
15. Attach the exhaust line to the outlet of the pump.
16. Turn on the pump and flush its lines for at least 5 minutes.
17. Turn off the pump
18. Attach the previously filled sample bag to the outlet of the pump.
19. Run the pump for exactly 2 minutes (adding the 700 ppm standard at low flow to the room air in the bag).
20. Close the bag's valve.
21. Repeat steps 7 to 20 four more times.
22. Measure the CO concentration in each of the five diluted bags with the Model 48 CO analyzer.
23. Calculate the average dilution ratio in the bags.

The average dilution ratio was calculated by obtaining the average measured CO concentration in the diluted standards and using the following equation:

$$DilutionRatio = \frac{700\ ppm}{Average\ concentration\ of\ diluted\ standards\ (ppm)} \qquad (4.1)$$

As mentioned before, the dilution ratio was measured at the start of each day of exhaust gas analysis.

After the dilution ratio was calculated, exhaust gas analysis was begun. The procedure for dilution and measurement of the exhaust gas samples was similar to the procedure used to determine the dilution ratio. It is detailed below:

1. Re-zero the analyzer with zero gas (if necessary).
2. Calibrate the span of the analyzer using 700 ppm CO standard.
3. If low flow adapter is attached, remove it from the pump inlet.
4. Run pump for approximately 1 minute to flush all lines with room air.
5. Turn off the pump.
6. Attach clean sample bag to the outlet of the pump.
7. Run the pump for exactly 1 minute (filling the sample bag with room air).
8. Close the valve on the sample bag.
9. Turn off the pump.
10. Repeat steps 6 through 9 four more times.
11. Attach the low flow adapter (with permanently set low flow screw) to the inlet of pump.
12. Attach the raw exhaust sample bag to the inlet of the low flow adapter (pump inlet).
13. Attach the exhaust line to the outlet of the pump.
14. Turn on the pump and flush its lines for at least 5 minutes.
15. Turn off the pump
16. Attach one of the bags previously filled with room air to the outlet of the pump.
17. Run the pump for exactly 2 minutes (adding the raw exhaust sample to the room air in the bag).
18. Close the bag's valve.
19. Turn off the pump.
20. Repeat steps 16 to 19 four more times.
21. Measure the CO concentration in each of the five diluted bags with the Model 48 CO analyzer.
22. Calculate the average concentration of the diluted exhaust samples.
23. Calculate the actual exhaust sample concentration using the appropriate dilution ratio.

The actual exhaust sample concentration was calculated by averaging the concentrations measured in the diluted exhaust samples and using the following equation:

$$Exhaust\ CO\ Conc = (Dilution\ Ratio)(Average\ Concentration\ of\ Diluted\ Samples) \quad (4.2)$$

Five dilutions were made for each exhaust sample in an effort to decrease the error introduced by diluting the raw exhaust.

CHAPTER 5

TASK 1: DATA REDUCTION

5.1 Calculation of Dry Exhaust Mass Flow Rate

In order to convert the exhaust CO concentrations to mass-based values, the dry mass flow rate of the snowmobile's exhaust was needed. However, the LAFE was used to measure volumetric air flow into the engine. Therefore, this data needed to be modified to approximate the exhaust flow rate. This involved assuming an air/fuel ratio and correcting the measured flow rate for the addition of fuel. The exhaust flow was then converted to a dry basis. The specific calculations are detailed below.

The first step in the air flow data reduction was to convert the pressure drop measured across the LAFE into the volumetric flow entering the engine. This was done using the calibration curve located in Appendix B. The indicated flow from the calibration curve was then corrected for temperature with the following equation (specified by the manufacturer):

$$Actual\ Flow = Indicated\ Flow\left(\frac{Viscosity\ @\ 70F}{Viscosity\ @\ Test\ Temperature}\right) \qquad (5.1)$$

This yielded the volumetric flow rate of air into the snowmobile's engine in actual cubic feet per minute (acfm).

The next step was to convert the inlet volumetric flow rate into a mass flow rate. This was accomplished by using a form of the ideal gas law detailed in Equation 5.2:

$$\frac{Mass\ of\ air\ into\ engine}{Time} = \left(\frac{Volume\ of\ air\ into\ engine}{Time}\right)\left(\frac{(MW_{air})(P)}{(R_U)(T)}\right) \qquad (5.2)$$

Where MW_{air} is the molecular weight of the air, P is the air pressure, R_U is the universal gas constant and T is the absolute temperature of the air flowing into the engine. Care was taken to insure that all necessary unit conversions were performed.

Next, the fuel/air equivalence ratio in the engine was estimated from the CO concentration measured in the exhaust sample and a graph of engine-out emissions as a function of the fuel/air equivalence ratio. A fuel/air equivalence ratio was estimated for each exhaust sample (not just for each speed tested). The fuel/air equivalence ratio, $\Phi_{F/A}$, is defined as the F/A ratio in the engine divided by the F/A ratio of stoichiometric combustion. The graph used to estimate the equivalence ratio is located in Figure 8.

It should be noted that estimation of the F/A equivalence ratio was necessary to correct inlet flow measurements for the addition of fuel. However, because the air flow into the engine is always much greater than the fuel flow into the engine, the final calculation of the mass flow rate of the exhaust is not greatly influenced by this value. It is estimated that a maximum error of ±3% would be introduced by the worst possible estimation of the F/A equivalence ratio.

Once the an air/fuel ratio was estimated, the following equation of combustion (for rich combustion) was balanced for each sample:

$$CH_{1.85} + \left(\frac{Stoich\ mol\ air}{mol\ fuel}\right)\left(\frac{1}{\Phi_{F/A}}\right)(O_2 + 3.76N_2) \rightarrow \mathbf{A}CO_2 + \mathbf{B}H_2O + \mathbf{C}N_2 + \mathbf{D}CO + \mathbf{E}H_2 \qquad (5.3)$$

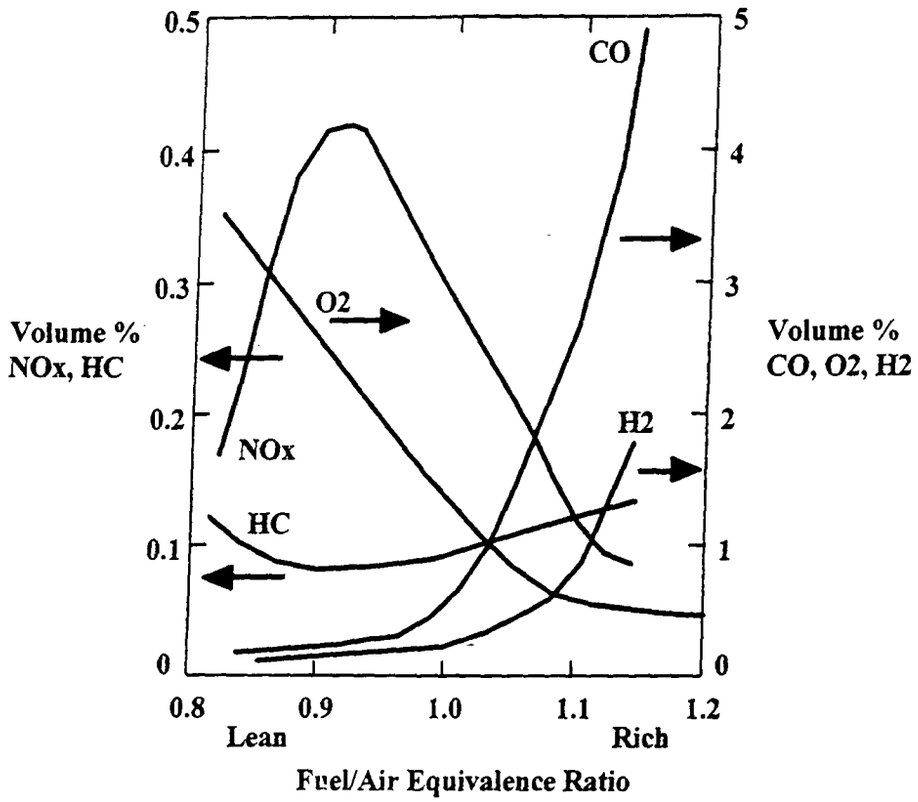

Figure 8 *Graph of Engine Emissions Vs. Fuel/Air Equivalence Ratio (Stone,1992)*

The capital letters in bold are the moles of the appropriate molecule in the balanced equation and the value for the stoichiometric moles of air/mole of fuel is 1.4625. Note that the fuel in Equation 5.3 is estimated at $CH_{1.85}$. This estimation neglects the small amount of oil burned in the combustion chamber.

Equation 5.3 contains five unknowns. Therefore, five equations were necessary to balance it. The first four equations were determined with carbon, hydrogen, nitrogen, and oxygen balances. The fifth equation came by assuming that the water gas equilibrium is the sole determinant of the burned gas composition (as described in Stone, 1992). The water gas reaction is expressed as:

$$CO_2 + H_2 \longleftrightarrow CO + H_2O \tag{5.4}$$

and the equilibrium constant, k, for the water gas reaction is:

$$k = \frac{P_{H_2O} P_{CO}}{P_{H_2} P_{CO_2}} \tag{5.5}$$

Where P_X is the partial pressure of x. Recalling that the partial pressure of a molecule is expressed by:

$$P_X = \left(\frac{moles\ of\ X}{total\ number\ of\ moles} P_T \right) \tag{5.6}$$

Where P_T is the total pressure. Equation 5.5 can be expressed in the following manner:

$$k = \frac{(moles\ of\ H_2O)(moles\ of\ CO)}{(moles\ of\ H_2)(moles\ of\ CO_2)} \tag{5.7}$$

Using the coefficients from Equation 5.3, K can be expressed as follows:

$$k = \frac{\mathbf{DB}}{\mathbf{AE}} \tag{5.8}$$

It is this relationship that was used as the fifth equation needed to balance the combustion equation (Stone, 1992).

The value of the equilibrium constant, k, is temperature dependent. Therefore, it was necessary to determine the appropriate temperature to use when looking up the value of the equilibrium constant. This was accomplished by assuming that the equilibrium composition was "frozen" (fixed in composition) at a temperature of 1400 K. This temperature is recommended by Obert in his book, *Internal Combustion Engines and Air Pollution* (Obert, 1973). At this temperature, the value of the equilibrium constant, K, is 2.153 (Cengel and Boles, 1989).

Once the combustion equation was balanced, the following quantities were calculated using the balanced combustion equation: the mass of fuel/mass of air, the mass of dry products/mole fuel, the mass of wet products/mole of fuel, and the molecular weight of the dry exhaust gases. The appropriate equations are as follows:

$$\frac{mass\ of\ fuel}{mass\ of\ air} = \frac{MW_{fuel}}{\left(\frac{1.4625}{\Phi_{F/A}}\right)(MW_{O_2} + 3.76\,MW_{N_2})} \tag{5.9}$$

$$\frac{mass\ of\ dry\ products}{mole\ fuel} = \mathbf{A}(MW_{CO_2}) + \mathbf{C}(MW_{N_2}) + \mathbf{D}(MW_{CO}) + \mathbf{E}(MW_{H_2}) \tag{5.10}$$

$$\frac{mass\ wet\ products}{mole\ fuel} = \mathbf{A}(MW_{CO_2}) + \mathbf{B}(MW_{H_2O}) + \mathbf{C}(MW_{N_2}) + \mathbf{D}(MW_{CO}) + \mathbf{E}(MW_{H_2}) \tag{5.11}$$

$$molecular\ weight\ of\ dry\ exhaust = \left(\frac{mass\ of\ dry\ products}{mole\ fuel}\right)\left(\frac{1}{\mathbf{A}+\mathbf{C}+\mathbf{D}+\mathbf{E}}\right) \tag{5.12}$$

Where MW_X is the molecular weight of X and all other symbols are as previously defined.

The dry mass flow rate of the exhaust was then calculated via the following two equations:

$$\frac{mass\ of\ exhaust\ (wet)}{time} = \left(\frac{mass\ of\ air\ into\ engine}{time}\right)\left(1 + \frac{mass\ of\ fuel}{mass\ of\ air}\right) \tag{5.13}$$

$$\frac{mass\ of\ exhaust\ (dry)}{time} = \left(\frac{mass\ exhaust\ (wet)}{time}\right)\left(\frac{mass\ dry\ products}{mole\ fuel}\right)\left(\frac{mole\ fuel}{mass\ wet\ products}\right) \tag{5.14}$$

Equation 5.14 yields the desired quantity, the mass flow rate of the snowmobile's exhaust on a dry basis.

5.2 Calculation of CO Mass Emission Rate

The final step in the data reduction of Task 1 was to calculate the CO mass emission rate of the snowmobile. The following equation was used:

$$\frac{mass\ CO}{time} = \left(\frac{conc.\ of\ CO\ in\ exhaust\ in\ ppm}{10^6}\right)\left(\frac{MW_{CO}}{MW_{dry\ exhaust}}\right)\left(\frac{mass\ of\ exhaust\ (dry)}{time}\right) \qquad (5.15)$$

Finally, the CO emitted as a function of distance traveled was calculated as follows:

$$\frac{mass\ of\ CO}{distance} = \left(\frac{mass\ CO}{time}\right)\left(\frac{1}{snowmobile\ speed}\right) \qquad (5.16)$$

An example calculation using Equations 5.1 through 5.16 is located in Appendix C.

CHAPTER 6

TASK 1: RESULTS AND DISCUSSION OF RESULTS

6.1 Steady-State CO Emissions Results

Steady-state mass emissions of CO were measured and calculated at speeds of 10, 20, 30 ,and 40 mph. All of the raw data and intermediate assumptions used to calculate the CO mass emission rates are located in Appendix D. The final CO emission results are shown graphically in Figures 9 and 10. Figure 9 plots the CO emissions in grams/hour as a function of the snowmobile speed. Figure 10 plots the snowmobile's emission of CO in grams/mile as a function of speed. In both graphs, the reduced data are represented with a ○. The mean of the data at each speed is represented with a ●.

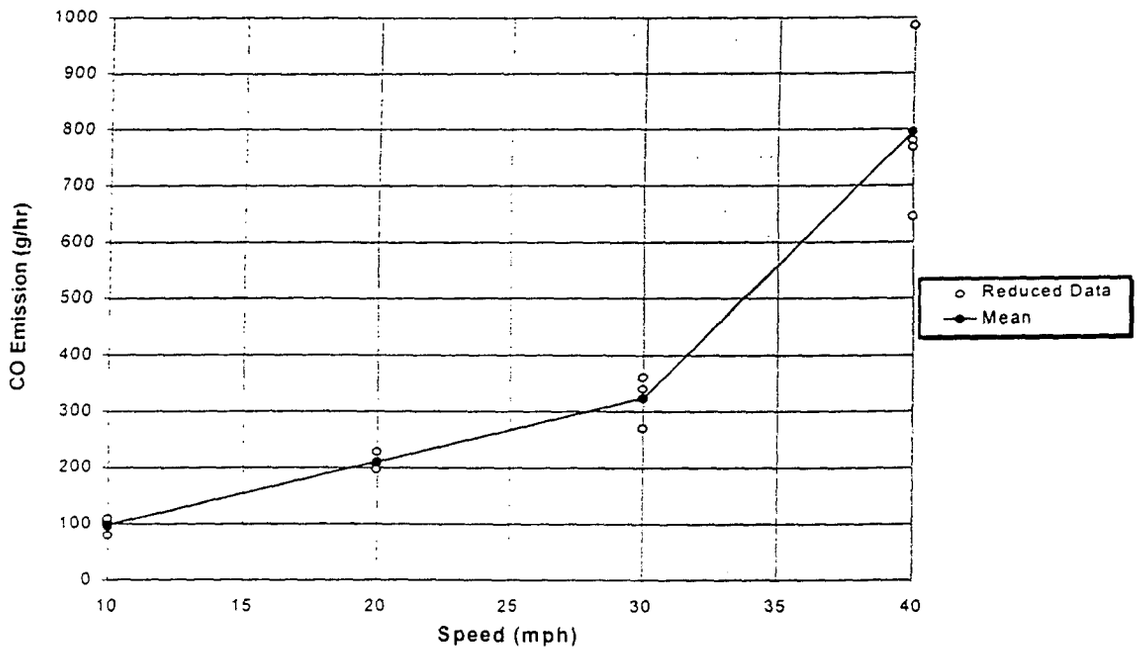

Figure 9 *Graph of CO Emission in g/hr vs. Snowmobile Speed*

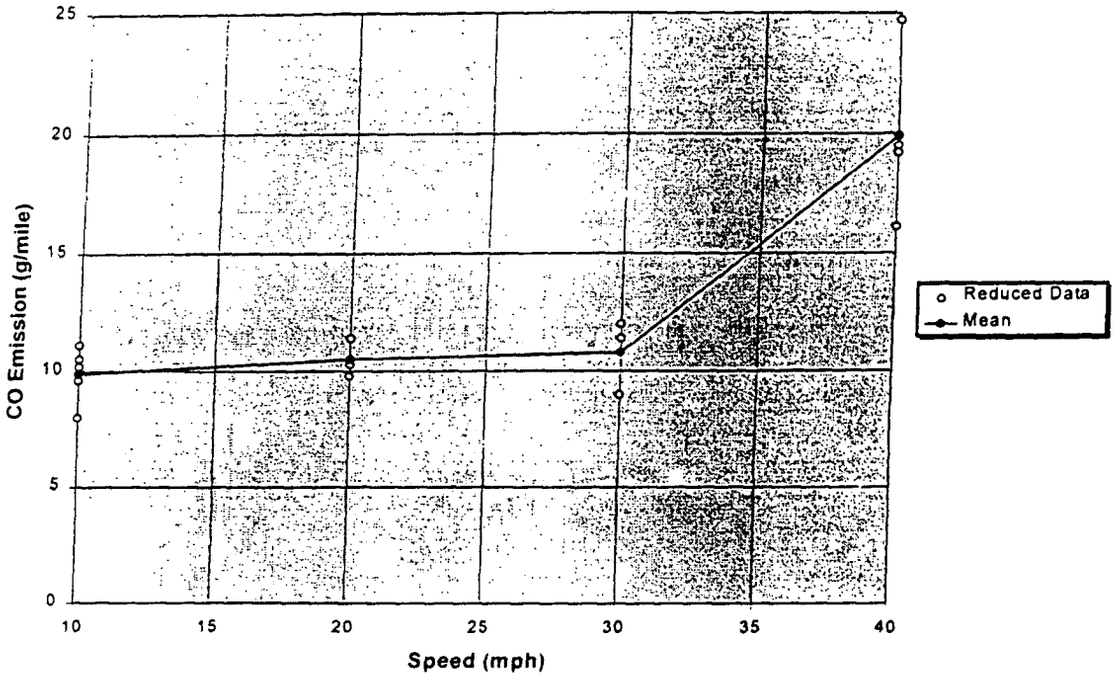

Figure 10 *Graph of CO Em'ssion in g/mile vs. Snowmobile Speed*

These calculated emission rates are also reported in Table 2. Table 2 also includes the mean and 90% confidence interval of the CO emission rates at each speed.

Some uncertainty was introduced into the emission results since the magnehelic gage was only able to be read to the closest 0.1 inches of H_2O. The uncertainty varied with snowmobile speed and was approximately ±25%, ±15%, ±10%, and ±7% at speeds of 10, 20, 30, and 40 mph respectively.

6.2 Discussion of Steady-State CO Emission Results

At first glance, the steady-state emission values measured during Task 1 appear to be quite low*. However, when one considers that the emissions were measured under

* Because of this concern, the airflow rates were double checked with a quick calculation. See Appendix E.

Table 2 *Results of Steady-State CO Emission Testing*

Speed (mph)	CO Emission (g/hr)	Mean (g/hr) @ Speed	90% Confidence Interval of Mean	CO Emission (g/mile)	Mean (g/mile) @ Speed	90% Confidence Interval of Mean
10	80	99	± 11	8.0	9.9	± 1.1
	96			9.6		
	102			10.2		
	105			10.5		
	110			11.1		
20	207	211	± 27	10.3	10.5	± 1.4
	228			11.4		
	197			9.8		
30	341	324	± 57	11.4	10.8	± 1.9
	361			12.0		
	323			10.8		
	270			9.0		
40	780	795	± 166	19.5	19.9	± 4.2
	768			19.2		
	986			21.7		
	645			16.1		

steady-state conditions, the emissions are seen to be of the same magnitude as emissions measured by other researchers under similar conditions. Under steady-state conditions, the snowmobile is operating under relatively low load. The Southwest Research Institute study (discussed in the Literature Review) measured emissions based upon load and rpm. Their results showed that two of the snowmobiles (the Rotax 248 and the Arctic Cat 440) had CO emissions ranging from 21 to 390 g/hr and 22 to 300 g/hr under loads ranging from 0 to 1/2 of the full load. These results are of the same magnitude as the CO emissions measured in this study.

Another sources (Heavner, 1994) has reported that snowmobiles may emit as much as 225 times the amount of CO as an automobile. The current national CO emission standard for new cars is 3.4 g/mile (Black, 1991). The measured snowmobile CO values obtained in this study ranged from 9.9 to 19.9 g/mile. While these values are still larger than current emission standards for automobiles, they are certainly not on the order of 200 times greater.

Again, this discrepancy can be explained by realizing that automobile emissions are measured while the vehicle is driven according to a prescribed driving schedule on a chassis dynamometer. Therefore, the CO emission standard for automobiles represents the average CO emitted from a vehicle under a variety of driving conditions (including acceleration, idling, etc.). The data obtained in this study represent snowmobile CO emissions under steady-state driving conditions only. Therefore it is improper for the CO emissions measured during Task 1 to be directly compared to automobile emission

standards. In order to compare the snowmobile emission results measured in this study to automobile emissions, steady-state CO emissions from an automobile must be known.

A recent study performed at the University of Tennessee did measure steady-state CO emissions from a 1988 Chevrolet Corsica (Sluder, 1995). This study measured both engine-out CO and post-catalyst CO emissions under steady-state conditions at a variety of speeds and gear ratios. For speeds ranging from 10 to 40 mph the steady-state engine-out CO emissions from the 1988 Corsica ranged from 3.7 to 17.0 g/mile. These values are on the same order of magnitude as the snowmobile emissions measured for this dissertation (9.9 to 19.9 g/mile). However, the 1988 Corsica (like most current automobiles) is equipped with a catalyst to reduce emissions. Therefore, the actual amount of CO emitted to the environment was much less. The Corsica's post-catalyst CO emission rate for steady-state speeds ranging from 10-40 mph ranged from 0.01 to 0.04 g/mile. These values are approximately 1000 times smaller than the steady-state snowmobile emissions measured for this dissertation. Therefore, the steady-state snowmobile emissions measured in this dissertation do support the claim that one snowmobile may produce as much CO as 225 (or more) current automobiles.

6.3 Idle and Acceleration CO Emission Results

In addition to steady-state CO emission values, idle and acceleration emissions were also investigated during Task 1. The raw data are located in Appendix D. Only final results are reported here.

While the snowmobile was idling, the exhaust concentration of CO was measured to be 5,138 ppm. However, the snowmobile required so little air while idling that the airflow into the engine was unmeasurable by the LAFE. Therefore, in order to estimate a maximum mass based emission rate, the air flow into the engine was assumed to be the minimum detectable flow rate of the LAFE. This resulted in an estimated maximum mass emission rate of 5.6 grams of CO per hour at idle.

While the snowmobile was accelerating, the concentration of CO in it's exhaust was 69,121 ppm. With an assumed fuel air equivalence of 1.25 and a measured intake airflow of 13.94 acfm, the mass emission rate of CO was calculated to be 2,027 g/hr, which is substantially greater than the steady-state emission of 795 g/hour at 40 mph.

CHAPTER 7

TASK 2: PURPOSE AND DESIGN

7.1 Purpose of Task 2

The purpose of Task 2 was to measure the amount of CO that a person riding on a second snowmobile behind the lead snowmobile is exposed to as a function of both the lead snowmobile's speed and the distance between the snowmobiles. Therefore, measurements of CO concentrations were taken at five different fixed distances behind the lead snowmobile. The measurements were taken both directly on centerline behind the lead snowmobile and 15 feet off-centerline. The distances between the lead and the second (exposed) snowmobiler ranged from 25 feet to 125 feet. Exposure at four different speeds was investigated (the same speeds used in Task 1). Additionally, CO concentrations were measured at the second snowmobile without the lead snowmobile in an effort to determine the amount of self-exposure occurring at each speed. Finally, photographic data on the behavior of the snowmobile's wake were taken with the use of smoke bombs.

7.2 Task 2 Sample Collection Equipment

Task 2 involved the collection of CO samples while riding at a specified distance behind a moving snowmobile. Therefore, the equipment used to collect samples needed to be portable, durable, and easily activated with only one hand. This was accomplished

by using the same SKC universal sampling pump used in Task 1. The only difference being that the pump inlet was opened to ambient air rather than connected to the exhaust sampling train. This was a convenient system for the researcher, as the pump was able to be worn in a special carrying case, allowing hands-free operation. The pump outlet was connected to a 2 liter Tedlar® sampling bag.

The inlet to the pump was located at approximately chest height, directly in front of the researcher. There was some concern that this would yield lower results than if the sample were located to the side of the snowmobile. Preliminary tests were run at 20 mph, 40 feet behind a lead snowmobile with the pump inlet in both locations. With the pump directly in front of the researcher, concentrations of 9.4 and 8.6 ppm CO were measured. With the pump to the side of the snowmobile, concentrations of 10.4 and 5.9 ppm CO were measured. It was concluded that a sampling location directly in front of the researcher was adequate.

Two snowmobiles were used to collect samples during Task 2. The lead snowmobile (the one producing the CO being measured) was the same 1992 Polaris Indy 500 used in Task 1. The second snowmobile was also a Polaris Indy 500, but it was never used as the lead snowmobile as its emission characteristics might have differed from the original snowmobile tested during Task 1

The distance between the two snowmobiles needed to remain constant while samples were collected. Therefore, a piece of bright yellow rope of the proper length was tied to the rear of the lead snowmobile. In this way, the second snowmobile driver had a reference to determine the proper spacing between the snowmobiles. Five different

pieces of rope were used, one for each distance measured. A picture of the two snowmobiles separated by the length of rope is located in Figure 11.

Meteorological conditions were also measured during Task 2. All equipment was the same as in Task 1. However, it was also necessary to estimate the stability category present during testing. To accomplish this task, the researcher called a ski resort located in the valley to obtain the air temperature 4000 feet above the valley floor (at the top of the mountain). This allowed the stability class to be approximated from the vertical temperature profile.

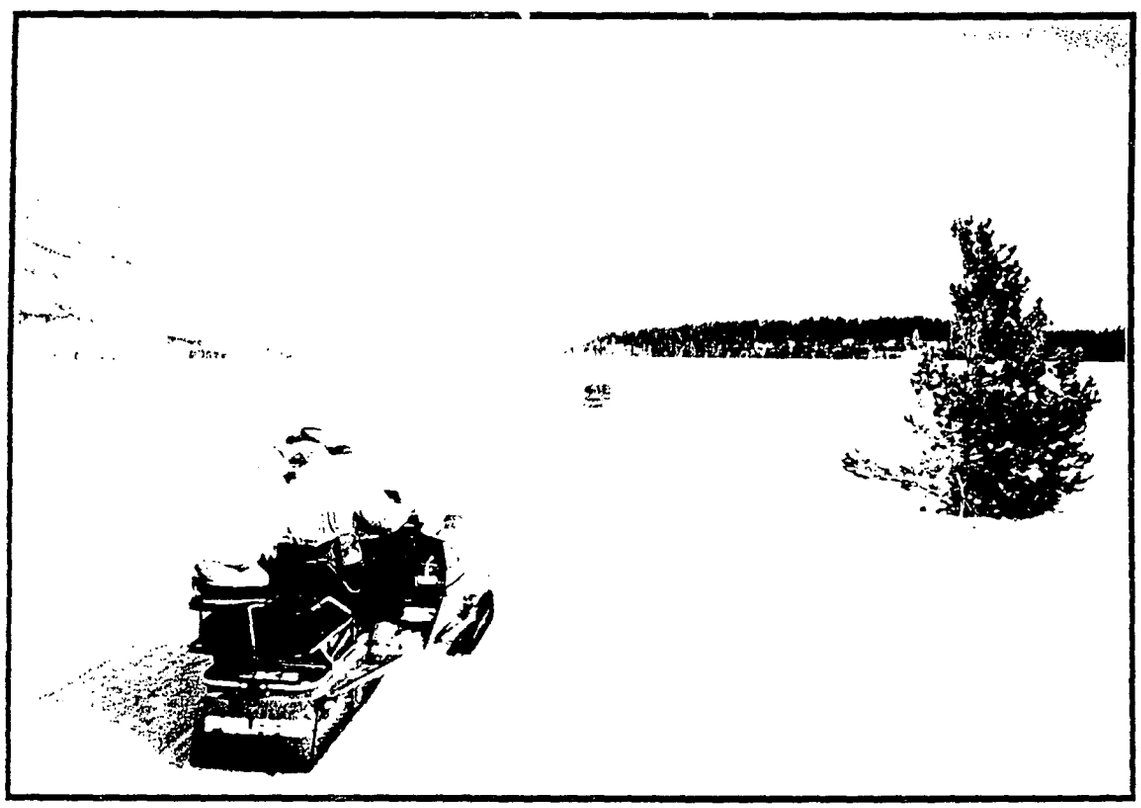

Figure 11 *Picture of Two Snowmobiles During Task 2 Data Collection*

7.3 Task 2 Sample Collection Procedure

Each day before exposure data were taken, the weather conditions were evaluated. If it was windy outside (greater than 2 mph) or if it was too cold (less than 10 degrees F below zero) testing was aborted for that day. It was extremely important to only collect exposure data on stable days. This prevented the wind from "blowing" the exhaust out of the path of the second snowmobile. Extremely cold days were avoided in an effort to prevent the researcher from becoming frostbitten. If the weather looked favorable, the ski resort was called and the temperature at 4000 feet above the valley floor was recorded.

Upon arrival at the test site, meteorological conditions were recorded. These included temperature, wind speed, wind direction, and snow (trail) condition. After the weather conditions were recorded, all equipment was double checked. If everything was satisfactory, both snowmobiles were started and driven to the appropriate location along trail. This allowed both snowmobiles to warm-up and reach standard operating conditions.

Each day of testing, exposure samples were taken at distances of 25, 50, 75, 100, and 125 feet behind the first snowmobile both along the centerline and at 15 feet off-centerline. Speeds of 10, 20, 30, and 40 mph were used. Additionally, exposure samples were taken at each speed without the lead snowmobile. The following procedure was used for each sample:

1. A new sample bag was prepared for collection by attaching it to the researcher and opening its valve.
2. If a new distance was being tested, the rope of the appropriate length was attached to the rear of the lead snowmobile.

3. The bag number, test speed, distance behind the lead snowmobile, centerline/off-centerline position, wind speed, and wind direction relative to the trail were recorded.
4. The pump was activated (flow rate = 1 l/min).
5. The snowmobiles was accelerated to the appropriate speed.
6. The driver of the lead snowmobile signaled that the desired speed was reached.
7. The speed was held constant for one-half of a minute.
8. The pump outlet tubing was attached to the sample bag.
9. The bag was allowed to fill (approximately 2 minutes).
10. The roberts valve on the bag was closed.
11. Both snowmobiles were brought safely to a stop.
12. The sample bag was removed and strapped to the researcher's backpack.

This procedure was used to take all exposure samples. However, when taking the self-exposure samples, the lead snowmobile was not present.

7.4 Task 2 Sample Analysis Equipment and Procedure

The CO in the exposure samples was measured with the Thermo Environmental Instruments Model 48 CO analyzer used for Task 1 analysis. This time, however, the samples did not require dilution. Therefore, the analysis simply required the following steps:

1. Turn on the CO analyzer and allow it to stabilize.
2. Zero the analyzer with zero gas.
3. Calibrate the span of the analyzer using the 20 ppm CO standard.
4. Measure the CO concentration in each of the sample bags with the Model 48 CO analyzer.
5. Clean used sample bags by flushing three times with room air.

A picture of an exposure sample being analyzed is located in Figure 12.

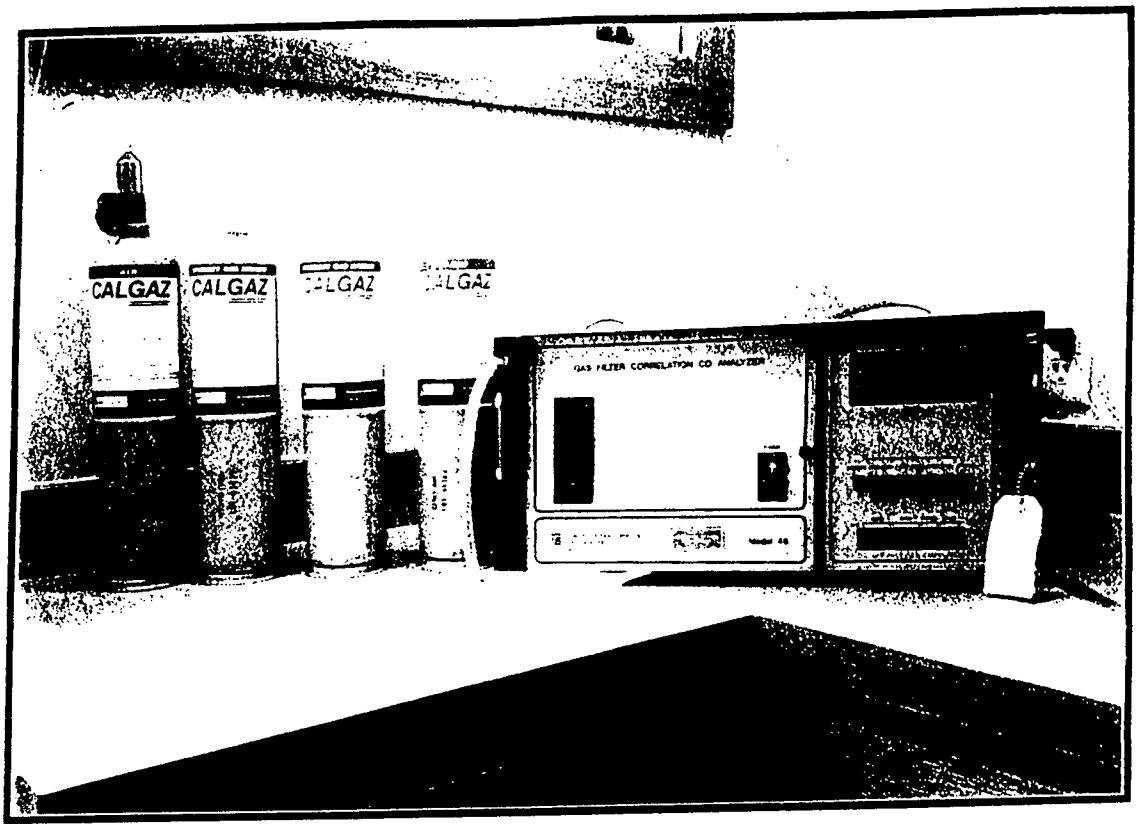

Figure 12 *Picture of Exposure Sample Being Analyzed*

CHAPTER 8

TASK 2: RESULTS AND DISCUSSION OF RESULTS

8.1 Task 2 Self-Exposure Results and Discussion

The concentration of CO which a driver is exposed to from his own snowmobile was measured at speeds of 10, 20, 30, and 40 mph. All of the raw data are located in Appendix F. The final CO self-exposure results (corrected for background CO) are shown graphically in Figure 13. In this graph, the reduced data are represented with a O. The mean of the data at each speed is represented with a ●. Table 3 also lists these results in tabular form.

The average of the CO concentrations from self-exposure at each speed ranged

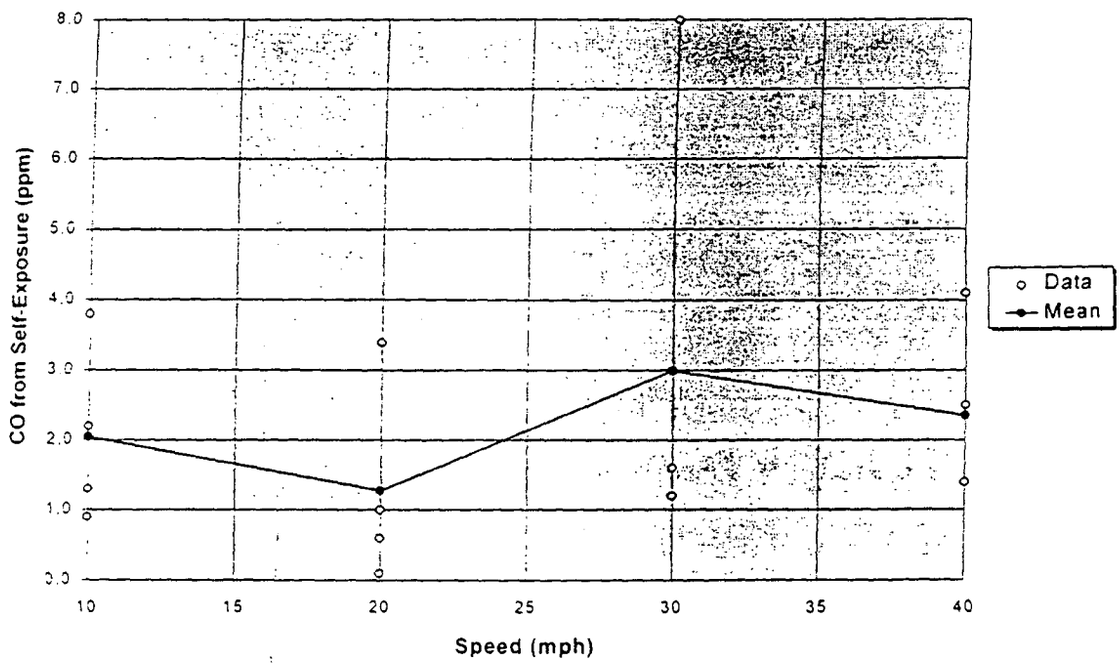

Figure 13 *Graph of CO from Self-Exposure Vs. Snowmobile Speed*

Table 3 *Results of Self-Exposure Testing*

Speed (mph)	Average Corrected CO (ppm) From Self-Exposure	90% Confidence Interval (ppm)
10	2.1	± 1.5
20	1.3	± 1.7
30	3.0	± 3.9
40	2.4	± 1.5

from 1.3 ppm to 3.0 ppm (with an individual data point as high as 8 ppm). The values appear to be independent of speed (when one looks at the 90% confidence interval) and are a significant source of CO exposure.

It is believed that the self-exposure results were influenced by two phenomena. The first being that the exhaust outlet of the snowmobile was located in front of the driver, allowing some of the exhaust to be mixed in such a way as to expose the driver. The second phenomenon believed to influence self-exposure results was the inability of the driver to maintain a constant speed during testing. During testing, the snowmobile driver would actually accelerate and decelerate slightly in an effort to maintain a constant speed. It is believed that while decelerating, the wake could have overtaken the snowmobile, causing exposure to pollution from the snowmobile being ridden. This explains the variability in the data, as the ability to maintain a constant speed varied with each run. Therefore, it is speculated that self-exposure concentrations would be greater if the snowmobiler was either idling or decelerating, rather than running under steady-state conditions.

The means of the concentrations of CO from self-exposure were used (along with the background concentration) to correct all of the remaining data collected during Task 2. Therefore, exposure concentrations reported in the remainder of this chapter represent CO exposure from the lead snowmobile only. Additionally, if one uses the model developed in Chapter 9 to predict total CO exposure, the appropriate self-exposure (based upon speed) should be added to the predicted concentration.

8.2 Task 2 Centerline Exposure Results and Discussion

The concentration of CO to which a driver is exposed as a result of a snowmobile traveling in front of him was measured along the centerline of travel at speeds of 10, 20, 30, and 40 mph and distances of 25, 50, 75, 100, and 125 ft behind the lead snowmobile. All of the raw data are located in Appendix F. The final centerline exposure results are shown graphically in Figure 14. In Figure 14, each value represents the average of 4 to 5 independent tests, as reported in Appendix F.

The data in Figure 14 indicate the following trends. Centerline CO concentrations increased with increasing speed (at the same distance). This is as expected due to the greater amount of CO emitted at higher speeds as well as the reduced time between emission and exposure (possibly resulting in less dispersion). Centerline CO concentrations decreased with increasing distance from the lead snowmobile. This is as would be expected as there is more time for dispersion the further the distance behind the lead snowmobile.

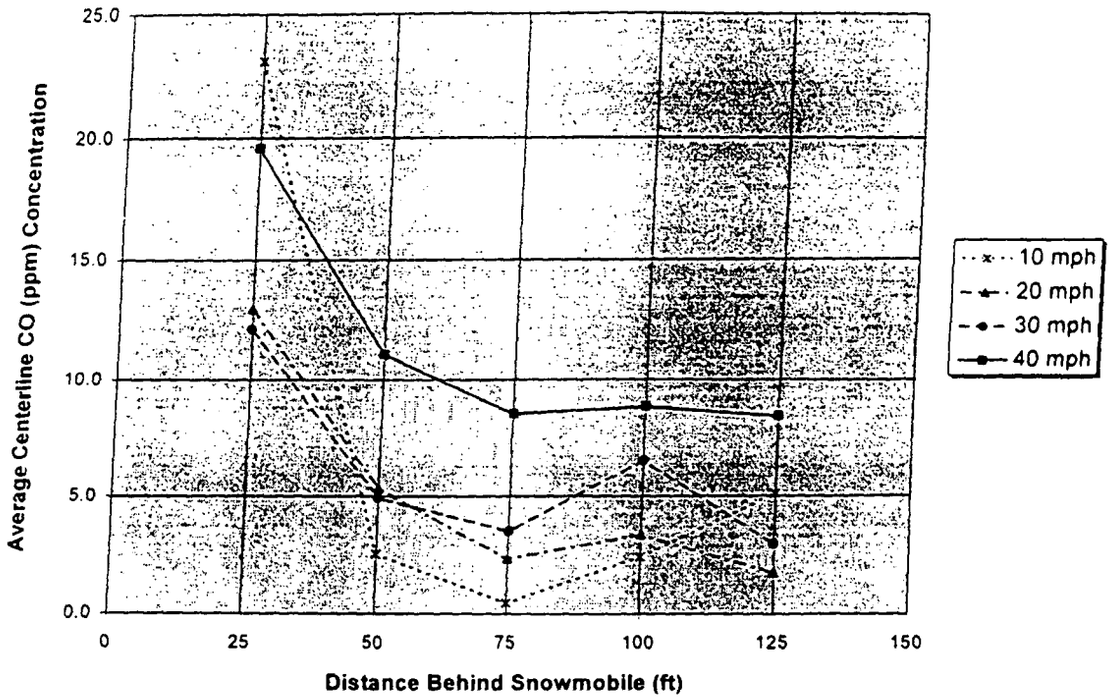

Figure 14 *Graph of Average Centerline CO Exposure*

There do appear to be exceptions to these trends. One exception occurs at 25 ft and 10 mph. Here, the average CO concentration was measured to be higher than the average CO concentrations at faster speeds. This could be attributed to experimental error. Table 4 lists the results of the centerline exposure testing and includes the 90% confidence interval at each speed and distance. At 25 ft and 10 mph, the 90% confidence interval is relatively large (± 10 ppm). Additionally, it was much easier for the driver of the second snowmobile to drive close to the lead snowmobile (25 feet) at 10 mph than at the faster speeds. Therefore, the data at this location may have actually been taken closer to the lead snowmobile than at the higher speeds.

Another exception to the trends occurs at 125 feet and 10 mph., Here, the average CO concentration was measured to be higher than the average CO concentrations at faster

Table 4 *Results of Centerline Exposure Testing*

Speed (mph)	Distance (ft)	Average CO (ppm) Exposure	90% Confidence Interval (ppm)
10	25	23.1	± 10.0
	50	2.6	± 2.7
	75	0.5	± 0.8
	100	2.4	± 4.2
	125	5.1	± 4.2
20	25	13.0	± 4.8
	50	5.4	± 3.6
	75	2.4	± 3.9
	100	3.4	± 1.1
	125	1.8	± 1.5
30	25	12.1	± 1.5
	50	5.0	± 3.5
	75	3.5	± 4.9
	100	6.6	± 5.3
	125	3.0	± 1.7
40	25	19.6	± 7.2
	50	11.1	± 2.4
	75	8.6	± 2.6
	100	8.9	± 3.3
	125	8.4	± 1.6

speeds. This, too, can be attributed to experimental error. The 90% confidence interval for this data point is ± 4.2 ppm. Additionally, it is believed that the wind had more of an influence on this data point than any other. There was more time between snowmobiles at this far distance and slow speed than under any other condition tested.

Finally, there are also several data points which are higher than data measured at the same speed, closer to the snowmobile. It is believed that this can be attributed to experimental error.

8.3 Task 2 Off-Centerline Exposure Results and Discussion

The concentration of CO which a driver is exposed to from a snowmobile traveling in front of him was measured 15 feet off of the centerline of travel at speeds of 10, 20, 30 ,and 40 mph and distances of 25, 50, 75, 100, and 125 ft behind the lead snowmobile. All of the raw data are located in Appendix F. The final off-centerline exposure results are shown graphically in Figure 15. Each value plotted in Figure 15 represents the average of 4 to 5 independent tests, as reported in Appendix F. A summary of these results are also listed in Table 5.

The data in Figure 15 allow the following observations to be made. First, it appears that at speeds of 30 mph and 40 mph, the measured off-centerline CO concentrations were effectively zero at every location. It is this researcher's belief that this occurred because CO measurements were not taken in the wake of the snowmobile. The wake had not had enough time to spread to a distance of 15 feet off-centerline. In order to measure exposure concentrations at 30 mph or 40 mph, samples should have

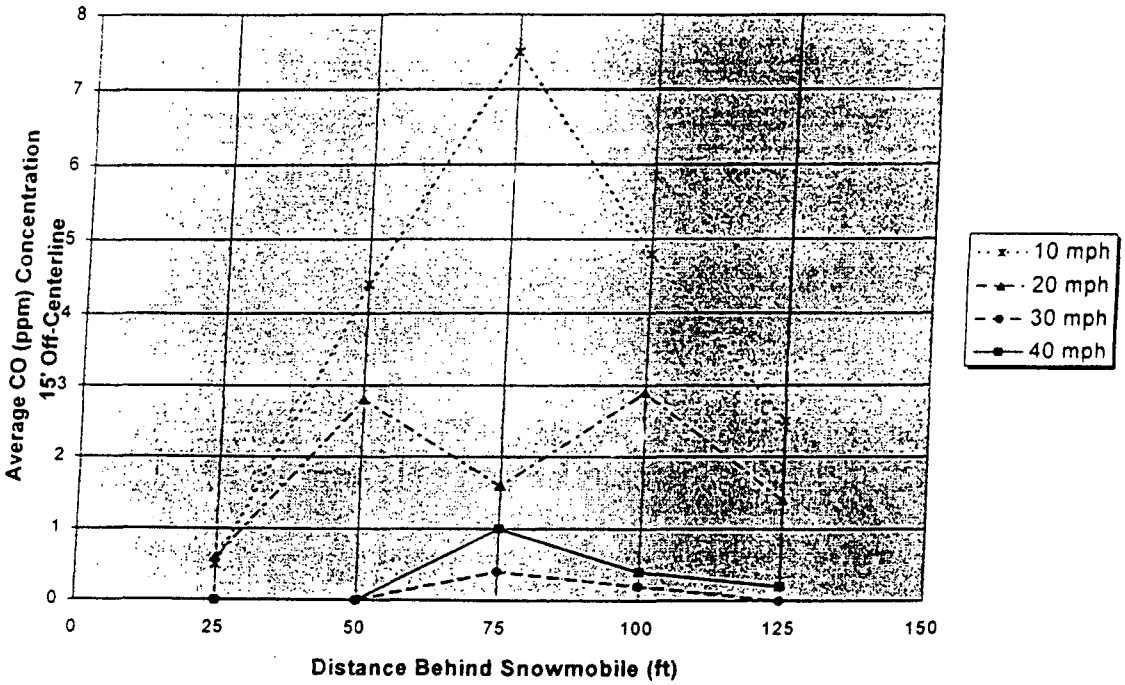

Figure 15 *Graph of Average CO Exposure 15 Feet Off-Centerline*

been taken either closer to the centerline of the lead snowmobile or further away from the lead snowmobile. These data are still useful, however, in model development as they provide information regarding the size and spread of the vehicle's wake.

At speeds of 10 and 20 mph, significant CO concentrations were measured at distances greater than 25 feet behind the lead snowmobile. This is to be expected since for a given separation *distance* there is more *time* separation between the two snowmobiles as the speed decreases. This increased time increases the distance that the wake can be transported off-centerline by the wind and would allow more wake dispersion to take place.

Table 5 *Results of Exposure Testing 15 Feet Off-Centerline*

Speed (mph)	Distance (ft)	Average CO (ppm) Exposure	90% Confidence Interval (ppm)
10	25	0.5	± 0.9
	50	4.4	± 3.4
	75	7.5	± 15.8
	100	4.8	± 7.1
	125	2.5	± 5.6
20	25	0.6	± 0.7
	50	2.8	± 2.6
	75	1.6	± 1.4
	100	2.9	± 5.6
	125	1.4	± 1.8
30	25	0	± 0.4
	50	0	± 1.2
	75	0.4	± 1.7
	100	0.2	± 1.2
	125	0	± 0.6
40	25	0	± 0.9
	50	0	± 0.7
	75	0.7	± 1.2
	100	0.1	± 1.9
	125	0.2	± 0.4

It should also be noted that at 10 and 20 mph the off-centerline CO concentrations were comparable to the corresponding centerline CO concentrations at distances greater than 25 feet (when considering the 90% confidence interval). This supports the idea that the concentrations observed at 10 and 20 mph off-centerline were caused by bulk transport of the wake, rather than by atmospheric dispersion.

8.4 Task 2 Photographic Data and Discussion

A visual representation of the snowmobile's wake was obtained on video tape at both 10 mph and 40 mph. This was accomplished by placing a smoke bomb in a small container at the rear of the snowmobile. The snowmobile was then driven at a constant speed (of both 10 and 40 mph) while being video taped.

An analysis of the video tape indicated that the size of the wake at 10 mph and the size of the wake at 40 mph were of the same magnitude. However, the smoke was much harder to see at 40 mph (the smoke emitted per unit distance traveled at 10 mph was 4 times that at 40 mph). The initial height of the wake was around 0.5 meters at both 10 mph and 40 mph. The wake then grew very slowly, never reaching a height greater than 1.5 m (within 100 feet behind the lead snowmobile). A picture of the snowmobile's wake at 10 mph is located in Figure 16.

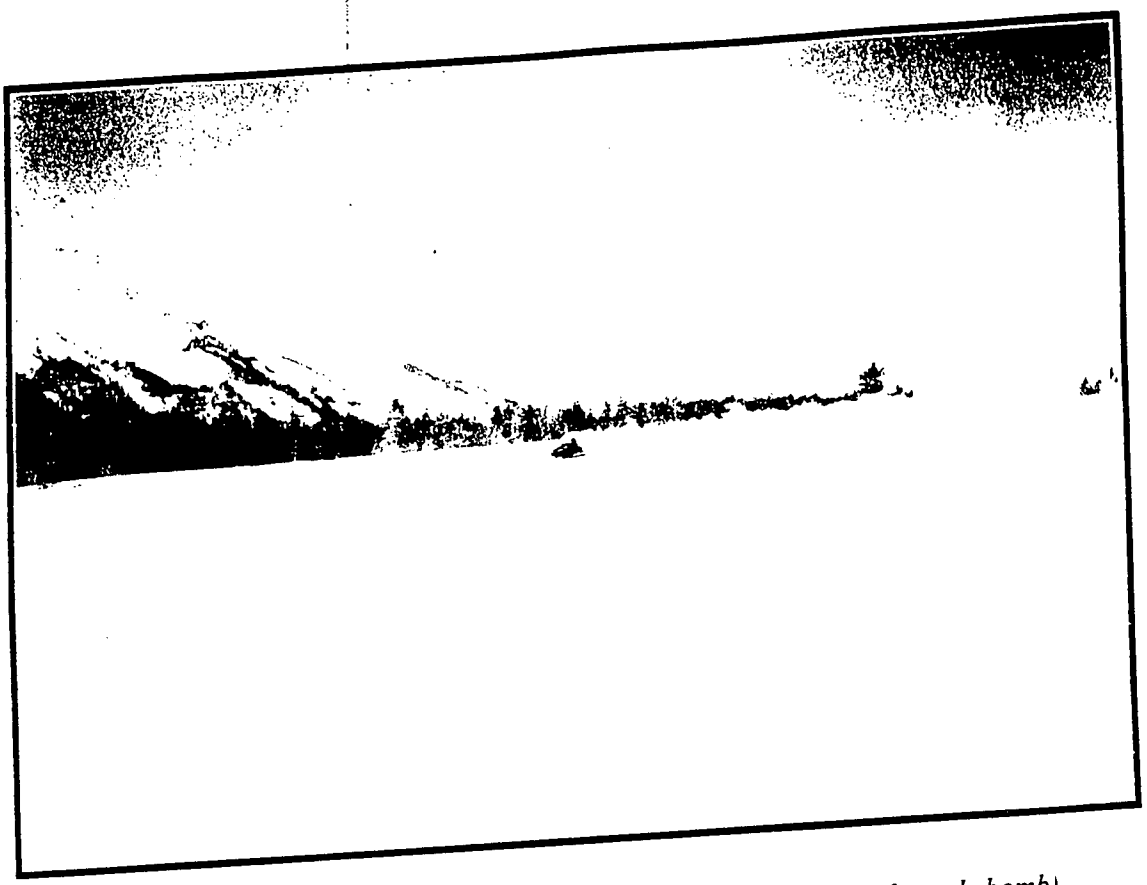

Figure 16 *Picture of Snowmobile Wake at 10 mph (simulated with smokebomb)*

CHAPTER 9

TASK 3: MODEL DEVELOPMENT

9.1 Purpose of Task 3

The purpose of Task Three was to develop a model which could be used to predict exposure to CO (or other pollutants) while traveling in the wake of another vehicle. As it was desired for the model to accurately represent physical reality, three phenomena were observed/contemplated prior to model development. These included the size and shape of the wake as a function of distance behind the snowmobile, the distribution of pollutants along the snowmobile's path of travel, and the distribution of pollutants within a cross-section of the wake.

9.2 Observations Regarding the Wake Size and Shape

As discussed in Section 8.4, visual analysis of the snowmobile's wake allowed several general conclusions to be drawn. First, there was no significant difference in the size of the wake between 10 mph and 40 mph. This is consistent with Equations 3.3 and 3.4 in the Literature Review. Both of these equations express the radius (or height) of the wake as a function of distance, not vehicle speed. Therefore, it is expected that the radius/size of the wake grows as a function of distance behind the snowmobile, but independent of the speed of the snowmobile.

Visual analysis also revealed that the height of the wake started at approximately 0.5 m and grew very slowly. The height of the wake remained below 1.5 meters as far as was visually recorded (approximately 100 feet behind the snowmobile). Therefore, growth of the wake was on the order of 1 meter of height/100 feet behind the lead snowmobile. This growth rate is much smaller than would be predicted using standard Gaussian dispersion curves. Even under the most stable conditions (F stability...which is valid only at night) CALINE3 predicts that σ_Z will grow from approximately 1.1 meters (1 foot downwind of the source) to 4.5 meters (101 feet downwind from the source). Assuming that the height of the wake is equal to $2.15\sigma_Z$, CALINE3 predicts a *minimum* growth of 7.3 meters over a distance of 100 feet. Clearly, this is not the case. The actual growth of the wake is less than 1/7 of this *minimum* predicted value. Therefore, it is concluded that at the distances of interest (x less than 125 feet) the growth of the wake is dominated by wake induced turbulence, not atmospheric dispersion, in the sense that one would normally apply dispersion.

Exposure measurements taken off-centerline at 30 and 40 mph clearly indicate that the wake does not grow enough to allow measurement of CO 15 feet off-centerline at distances less than 125 feet from the lead snowmobile. However, CO measurements *were* obtained at both 10 and 20 mph, 15 feet off-centerline. This may be explained by one of two phenomena. Either the size of the wake is dependent upon snowmobile speed or some other factor was transporting the wake off-centerline at slower speeds. Because both the visual data and the literature indicate that the growth of the wake *is* a function of

distance, it can only be concluded that some other factor was causing CO to be measured 15 feet off-centerline at 10 and 20 mph.

It is believed that this other factor was the wind. At slower speeds, the wind has more time to transport the wake off-centerline (as a function of distance behind the snowmobile) than at higher speeds. This general phenomenon is illustrated in Figure 17.

More specifically, the wind speed ranged from 0 to 2 m/s and averaged about 1 m/s during testing. Assuming that the wind is blowing perpendicular to the path of the snowmobile (a worst case displacement situation), the distance off-centerline (y) that the wind could transport the wake (at distance x behind the snowmobile) is calculated from the following equation:

$$y = \frac{ux}{V_c} \tag{9.1}$$

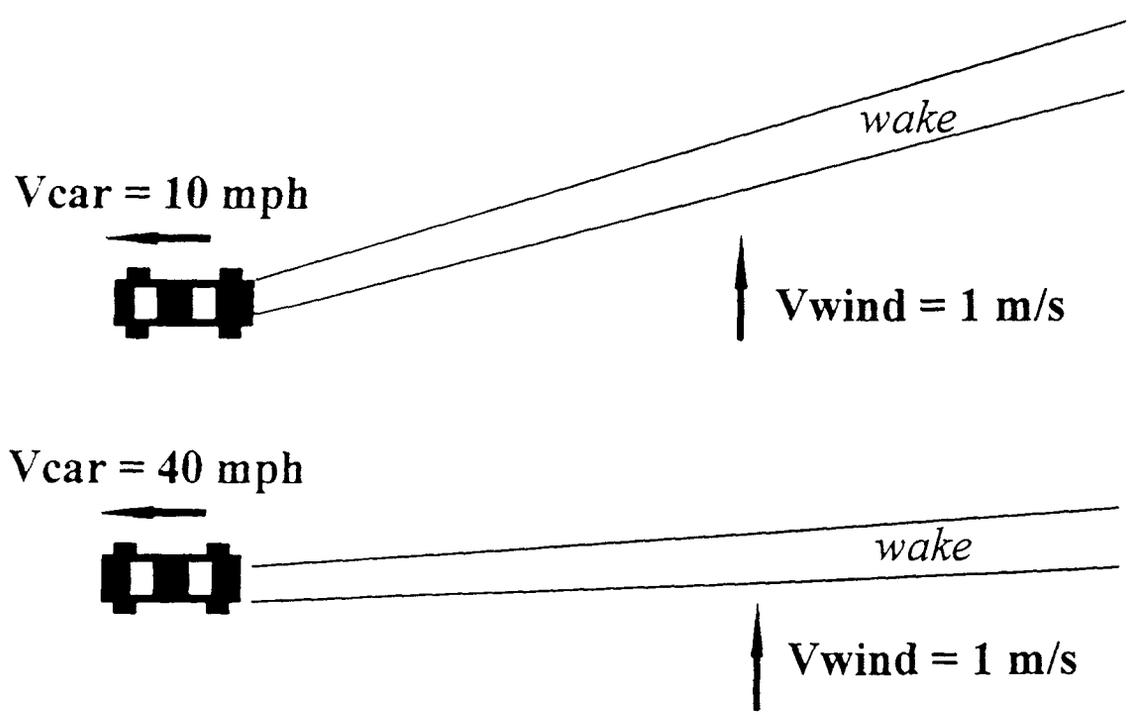

Figure 17 *Representation of the Effect of Wind at Different Vehicle Speeds*

where y is the distance off-centerline, u is the windspeed, V_V is the speed of the snowmobile and x is the distance behind the snowmobile. Assuming that u=1 m/s and x=125 feet, y is calculated at 28, 14, 7, and 3.5 feet at speeds of 10, 20, 30, and 40 mph respectively. Therefore, when the windspeed was 1 m/s and perpendicular to the direction of travel, the wind would have been able to transport the wake more than 14 feet off-centerline (125 feet behind the lead snowmobile) at speeds of 10 and 20 mph but not at speeds of 30 or 40 mph. This is the trend indicated by the exposure measurements. Therefore, evidence indicates that CO concentrations measured 15 feet off-centerline at 10 and 20 mph may have been influenced primarily by bulk transport of the wake by wind, rather than by the growth of the wake itself.

Additionally, if one considers that models in the literature consider a vehicle's wake as semi-circular in cross section (height=2*width), and that the height of the wake remained less than 1.5 meters (less than 100 feet behind the snowmobile), it seems logical to conclude that the width of the snowmobile's wake remained less than 3 meters (at distances less than 100 feet behind the snowmobile). Three meters is approximately 10 feet. Therefore, this coincides with a growth of 5 feet off-centerline (much less than 15 feet). This supports the conclusion that at 10 and 20 mph the wake of the snowmobile did not grow to a distance of 15 feet off-centerline, but was likely transported there by the wind.

Finally, the off-centerline concentrations measured at 10 and 20 mph are comparable to the corresponding centerline values (at distances greater than 25 feet) when one takes into account the 90% confidence intervals of the means. This further

supports the idea that bulk transport is responsible for the observed off-centerline concentrations at 10 and 20 mph (otherwise, the off-centerline values would be less than the centerline values).

As a result of these observations, it is concluded that the size of the wake should meet the following criteria if the model is to accurately represent physical reality. First, the size of the wake must vary as a function of distance behind the snowmobile. Second, at distances less than 100 feet behind the snowmobile, the height of the wake must remain less than 1.5 meters (5 feet). And third, at distances less than 125 feet behind the snowmobile, the half-width of the wake must not be greater than 4.5 meters (15 feet).

9.3 Observations Regarding the Distribution of Pollutants Along the Path of Travel

Visual data regarding the wake of a snowmobile indicated that the smoke in the wake became less visible (more diluted) at higher speeds even though the size of the wake was the same. Therefore, dilution of pollution in the wake increased with increasing speed. Phrased another way, the pollutant concentration in the wake is inversely related to the speed of the snowmobile for constant pollutant release rates.

This phenomena is illustrated best by Figure 18. Figure 18 shows two vehicles both with a hypothetical emission rate of 4●/sec. One of the vehicles is traveling at a speed of 1 box/second while the other is moving at 4 boxes/second. It is clear that the number of ●s that are left in each box is inversely proportional to the speed of the vehicle.

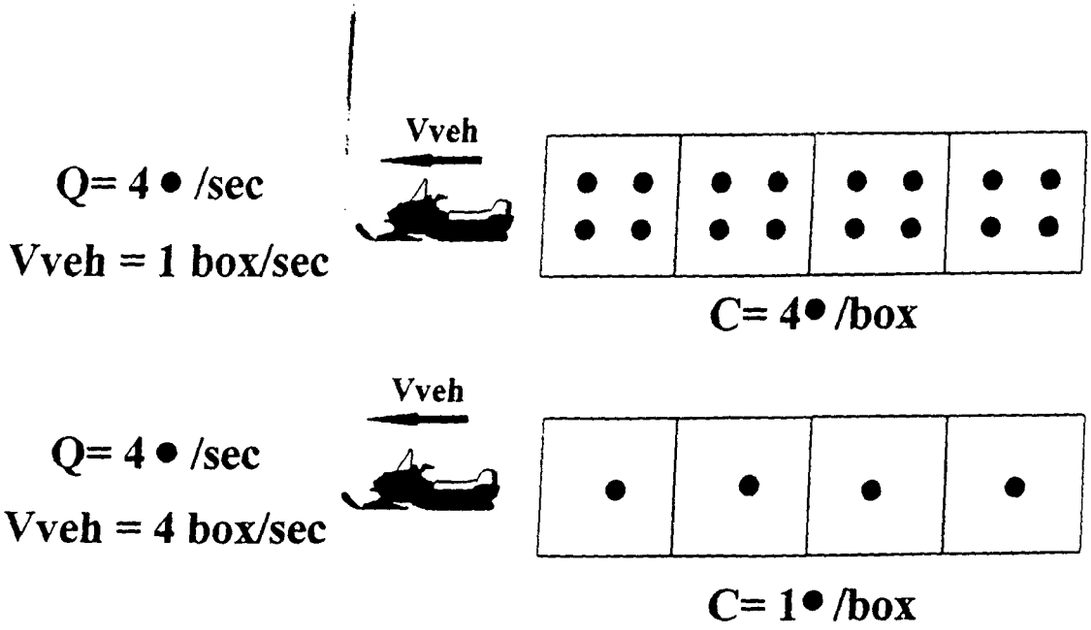

Figure 18 *Representation of the Relationship Between Concentration and Vehicle Speed*

Now, let us imagine that the boxes themselves can move (at a speed slower than the vehicles). Figure 19 illustrates this situation. In Figure 19, both vehicles are traveling at 4 boxes/second and have an emission rate of 4●/sec. However, one of the vehicles drives in front of fixed boxes while the other drives in front of boxes moving with a velocity of 1 box/second. This illustrates the fact that the number of ●s that are left in each box is inversely proportional to the relative velocity between the vehicle and the box.

It is this scenario which is analogous to the distribution of pollution along the travel path in the wake of a snowmobile. The snowmobile itself is moving, leaving behind pollutant concentrations which are inversely proportional to its speed (if the source strength is constant). However, the snowmobile is also imparting momentum to the air it travels through, causing the wake itself to have a velocity (this corresponds to

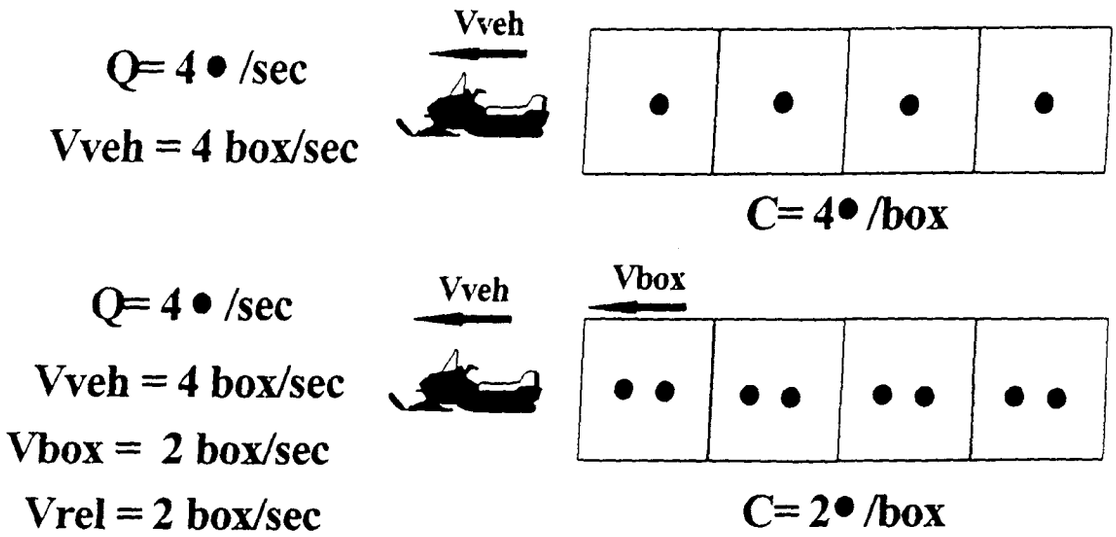

Figure 19 *Representation of the Relationship Between Concentration and Relative Velocity*

the moving boxes in the analogy). Therefore, for the model to accurately represent physical reality, the concentration of pollution in the wake of the vehicle should be inversely proportional to the relative velocity between the snowmobile and its wake. One should note that the velocity of the wake is a function of distance and approaches zero with increasing distance behind the snowmobile. Therefore, far behind the snowmobile, the concentration of pollution in the wake reduces to an inverse relationship with the speed of the snowmobile only.

9.4 Thoughts on the Pollutant Distribution In a Cross-Section of the Wake

If the conclusions regarding the spread of the wake are correct (i.e. measurements obtained at 10 and 20 mph. 15 ft off-centerline were from bulk transport of the wake due to wind), there were no CO measurements taken to provide an estimate of the pollutant

distribution across a cross-section of the wake. Only centerline concentrations were measured in the wake itself.

Therefore, an appropriate method for modeling the pollutant distribution in a cross-section of the wake must be based solely upon good engineering judgment. However, the following evidence does exist: the growth of the wake was dominated by turbulence and not atmospheric dispersion, the growth of the wake was very slow, and mixing/swirling in the wake of the snowmobile was observed visually. Therefore, it is believed that wake-induced turbulence caused significant mixing of pollution in the wake. In addition, the second snowmobile also had the opportunity to cause further mixing. Because of this observed mixing, the most appropriate assumption regarding the distribution of pollution in a cross-section of the wake is that the pollution is distributed uniformly. In other words, the concentration of the pollutant of interest is constant across a cross-section of the wake. This is the best assumption that can be made with the available data.

9.5 Model of Exposure in the Wake of the Snowmobile

A model which predicts exposure to pollution while traveling in the wake of a snowmobile which satisfies the all of the observations described in Sections 9.2, 9.3, and 9.4 is represented by the following equation:

$$C = \frac{Q}{(V_s - V_w) A_w} \tag{9.2}$$

where C is the concentration in mass/volume, Q is the emission rate in mass/time, V_V is the velocity of the snowmobile, V_W is the velocity of the wake (a function of x), A_W is the cross-sectional area of the wake (a function of x), and x is the distance behind the snowmobile. This model basically represents the concentration as a mass flow rate (Q) per unit volume flow rate (velocity*A_W).

If a cross-section of the wake is modeled as semicircular in area (as stated in the literature), Equation 9.2 becomes:

$$C = \frac{Q}{(V_V - V_W)\left(\frac{\pi R_W^{\,2}}{2}\right)} \tag{9.3}$$

where R_W is the radius of the wake (a function of x).

Equation 3.2 in the Literature Review is a simple equation for V_W. Substituting this into Equation 9.3 and manipulating algebraically gives the following:

$$C = \frac{2Q}{V_V(\pi R_W^{\,2} - C_D A_V)} \tag{9.4}$$

where C_D is the coefficient of drag and A_V is the frontal area of the snowmobile. This equation represents one possible model which can be used to predict exposure to pollution while traveling in the wake of a vehicle. All quantities are known except for R_W as a function of distance behind the snowmobile. Equations 3.3 and 3.4 should not be used to estimate R_W as they do not account for the effect the second snowmobile has on the spread of the wake. Therefore, an equation for the radius of the wake as a function of distance behind the snowmobile which accounts for the effect of the second snowmobile must be determined empirically from the available data.

It should be noted that the model expressed by Equation 9.4 was developed under the assumptions that the effects of wind and atmospheric dispersion are negligible.

9.6 Effective Radius of the Wake as a Function of Distance Behind the Snowmobile

As mentioned in the previous section, a relationship describing the radius of the wake as a function of distance behind the lead snowmobile is required in order to use Equation 9.3 to predict exposure to pollution while traveling in the wake of a snowmobile. Therefore, the data obtained in Tasks 1 and 2 were used along with Equation 9.5 to determine this relationship empirically. Rearranging Equation 9.4 and solving for the radius of the wake:

$$R_W = \left[\frac{2}{\pi}\left(\frac{Q}{C V_V} + \frac{C_D A_V}{2}\right)\right]^{1/2} \tag{9.5}$$

where all variables are as previously defined. The frontal area of the snowmobile used for during testing was approximately 1.3 m^2. There is no published information regarding the coefficient of drag for a snowmobile, but a good estimate is around 0.5 (this is based on the fact that the most streamlined automobile has a C_D of 0.3 and that flat-faced antique cars have a C_D of 0.9) (White, 1986).

These estimates, along with the data collected in Tasks 1 and 2 were used to solve for the radius of wake the at each centerline sample taken. It should be noted that radii were not calculated for centerline values which were equal to zero (it is clear that the wind had blown the wake out of the path of the second snowmobile). It should also be noted that radii were calculated for all other measured concentrations (even those which

were relatively small). Therefore, the empirical relationship for the radius of the wake may not necessarily represent the true wake radius. It will, however, be useful for determining actual exposure to pollution in the wake of a snowmobile.

The calculated values of R_W were plotted on a graph as a function of distance behind the lead snowmobile. This graph is shown in Figure 20. Note that the empirical values for the radius of the wake vary by a factor of 2 to 3. At first glance, this variation appears large. However, when viewed within the context of other air pollution work this magnitude of variation is common/acceptable. For example, Turner's values of σ_Z are expected to be correct only within a factor of 2 (Turner, 1970).

The power law approximation for R_W which yields the desired modeling results is

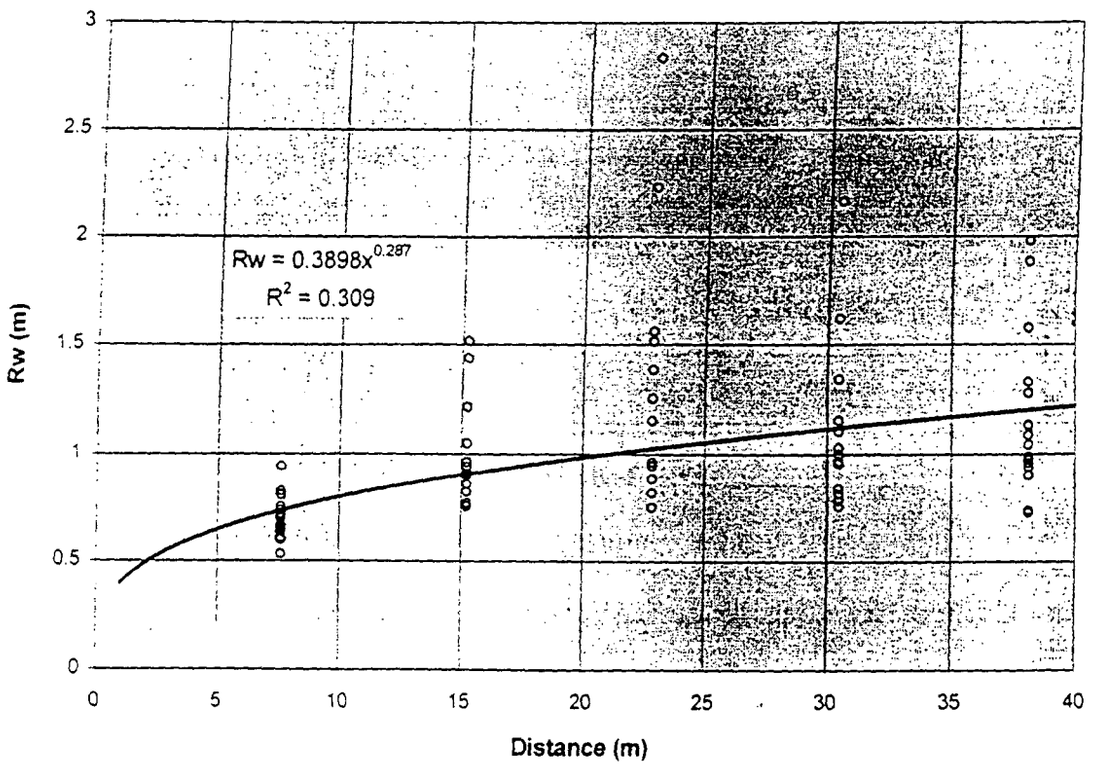

Figure 20 *Graph of Effective Wake Radius Calculated from Experimental Data vs. Distance Behind the Lead Snowmobile*

given by:

$$R_W = 0.3898x^{0.287} \tag{9.6}$$

where R_W and x are in meters. Also, x should be greater than or equal to 7.6 m (25 ft). This is important as Equation 9.6 is not mathematically correct at distances close to the snowmobile (made obvious by the fact that the wake radius is calculated to be zero at the snowmobile).

Recall that the Literature Review revealed that the height of the wake is, in theory, proportional to $x^{0.25}$ (Equation 3.4). The empirical relationship determined for the radius of the wake (as described by Equation 9.6) states that the radius of the wake is proportional to $x^{0.287}$. Thus, the empirically determined relationship is in reasonable agreement with wake theory. The only difference is that the empirical relationship predicts a slightly faster growth rate of R_W than does the wake theory. It is believed that this discrepancy can be attributed to turbulence caused by the second snowmobile.

Again it should be noted that Equation 9.6 should be used only for distances greater than or equal to 7.6 meters (25 feet). Additionally, the atmosphere should be stable, with a windspeed less than 2 m/s.

9.7 Summary

In conclusion, a model to predict exposure to pollution while traveling in the wake of a snowmobile which accurately represents physical reality is described by Equation 9.5. The model is valid only under stable atmospheric conditions with windspeeds less than 2 m/s. The effect of wind direction is neglected in the model. The

model requires information regarding the size of the wake as a function of distance behind the snowmobile. An empirical relationship for the effective wake radius is described by Equation 9.6. The performance of the model is investigated in Chapter 10.

CHAPTER 10

TASK 3: MODEL PERFORMANCE

10.1 CO Exposure Predicted by the Model

The model described by equations 9.4 and 9.6 was used to predict exposure to CO while traveling in the wake of another snowmobile. Concentrations were calculated at distances of 25, 50, 75, 100, and 125 feet and speeds of 10, 20, 30, and 40 mph. The steady-state emission factors measured in Task One were used as the source terms (99, 211, 324, and 795 g/hour at speeds of 10, 20, 30 and 40 mph, respectively). The frontal area of the vehicle was estimated to be 1.3 m^2 and the coefficient of drag of the snowmobile was estimated at 0.5. Figure 21 shows a graph of the predicted CO concentrations as a function of speed and distance behind the lead snowmobile. Concentrations were predicted at speeds of 10, 20, 30, and 40 mph at distances of 25, 50, 75, 100, and 125 feet. These are the same speeds and locations at which exposure measurements were taken during Task 2. The model predicts that the concentration increases with increasing vehicle speed (due to the larger source term) and that the concentration decreases with distance from the snowmobile (due to the increasing size of the wake).

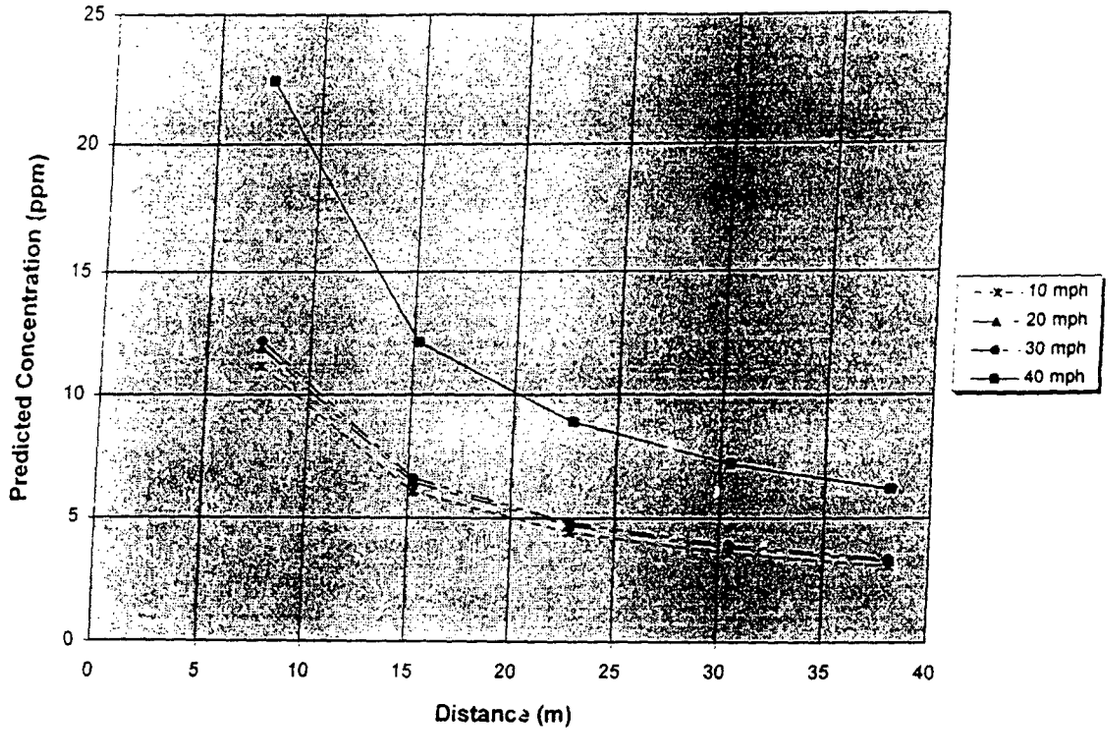

Figure 21 *Graph of Predicted CO vs. Speed and Distance Behind the Lead Snowmobile*

10.2 Comparison of Predicted Exposure to Actual Exposure

A scatter plot of the CO exposure predicted by the model versus all of the measured CO data (for each speed and location) is located in Figure 22. The line drawn on the plot indicates the best fit of the data. If, on average, the model were to accurately predict exposure to CO, the slope of this line would be one. The equation of the best fit is:

$$C_{MEASURED} = 1.05 C_{PREDICTED} \qquad (10.1)$$

Therefore it may be concluded that, on average, the model predicts the measured exposures within 5%.

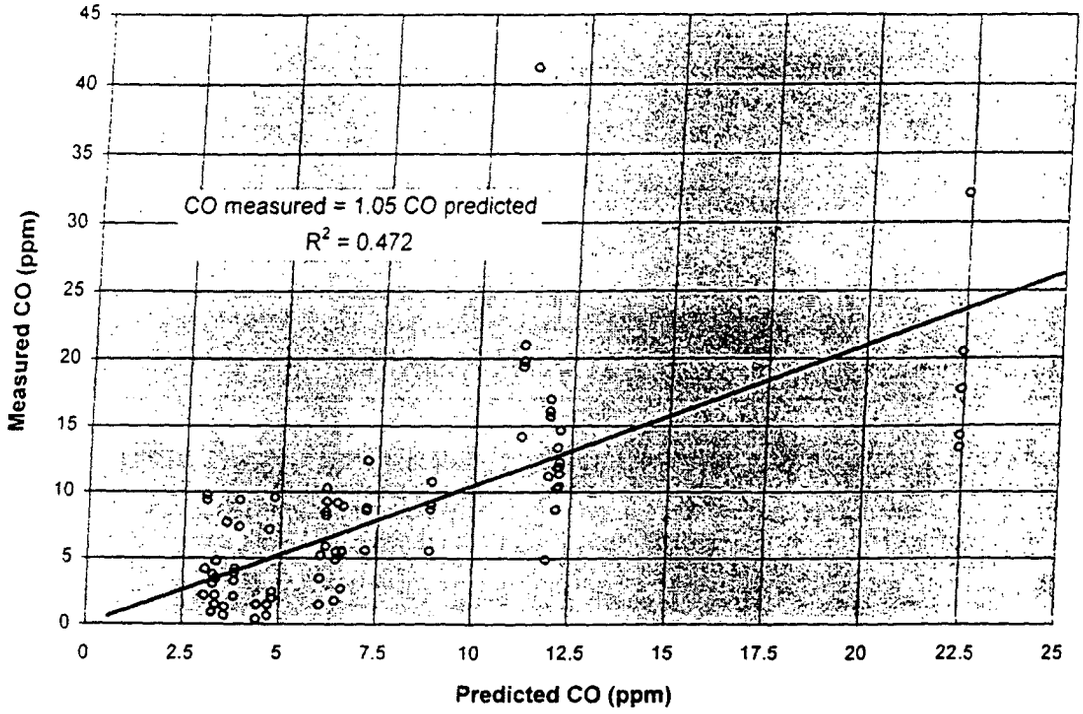

Figure 22 *Scatterplot of Measured CO Exposure vs. Predicted CO Exposure*

An examination of the scatter plot also shows that the data varies by a factor of around 2-3 (and by a factor of four for a few data points). Therefore, CO predictions made by the model should only be expected to be valid only within a factor of 3 or so. This is along the lines of performance of other air pollution models. For example, Gaussian dispersion predictions using Turner's sigma's are only expected to be correct within a factor of 3 (Turner 1970).

Another method of evaluating the performance of the model is to examine its predictions relative to the average measured exposure at each speed and distance. Table 6 provides such a comparison. Listed in Table 6 are the CO concentrations predicted by the model, the average of the CO concentrations measured during Task 2, and the 90%

Table 6 *Comparison of Predicted CO to Average Measured CO*

Speed (mph)	Distance (ft)	Predicted CO Exposure (ppm)	Average CO Exposure (ppm)	90% Confidence Interval (ppm)
10	25	**11.2**	23.1	± 10.0
	50	**6.0**	2.6	± 2.7
	75	**4.4**	0.5	± 0.8
	100	3.6	2.4	± 4.2
	125	3.1	5.1	± 4.2
20	25	11.9	13.0	± 4.8
	50	6.4	5.4	± 3.6
	75	4.7	2.4	± 3.9
	100	3.8	3.4	± 1.1
	125	3.3	1.8	± 1.6
30	25	12.2	12.1	± 1.5
	50	6.6	5.0	± 3.5
	75	4.8	3.5	± 4.9
	100	3.9	6.6	± 5.3
	125	3.4	3.0	± 1.7
40	25	22.4	19.6	± 7.2
	50	12.1	11.1	± 2.4
	75	8.9	8.6	± 2.6
	100	7.2	8.9	± 3.3
	125	6.2	8.4	± 1.8

confidence interval of the mean of the measured CO concentrations. Predicted CO concentrations which fall outside of the 90% confidence interval of the average measured concentrations are indicated in bold.

An examination of the data listed in Table 6 shows that only three out of twenty predictions fall outside of this confidence interval of the mean. Additionally, all of those which do fall outside of the 90% confidence interval of the mean appear to be attributable to experimental error or anomalies in the measured data (refer to Section 8.2).

10.3 Model Performance at Distances Close to the Snowmobile

The model described by Equations 9.4 and 9.6 is not mathematically correct at distances close to the snowmobile. Therefore, in no case should it be used to estimate driver exposure to pollution at distances close to the snowmobile which were not validated by experimental data (less than 25 feet). This is caused by two factors. First, the empirical relationship determined for the radius of the wake is not mathematically correct at distances close the snowmobile. Recall that Equation 9.6 predicts a wake radius of zero at the snowmobile, which is clearly not the case. Second, the equation used by the model to determine the velocity of the wake (Equation 3.2) was derived for the case of $x>>R_W$ close to the vehicle. Therefore, it does not accurately estimate the wake velocity close to the snowmobile. This can be seen clearly in Figure 23.

Figure 23 contains a graph of the ratio of the wake velocity to the snowmobile velocity as a function of distance as determined by Equation 3.2. At distances close to the snowmobile, this ratio is greater than one. In other words, the model predicts a wake

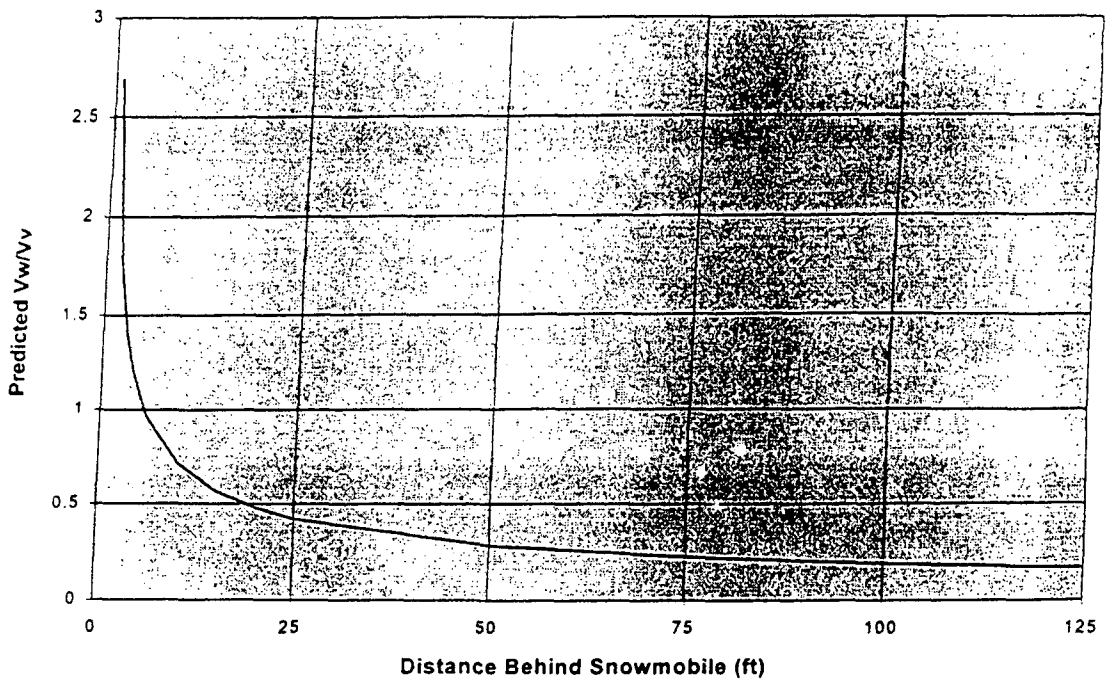

Figure 23 *Graph of Wake Velocity/Snowmobile Velocity Versus Distance Close to the Snowmobile*

velocity which is greater than the snowmobile velocity at distances close to the snowmobile. Clearly, this is not possible. Therefore, the model must not be used to predict concentrations close to the snowmobile.

This point may be further illustrated by using the model to calculate exposure at distances less than 25 feet behind the lead snowmobile. This is shown in Figure 24 (where all inputs are as in Section 10.1 except for distances). An examination of Figure 24, shows that the model predicts both negative concentrations and unrealistically high concentrations at distances close to the snowmobile. Therefore, it is clear that model usage must be limited to distances where x is large relative to the radius of the wake (as a general rule, x should be at least an order of magnitude greater than R_W).

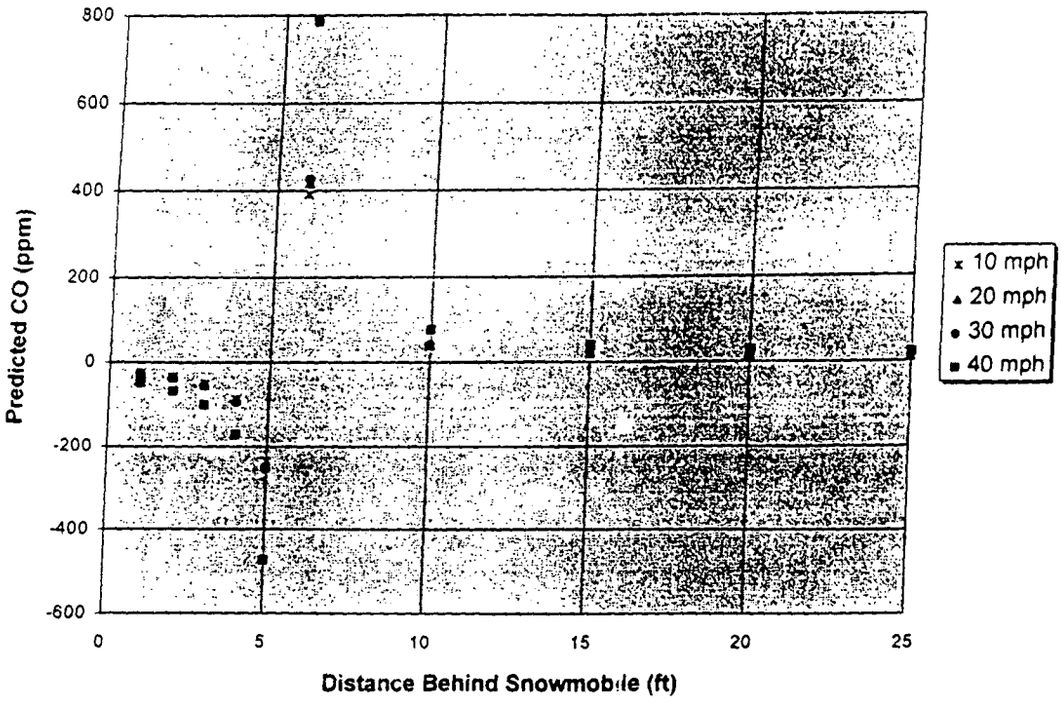

Figure 24 *Graph of Predicted Concentration Close to the Snowmobile*

10.4 Summary of Model Performance

A comparison of the model's predictions to the measured exposures indicates that the model adequately predicts exposure to pollution within the wake of a snowmobile at the speeds and distances considered in the project. The trends predicted by the model are the same as observed in field measurements. Predicted pollutant concentrations are expected to be correct within a factor of 3. The model is not valid and must not be used at distances close to the snowmobile ($x < 25$ feet).

CHAPTER 11

CONCLUSIONS AND IMPLICATIONS

11.1 Conclusions

As a result of this research, valuable information has been gained regarding the emission of CO from a snowmobile under steady-state conditions, regarding exposure to CO while riding in a wake of a snowmobile under steady-state conditions, and regarding an appropriate method to model this exposure.

Steady-state emission measurements of CO indicated that the snowmobile's CO emissions ranged from 9.9 g/mile at 10 mph to 19.9 g/mile at 40 mph. When one compares these values to tailpipe emissions from a modern automobile (0.01 to 0.04 g/mile) (Sluder, 1995), it is easy to see that the snowmobile used in this study emits significantly more CO under steady-state conditions than does a modern automobile.

Average exposure measurements taken at distances between 25 and 125 feet behind the lead snowmobile and at speeds ranging from 10 to 40 mph were as high as 23 ppm. with individual measurements as high as 45 ppm. The 1-hour National Ambient Air Quality Standard for CO is 35 ppm and the 8-hour National Ambient Air Quality Standard for CO is 8 ppm. When one considers that snowmobilers may travel behind more than one snowmobile for sustained intervals (three hours), it is clear that significant exposure to CO may occur while traveling on a snowmobile trail.

A simple model to predict exposure to CO while traveling in the wake of a snowmobile was developed for stable atmospheric conditions. This model neglects the effect of wind. It is expected that predictions will be correct within a factor of three if the speed of interest is between 10 and 40 mph and if the distance of interest is between 25 and 125 feet. No information regarding the performance of the model under other atmospheric conditions or at other speeds and distances is available. The model must not be used to predict exposure at distances close to the first snowmobile.

It may be possible to use the model to predict exposure to CO while traveling in the wake of multiple snowmobiles. This would simply be done by superposition. However, no data has been collected to verify the validity of this approach.

11.2 Implications

The major implication of this research is that it is possible for snowmobilers to be exposed to significant concentrations of CO if traveling on a snowmobile trail either behind a number of snowmobiles or for an extended period of time. However, it may be possible to decrease one's exposure by traveling off-centerline and upwind of other snowmobiles.

11.3 Recommendations for Future Study

It is recommended that further research be performed to allow the model to predict exposure to pollution under atmospheric conditions other than stable and at higher wind speeds. This will allow scenarios other than the worst-case to be evaluated.

It is also recommended that the empirical relationship for the radius of the wake be investigated in order to more firmly ground the model in physical reality as well as to allow the model to be used for any type of vehicle (not just snowmobiles). The effect of atmospheric stability on the growth of the wake (if any) should also be investigated.

This study focused only on CO emissions from a snowmobile. It is recommended that tests be performed in an effort to characterize steady-state emission values for UHCs from snowmobiles. This will allow the model developed in the research to be used to predict exposure to UHCs while traveling in the wake of a snowmobile.

Steady-state self-exposure results measured in this research were higher than expected and were a significant source of driver exposure to CO. It believed that self-exposure becomes even more significant if the snowmobile is idling or decelerating. Therefore, it is recommended that self-exposure measurements be taken under deceleration and while idling.

It is expected that superposition may be used to predict exposure when traveling behind multiple snowmobiles. However, there is not data to verify this. Therefore, it is recommended that further research be done to investigate the model's ability to predict exposure when traveling behind multiple snowmobiles.

Finally, it is recommended that non-steady-state emissions be investigated for both UHCs and CO. As shown in this study, emissions under acceleration were nearly three times greater than at 40 mph under steady-state conditions. This indicates that substantially greater exposure could occur under non-steady-state conditions.

REFERENCES

REFERENCES

Associated Press, "'Biler's Spending Lots of Time, Bucks in Wyoming," *Jackson Hole Daily*, February 6, 1995.

Beaton, J.L., Ranzieri, A.J., Shirley, E.C., and Skog, J.B., *Mathematical Approach to Estimating Highway Impact on Air Quality,* Volume IV, FWHA-RD-72-36, Washington, D.C., 1972.

Bensen, P.E., "CALINE3 - A Versatile Dispersion Model to Predicting Air Pollutant Levels Near Highways and Arterial Streets," 1979, FHWA/CA/TL-79/23.

Bensen, P.E., "Modifications to the Gaussian Vertical Dispersion Parameter, σ_z, Near Roadways," *Atmospheric Environment*, 1982, Vol. 16, 1399-1405.

Black, F.M., "Control of Motor Vehicle Emissions - The U.S. Experience", *Critical Reviews in Environmental Control*, 21(5,6), 373-410, 1991.

Bullen, J.A. and Maldonado, C., "Modeling Carbon Monoxide Dispersion from Roadways," *Environmental Science and Technology*, 1977, Vol. 11, 1071-1076.

Brice, R.M. and Roesler, J.F., "The Exposure to Carbon Monoxide of Occupants of Vehicles Moving in Heavy Traffic," *Journal of the Air Pollution Control Association*, 1966, Vol. 16, No. 11, 597-601.

Calder, K.L., "On Estimating Air Pollution Concentrations From a Highway in an Oblique Wind," *Atmospheric Environment*, 1973, No. 7, 863-868.

Cengel, Y.A. and Boles, M.A., *Thermodynamics: An Engineering Approach*, McGraw-Hill, 1989.

Chan, C.C., Ozkaynak, H., Spengler, J.D., and Sheldon, L., "Driver Exposure to Volatile Organic Compounds, CO, Ozone, and NO_2 Under Different Driving Conditions," *Environmental Science and Technology*, 1991, Vol. 25, No. 5, 964-972.

Chock, D.P. "The General Motors Sulfate Dispersal Experiment - An Overview of the Wind, Temperature, and Concentration Fields," *Atmospheric* Environment, 1977, Vol. 11, 553-559.

Chock, D.P., "Assessment of the EPA HIWAY Model," *Journal of Applied Meteorology*, 1977, Vol. 27, No. 1, 39-45.

Chock, D.P., "A Simple Line Source Model For Dispersion Near Roadways," *Atmospheric Environment*, 1978, Vol. 12, 823-829.

Chock, D.P., Colwill, D.M. and Hickman, A.J., "Exposure of Drivers to Carbon Monoxide," *Journal of the Air Pollution Control* Association, 1980, Vol. 30, No. 12, 1316-1319.

Eskridge, R.E. and Hunt, J.C., "Highway modeling - I. Prediction of Velocity and Turbulence Fields in the Wakes of Vehicles," *Journal of Applied Meteorology*, 1979, Vol. 18, 387-400.

Eskridge, R.E., Hunt, J.C., Clark, T.L., and Demerhian, K.L., "Highway Modeling, Part II: Advection and Diffusion of SF_6 Tracer Gas," *Journal of Applied* Meteorology, 1979, Vol. 18, 401-412.

Eskridge, R.E., and Thompson, R.S., "Experimental and Theoretical Study of the Wake of a Block-shaped Vehicle in a Shear-Free Boundary Flow," *Atmospheric Environment*, 1982, Vol. 16, No. 12, 2821-2836.

Eskridge, R.E., Petersen, W.B., and Rao, S.T., "Turbulent Diffusion Behind Vehicles: Effect of Traffic Speed on Pollutant Concentrations," *Journal of the Air and Waste Management* Association, 1991, Vol. 41, 312-317.

Fay, J.A., *Introduction to Fluid Mechanics*, MIT Press, Cambridge, 1994.

Flachsbart, P.G., Howes, J.E., Mack, G.A., and Rodes, C.E., "Carbon Monoxide Exposures of Washington Commuters," *Journal of the Air Pollution Control Association*, 1987, Vol. 37, No. 2, 135-142.

Gronskei, K.E., "The Influence of Car Speed on Dispersion of Exhaust Gases," *Atmospheric Environment*, 1988, Vol. 22, No. 2, 273-281.

Green, N.J, Bullin, J.A., and Plasek, J.C., "Dispersion of Carbon Monoxide from Roadways at Low Windspeeds," *Journal of the Air Pollution Control Association*, 1979, Vol. 29, 1057-1061.

Hare, C.T., and Springer, K.J., "Exhaust Emissions From Uncontrolled Vehicles and Related Equipment Using Internal Combustion Engines: Part 7 - Snowmobiles," NTIS Final Report, April 1974, PB235751.

Hare, C.T., Springer, K.J., and Huls, T. A., "Snowmobile Emissions and Their Impact," SAE 740735, September 1974.

Heavner, R., Personal facsimile, National Park Service Air Quality Division, August 1994.

Houston, R., Archer, M., Moore, M., and Newmann, Ramon, "Development of a Durable Emissions Control System for an Automotive Two-stroke Engine," SAE 960361, 1996.

International Snowmobile Industry Association, "Statement on Snowmobile Emissions," Letter, May 1995.

Johnson, W.B., "Field Study of Near-roadway Diffusion Using a Fluorescent Dye Tracer," *Symposium on Atmospheric Diffusion and Air Pollution*, American Meteorological Society, 1974, 261-266.

Mayron, L.W., and Winterhalter, J.J., "Carbon Monoxide: A Danger to the Driver?" *Journal of the Air Pollution Control* Association, 1976, Vol. 26, No. 11, 1085-1088.

Obert, E.F., *Internal Combustion Engines and Air Pollution Third Edition*, Harper & Row, 1973.

Pasquill, F. *Atmospheric* Diffusion, Ellis Horwood Chichester, John Wiley, New York, 1974.

Pasquill, F. "Atmospheric Dispersion Parameters in Gaussian Plume Modeling; Part 2, Possible Requirements for Change in the Turner Workbook Values," U.S. EPA Document EPA-600/4-76-030b, 1976.

Petersen, W.B., and Allen, R., "Carbon Monoxide Exposures to Los Angeles Area Commuters," *Journal of the Air Pollution Control Association*, 1982, Vol. 32, No. 8, 826-833.

Rao, S.T., , G., Keenan, M.T., and Wilson, J.S., "An Evaluation of Some Commonly Used Highway Dispersion Models," *Journal of the Air Pollution Control Association*, Vol. 30, No. 3, 283-293.

Samson, P.J. "Atmospheric Transport and Dispersion of Air Pollutants Associated with Vehicular Emissions," *Air Pollution the Automobile and Public Health*, Health Effects Institute, National Academy Press, 1988.

Sluder, C. S., *Development of a Method for Determining Exhaust Emissions and Fuel Consumption of Vehicles in On-road Operation*, Master's Thesis, University of Tennessee, December 1995.

Stone, R., *Introduction to Internal Combustion Engines*, Society of Automotive Engineers, 1992.

Turner, D.B., "Workbook of Atmospheric Dispersion Estimates," U.S. Department of Health, Education and Welfare, PB 91 482, May 1970.

Wark, K. and Warner, C.F., *Air Pollution Its Origin and Control Second Edition*, Harper Collins Publishers, New York, 1981.

White, F.M., *Fluid Mechanics 2nd Edition*, McGraw-Hill Publishing Company, New York, 1986.

White, J.J.; Carroll, J.N.; Lourenco, J.G.; Downing-Iaali, A.; "Baseline and controlled Exhaust Emissions From Off-Highway Vehicle Engines," SAE 931541, 1993.

Wilkinson, T., "Snowed Under," *National Parks*, 1995, Vol. 69, no. 1-2, 32-37.

Zimmerman, J.R. and Thompson, R.S., "HIWAY: A Highway Air Pollution Model," Environmental Protection Agency, Research Triangle Park, North Carolina, 1974.

APPENDICES

APPENDIX A

EQUIPMENT LIST

CO Analyzer

Manufacturer:	Thermo Environmental Instruments
Model Number:	Model 48
Range:	0.1-1000 ppm
Min. Det. Limit:	0.1 ppm
Response Time:	30 seconds at 1 l/min flow
Cost:	N/A (loaned by Thermo Environmental for this project)

Laminar Air Flow Element

Manufacturer:	Meriam Instrument Company
Model Number:	Model 60 AC O2
Range:	0-30 acfm at 6 inches of water
Min. Det. Limit:	Dependent upon pressure measurement technique
Cost:	N/A (property of the University of Tennessee)

Universal Flow Air Sample Pump

Manufacturer:	SKC Inc.
Model Number:	Model 224-PCXR8 with low flow adapter
Range:	5 ml/min to 5 l/min
Run Time:	8 hours minimum at 4 l/min and 20" water back pressure
Operating Temp:	-4 °F to 113 °F
Cost:	N/A (loaned by SKC for this project)

Magnehelic Gage

Range:	0 to 6 inches of water
Min. Det. Limit:	0.2 inches of water
Cost:	N/A (property of the University of Tennessee)

Anemometer

Manufacturer:	Davis Instruments
Model:	Turbometer
Range:	0-45 m/s
Min. Det. Limit:	0.1 m/s
Accuracy:	± 3%
Cost:	$165.00 from Cole-Parmer Instrument Company

Sampling Bags

Manufacturer:	Environmental Supply Company, Inc.
Model:	BR9
Description:	2 mil sampling bag with roberts valve and grommet
Size:	2 liters (9"x9")
Cost:	$6.00/bag (reduced rate from ESC)

Drierite® Drying Tubes

Purchased From:	Cole-Parmer Instrument Company
Catalog Number:	H-06462-20
Cost:	$15.00 for pack of four

Calibration Gases and Regulator

Manufacturer:	Air Liquide
Gases and Conc.:	2 cylinders of zero gas
	1 cylinder of 20 ppm CO
	1 cylinder of 700 ppm CO
Cylinder Volume:	3.6 ft^3 (at stp)
Regulator Flow:	1.2 l/min (fixed)
Cost:	N/A (donated by Air Liquide for use in the study)

Snowmobile

Manufacturer:	Polaris
Model & Year:	1992 Indy 500
Engine:	488 cc two-stroke
Fuel Delivery:	Electronic injection
Cooling:	Liquid
Cost:	N/A (loaned by GTNP for use in this study)

Carbon Monoxide Badge Kit

Manufacturer:	Leak Tec
Response:	Color change at 50 ppm for 5 minutes
Purchased From:	American Gas and Chemical Co., Ltd.
Cost:	$21.00

Smoke Bombs

Manufacturer:	Superior
Purchased From:	Safety Master Corp.
Cost:	$4.25/bomb

Carbon Monoxide Alarm

Manufacturer: American Sensors

Response: Full alarm at: 100 ppm for 90 min
200 ppm for 35 min
400 ppm for 15 min
Low alarm at: 40-80 ppm for 90 min

Purchased From: K-Mart

Cost: $35.00

APPENDIX B

LAMINAR AIR FLOW ELEMENT CALIBRATION

The Meriam model 60 AC O2 LAFE was calibrated against a Meriam 50 MR2-2 LAFE (which had recently been factory calibrated). Both LAFEs were attached (in series) to the air intake of a Mercury Villager LS Minivan. The minivan was then driven on a chassis dynamometer at the University of Tennessee at several different speeds. The pressure drop across both LAFEs was measured with Omega PX650 series pressure transducers. The factory calibration curve for the Meriam 50 MR2-2 LAFE was used to calculate the air flowing into the engine at each speed. This data was then used to create a curve of air flow (at STP) vs pressure drop for the Meriam 60 AC 02. This calibration curve is shown below.

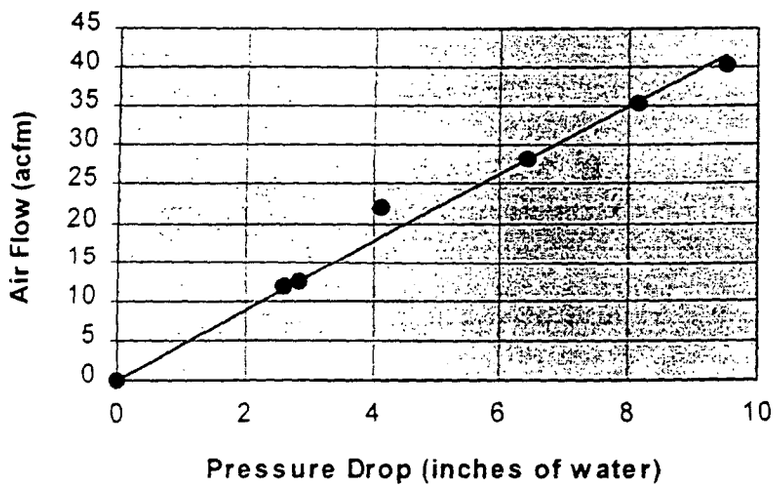

Calibration Curve for Meriam 60 AC O2 Laminar Air Flow Element (at STP)

APPENDIX C

SAMPLE EXHAUST MASS FLOW RATE CALCULATION

Problem:

Estimate the mass emission rate of CO from a snowmobile in both g/hr and g/mile. The following information is given: the air temperature is 8 degrees F, the pressure drop across the LAFE (calibration curve in Appendix B) is 1.5 inches of water, the snowmobile speed is 40 mph, and the concentration of CO in the exhaust is 48,346 ppm.

Solution:

The first step is to calculate the mass flow rate of air into the engine in acfm. First, the calibration curve is used to determine the indicated flow rate from the measured pressure drop across the LAFE.

$$Indicated\ Flow = 4.39(inches\ of\ H_2 0)$$
$$= 4.39(1.5) = 6.59\ acfm$$

The indicated flow is converted to the actual flow as in equation 5.1.

$$Actual\ Flow = 6.59(ratio\ of\ viscosities)$$
$$= 6.59(1.123)$$
$$= 7.4\ acfm$$

And finally, Equation 5.2 is used to calculate the mass of air into the engine per unit time.

$$\frac{Mass\ of\ air\ into\ engine}{Time} = \left(\frac{Volume\ of\ air\ into\ engine}{Time}\right)\left(\frac{(MW_{air})(P)}{(R_U)(T)}\right)$$

$$= 7.4\,acfm\,\frac{(28.97lb/lbmol)(14.7psia)}{\left(10.73\frac{psiaft^3}{lbmolR}\right)(468R)}$$

$$= 0.6276\ lbair/min$$

The next step is to assume a fuel/air equivalence ratio and solve the combustion equation. The appropriate fuel/air equivalence ratio is 1.15 for a CO concentration of 4.8% (from Figure 7). The combustion equation described by Equation 5.3 is determined with a mass balance and Equation 5.8. The following balanced combustion equation results:

$$CH_{1.85} + (1.4625)\left(\frac{1}{1.15}\right)(O_2 + 3.76N_2) \rightarrow 0.745CO_2 + 0.798H_2O + 4.78N_2 + 0.255CO + 0.127H_2$$

where the constants **A**, **B**, **C**, **D**, and **E** from Equation 5.3 are 0.745, 0.798, 4.78, 0.255, and 0.127 respectively.

The balanced combustion equation may now be used to calculate the mass of fuel/mass of air, the mass of dry products/mole of fuel, the mass of wet products/mole of fuel, and the molecular weight of the dry exhaust gases. The appropriate Equations are 5.9 through 5.12. This is shown below.

$$\frac{mass\ of\ fuel}{mass\ of\ air} = \frac{MW_{fuel}}{\left(\frac{1.4625}{\Phi_{F/A}}\right)(MW_{O_2} + 3.76\,MW_{N_2})}$$

$$= \frac{1.85 + 12}{\left(\frac{1.4625}{1.15}\right)(32 + 3.76(28))}$$

$$= 0.0793\frac{g\ fuel}{g\ air}$$

$$\frac{mass\ of\ dry\ products}{mole\ fuel} = \mathbf{A}(MW_{CO_2}) + \mathbf{C}(MW_{N_2}) + \mathbf{D}(MW_{CO}) + \mathbf{E}(MW_{H_2})$$

$$= 0.745(44) + 4.78(28) + 0.255(28) + 0.127(2)$$

$$= 174\frac{g\ dry\ product}{gmol\ fuel}$$

$$\frac{mass\ wet\ products}{mole\ fuel} = \mathbf{A}(MW_{CO_2}) + \mathbf{B}(MW_{H_2O}) + \mathbf{C}(MW_{N_2}) + \mathbf{D}(MW_{CO}) + \mathbf{E}(MW_{H_2})$$

$$= 0.745(44) + 0.798(18) + 4.78(28) + 0.255(28) + 0.127(2)$$

$$= 188\frac{g\ wet\ product}{gmol\ fuel}$$

$$molecular\ weight\ of\ dry\ exhaust = \left(\frac{mass\ of\ dry\ products}{mole\ fuel}\right)\left(\frac{1}{\mathbf{A}+\mathbf{C}+\mathbf{D}+\mathbf{E}}\right)$$

$$= \left(174\frac{g\ dry\ product}{gmol\ fuel}\right)\left(\frac{1}{0.745+4.78+0.255+0.127}\right)$$

$$= 29.46\frac{g\ dry\ product}{gmol\ dry\ product}$$

Equations 5.13 and 5.14 are now used to calculate the dry mass flow rate of the exhaust. This is shown below.

$$\frac{mass\ of\ exhaust\ (wet)}{time} = \left(\frac{mass\ of\ air\ into\ engine}{time}\right)\left(1+\frac{mass\ of\ fuel}{mass\ of\ air}\right)$$

$$= \left(0.6276\frac{lb\ air\ into\ engine}{\min}\right)(1+0.0793)$$

$$= 0.6774\frac{lb\ wet\ exhaust}{\min}$$

$$= 18.391\frac{g\ wet\ exhaust}{hr}$$

$$\frac{mass\ of\ exhaust\ (dry)}{time} = \left(\frac{mass\ exhaust\ (wet)}{time}\right)\left(\frac{mass\ dry\ products}{mole\ fuel}\right)\left(\frac{mole\ fuel}{mass\ wet\ products}\right)$$

$$= \left(18.391\frac{g\ wet\ exhaust}{hr}\right)\left(174\frac{g\ dry\ product}{gmol\ fuel}\right)\left(\frac{gmol\ fuel}{188g\ wet\ product}\right)$$

$$= 17.022\frac{g\ dry\ exhaust}{hr}$$

And finally, the desired mass emission rates may be calculated using Equations 5.15 and 5.16. This is shown below.

$$\frac{mass\ CO}{time} = \left(\frac{conc.\ of\ CO\ in\ exhaust\ in\ ppm}{10^6}\right)\left(\frac{MW_{CO}}{MW_{dry\ exhaust}}\right)\left(\frac{mass\ of\ exhaust\ (dry)}{time}\right)$$

$$= \left(\frac{48{,}346 gmols\ CO}{1{,}000{,}000 gmols\ dry\ exhaust}\right)\left(\frac{28\ {}^{g\ CO}/_{gmol\ CO}}{29.46\ {}^{g\ air}/_{gmol\ air}}\right)\left(17{,}022\frac{g\ dry\ exhaust}{hr}\right)$$

$$= 782\frac{g\ CO}{hr}$$

$$\frac{mass\ of\ CO}{distance} = \left(\frac{mass\ CO}{time}\right)\left(\frac{1}{snowmobile\ speed}\right)$$

$$= \left(782\frac{g\ CO}{hr}\right)\left(\frac{1}{40 mph}\right)$$

$$= 19.6\frac{g}{mile}$$

APPENDIX D

TASK 1 DATA

The following table contains all of the raw data collected during Task 1. These include the air temperature, the snowmobile speed, the engine rpm, the pressure drop across the LAFE, and the concentration measured in the diluted sample bags. This table also contains the following reduced data: the air flow rate into the engine, the exhaust dilution ratio, the calculated exhaust concentration for each diluted sample, the average calculated exhaust concentration for each exhaust sample, the assumed equivalence ratio, and the CO mass emission rate.

Table of Task 1 Exhaust Data

Date	Temp (F)	Speed in mph	RPM	dP "H2O	Air Flow (acfm)	Dil. Ratio	Dil Bag Conc (ppm)	Exhaust Conc (ppm)	Mean Exhaust Conc (ppm)	Std. Dev. of Exhaust Conc	Equiv Ratio	Grams of CO/hour
1.22.96	8	10	4800	0.4	1.97	81.2	233	18920	19096	600	1.05	80
						81.2	231	18757				
						81.2	243	19732				
						81.2	243	19732				
						81.2	224	18189				
						81.2	237	19244				
1.22.96	8	10	4500	0.4	1.97	81.2	220	17864	23121	1935	1.05	96
						81.2	278	22574				
						81.2	296	24035				
						81.2	293	23792				
						81.2	279	22655				
						81.2	315	25578				
						81.6	285	23256				
						81.6	297	24235				
						81.6	281	22930				
						81.6	290	23664				
						81.6	291	23746				
1.23.96	8	10	4800	0.4	1.97	80.5	300	24150	24375	1784	1.05	102
						80.5	319	25680				
						80.5	305	24553				
						80.5	323	26002				
						80.5	267	21494				

Table of Task 1 Exhaust Data (continued)

Date	Temp (F)	Speed in mph	RPM	dP "H2O	Air Flow (acfm)	Dil. Ratio	Dil Bag Conc (ppm)	Exhaust Conc (ppm)	Mean Exhaust Conc (ppm)	Std. Dev. of Exhaust Conc	Equiv Ratio	Grams of CO/hour
1/26/96	-6	10	5100	0.4	2.02	80.5	265	21333	23778	1416	1.05	105
						80.5	310	24955				
						80.5	311	25036				
						80.5	301	24231				
						80.5	299	24070				
						81.6	305	24888				
						81.6	281	22930				
						81.6	303	24725				
						81.6	262	21379				
						81.6	297	24235				
1/26/96	-6	10	4600	0.4	2.02	81.2	296	24035	25077	897	1.05	110
						81.2	311	25253				
						81.2	301	24441				
						81.2	314	25497				
						81.2	304	24685				
						81.2	327	26552				
1/22/96	8	20	5900	0.7	3.45	81.2	342	27770	27917	337	1.10	207
						81.2	346	28095				
						81.2	341	27689				
						81.2	350	28420				
						81.2	340	27608				
1/26/96	-6	20	5800	0.7	3.54	80.5	358	28819	29149	1130	1.10	228
						80.5	350	28175				
						80.5	363	29222				
						80.5	340	27370				
						81.6	370	30192				
						81.6	382	31171				
						81.6	353	28805				
						81.6	366	29866				
						81.6	352	28723				
2/11/96	15	20	5400	0.6	2.92	26.3	1130	29719	31816	1561	1.10	197
						26.3	1271	33427				
						26.3	1231	32375				
						26.3	1207	31744				
1/22/96	8	30	6000	1.0	4.93	82.7	387	32005	32220	466	1.10	341
						82.7	389	32170				
						82.7	389	32170				
						82.7	399	32997				
						82.7	384	31757				
1/23/96	8	30	6200	0.9	4.44	81.6	472	38515	37824	1990	1.10	361
						81.6	486	39658				
						81.6	460	37536				
						81.6	471	38434				
						81.6	415	33864				
						81.2	468	38002				
						81.2	496	40275				
						81.2	475	38570				
						81.2	438	35566				
1/26/96	-6	30	6100	1.0	5.06	80.5	382	30751	28846	1684	1.10	323
						80.5	383	30832				
						80.5	355	28578				
						80.5	354	28497				
						80.5	329	26485				
						80.5	347	27934				
2/11/96	15	30	6000	0.8	3.9	75.8	443	33655	32670	2033	1.10	270
						75.8	448	33958				
						75.8	391	29638				
						75.8	441	33428				

Table of Task 1 Exhaust Data (continued)

Date	Temp (F)	Speed in mph	RPM	dP "H2O	Air Flow (acfm)	Dil. Ratio	Dil Bag Conc (ppm)	Exhaust Conc (ppm)	Mean Exhaust Conc (ppm)	Std. Dev. of Exhaust Conc	Equiv Ratio	Grams of CO/hour
1/22/96	8	40	6600	1.5	7.4	82.7	552	45650	48346	2614	1.15	780
						82.7	552	45650				
						82.7	589	48710				
						82.7	614	50778				
						82.7	616	50943				
1/23/96	8	40	6400	1.5	7.4	81.2	573	46528	47583	906	1.15	768
						81.2	603	48964				
						81.2	588	47746				
						81.2	580	47096				
						81.2	586	47583				
1/26/96	-6	40	6800	1.5	7.59	80.5	695	55948	56946	1833	1.20	986
						80.5	746	60053				
						80.5	709	57075				
						80.5	698	56189				
						80.5	689	55465				
2/11/96	15	40	6200	1.3	6.33	75.8	626	47451	47405	1180	1.15	645
						75.8	602	45632				
						75.8	621	47072				
						75.8	643	48739				
						75.8	635	48133				
2/10/96	40	acc.	7000	3	13.94	82.7	802	66325	69121	2356	1.25	2027
						82.7	849	70212				
						82.7	837	69220				
						82.7	816	67483				
						82.7	875	72363				
1/29/96	-6	idle	1300	0.1	0.5*	81.6	61.6	5027	5136	224	1.0	5.6*
						81.6	60.3	4920				
						81.6	65.9	5377				
						81.6	62.8	5124				
						81.6	61.1	4986				
						81.6	60.5	4937				
						81.2	69.5	5643				
						81.2	62	5034				
						81.2	63	5116				
						81.2	64	5197				

* The airflow under idle was below detectable limits. Therefore, this represents a maximum expected idle emission.

APPENDIX E

QUICK CHECK OF EXPECTED AIR FLOW RATE

As the air flow rates measured in Task 1 appeared a bit low, a quick calculation was done to determine if they were of the appropriate magnitude. For the calculation, the weight of the snowmobile was assumed to be 500 lb (it is actually 511 lbs), the brake specific fuel consumption was assumed to be 0.575 lb fuel/hp-hr (taken from Houston et.al., 1996), and the coefficient of tractive resistance was assumed to be 0.1. Neglecting air drag, the power required to propel the snowmobile at constant speed is calculated by:

$$Power = (Weight)(f)(V_V)$$

where f is the coefficient of tractive resistance and V_V is the velocity of the snowmobile. From this, the fuel consumption can be calculated as follows:

$$m_{FUEL} = (brake\ specific\ fuel\ consumption)(Power)$$

where m_{FUEL} is the mass flow rate of the fuel in mass/time. Finally, the mass flow rate of air is calculated by the following equation:

$$airflow = \frac{(m_{FUEL})(A/F)}{\rho_{AIR}}$$

where the airflow is calculated in volume/time, A/F is the mass based air/fuel ratio, and ρ_{AIR} is the density of air.

An example calculation is shown below for the case of V_V = 40 mph.

$$Power = (Weight)(f)(V_v)$$

$$= (500lb)(0.1)\left(40\frac{miles}{hour}\right)\left(5280\frac{ft}{mile}\right)\left(\frac{hour}{3600sec}\right)\left(\frac{hp}{550\frac{ftlb}{\sec}}\right)$$

$$= 5.33\ horsepower$$

$$m_{FUEL} = (brake\ specific\ fuel\ consumption)(Power)$$

$$= \left(0.575\frac{lb}{hphr}\right)(5.33hp)\left(\frac{hr}{60min}\right)$$

$$= 0.0511\frac{lb\ fuel}{min}$$

$$airflow = \frac{(m_{FUEL})(A/F)}{\rho_{AIR}}$$

$$= \frac{\left(.0511\frac{lb\ fuel}{min}\right)\left(125\frac{lb\ air}{lb\ fuel}\right)}{0.0875\frac{lb\ air}{ft^3\ air}}$$

$$= 7.31\frac{ft^3}{\min} = 7.31\,acfm$$

This calculation was made for speeds of 10, 20, 30, and 40 mph and was plotted as a function of speed on the graph on the following page. Also included on this graph are the actual airflow measurements taken during Task 1. It is clear from the graph that the measured and calculated values are of the same magnitude.

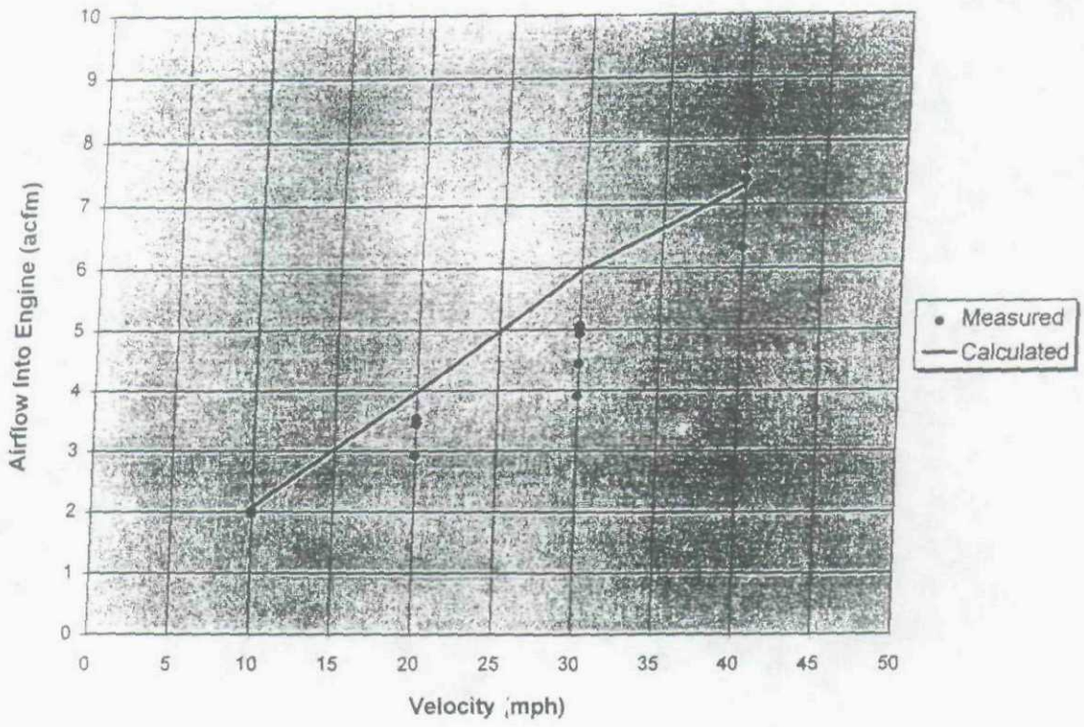

Comparison of Calculated Air Flow Rates to Measured Air Flow Rates as a Function of Snowmobile Speed

APPENDIX F

TASK 2 DATA

Self Exposure Data

The following table contains all of the raw data collected during the self-exposure measurements of Task 2. These include the date, the wind speed, the snowmobile speed, the background CO and the measured CO concentration This table also contains the self-exposure CO concentration corrected for the background CO.

Table of Self-Exposure Data

Date	Speed (mph)	Windspeed (m/s)	Measured CO (ppm)	Background CO (ppm)	Corrected CO (ppm)
2/11/96	10	1.1	1.3	0.4	0.9
2/12/96	10	2.0	4.1	0.3	3.8
2/13/96	10	1.0	2.4	0.2	2.2
2/16/96	10	0.6	1.8	0.5	1.3
2/11/96	20	1.1	1.0	0.4	0.6
2/12/96	20	2.0	3.7	0.3	3.4
2/13/96	20	1.0	1.2	0.2	1.0
2/16/96	20	0.6	0.6	0.5	0.1
2/11/96	30	1.1	1.6	0.4	1.2
2/12/96	30	2.0	8.3	0.3	8.0
2/13/96	30	1.0	1.8	0.2	1.6
2/16/96	30	0.6	1.7	0.5	1.2
2/11/96	40	1.1	1.8	0.4	1.4
2/12/96	40	2.0	4.4	0.3	4.1
2/13/96	40	1.0	1.6	0.2	1.4
2/16/96	40	0.6	3.0	0.5	2.5

Centerline Exposure Data

The following table contains all of the raw data collected during the centerline exposure measurements of Task 2. These include the snowmobile speed, the distance, the wind speed, the background CO, the CO from self-exposure (corrected for background CO), and the measured CO concentration This table also contains the corrected centerline CO concentration (corrected for the background CO and self-exposure).

Table of Centerline Exposure Data

Speed (mph)	Distance (ft)	Date	Wind (m/s)	Background CO (ppm)	Corrected Self Exposure CO (ppm)	Measured CO (ppm)	Corrected CO (ppm)
10	25	2/10/96	4.7	1.0	2.1	22.5	19.4
10	25	2/11/96	1.0	0.4	2.1	43.7	41.2
10	25	2/12/96	0.8	0.3	2 1	22.2	19.8
10	25	2/13/96	1.8	0.2	2.1	16.5	14.2
10	25	2/16/96	0.8	0.5	2.1	23.6	21.0
10	50	2/11/96	1.1	0.4	2.1	6.0	3.5
10	50	2/12/96	0.8	0.3	2.1	3.9	1.5
10	50	2/13/96	0.0	0.2	2.1	7.5	5.2
10	50	2/16/96	2.0	0.5	2.1	1.7	0.0
10	75	2/11/96	1.0	0.4	2.1	2.8	0.0
10	75	2/12/96	1.8	0.3	2.1	3.9	1.5
10	75	2/13/96	0.3	0.2	2.1	0.6	0.0
10	75	2/16/96	1.8	0.5	2.1	3.0	0.4
10	100	2/11/96	1.5	0.4	2.1	1.9	0.0
10	100	2/12/96	1.0	0.3	2.1	10.1	7.7
10	100	2/13/96	0.5	0.2	2.1	3.0	0.7
10	100	2/16/96	0.8	0.5	2.1	3.9	1.3
10	125	2/10/96	4.7	1.0	2.1	5.3	2.2
10	125	2/11/96	0.0	0.4	2.1	12.3	9.8
10	125	2/12/96	0.8	0.3	2.1	11.8	9.4
10	125	2/13/96	0.4	0.2	2.1	1.8	0.0
10	125	2/16/96	1.2	0.5	2.1	6.8	4.2
20	25	2/10/96	4.7	1.0	1.3	18.0	15.7
20	25	2/11/96	1.0	0.4	1.3	12.9	11.2
20	25	2/12/96	0.8	0.3	1.3	18.6	17.0
20	25	2/13/96	1.8	0.2	1.3	17.6	16.1
20	25	2/16/96	0.8	0.5	1.3	6.7	4.9
20	50	2/11/96	1.1	0.4	1.3	6.6	4.9
20	50	2/12/96	0.8	0.3	1.3	7.1	5.5
20	50	2/13/96	0.0	0.2	1.3	3.3	1.8
20	50	2/16/96	1.6	0.5	1.3	11.0	9.2

Table of Centerline Exposure Data (continued)

Speed (mph)	Distance (ft)	Date	Wind (m/s)	Background CO (ppm)	Corrected Self Exposure CO (ppm)	Measured CO (ppm)	Corrected CO (ppm)
20	75	2/11/96	1.0	0.4	1.3	3.2	1.5
20	75	2/12/96	1.8	0.3	1.3	8.8	7.2
20	75	2/13/96	0.3	0.2	1.3	1.7	0.0
20	75	2/16/96	1.8	0.5	1.3	2.5	0.7
20	100	2/11/96	1.5	0.4	1.3	5.6	3.9
20	100	2/12/96	1.0	0.3	1.3	3.7	2.1
20	100	2/13/96	0.5	0.2	1.3	5.7	4.2
20	100	2/16/96	0.8	0.5	1.3	5.1	3.3
20	125	2/10/96	4.7	1.0	1.3	3.3	1.0
20	125	2/11/96	0.0	0.4	1.3	4.8	3.1
20	125	2/12/96	0.8	0.3	1.3	2.5	0.9
20	125	2/13/96	0.4	0.2	1.3	1.6	0.0
20	125	2/16/96	1.2	0.5	1.3	5.6	3.8
30	25	2/10/96	4.7	1.0	3.0	15.4	11.4
30	25	2/11/96	1.0	0.4	3.0	13.8	10.4
30	25	2/12/96	0.8	0.3	3.0	18.0	14.7
30	25	2/13/96	1.8	0.2	3.0	15.5	12.3
30	25	2/16/96	0.8	0.5	3.0	15.4	11.9
30	50	2/11/96	1.1	0.4	3.0	12.3	8.9
30	50	2/12/96	0.8	0.3	3.0	8.8	5.5
30	50	2/13/96	0.0	0.2	3.0	5.9	2.7
30	50	2/16/96	2.0	0.5	3.0	6.2	2.7
30	75	2/11/96	1.0	0.4	3.0	5.4	2.0
30	75	2/12/96	1.8	0.3	3.0	12.9	9.6
30	75	2/13/96	0.3	0.2	3.0	1.8	0.0
30	75	2/16/96	1.8	0.5	3.0	6.0	2.5
30	100	2/11/96	1.5	0.4	3.0	12.8	9.4
30	100	2/12/96	1.0	0.3	3.0	12.7	9.4
30	100	2/13/96	0.5	0.2	3.0	2.0	0.0
30	100	2/16/96	0.8	0.5	3.0	10.9	7.4
30	125	2/10/96	4.7	1.0	3.0	8.8	4.8
30	125	2/12/96	0.8	0.3	3.0	6.8	3.5
30	125	2/13/96	0.4	0.2	3.0	4.7	1.5
30	125	2/16/96	1.2	0.5	3.0	5.7	2.2
40	25	2/10/96	4.7	1.0	2.4	17.7	14.3
40	25	2/11/96	1.0	0.4	2.4	20.5	17.7
40	25	2/12/96	0.8	0.3	2.4	23.2	20.5
40	25	2/13/96	1.8	0.2	2.4	16.0	13.4
40	25	2/16/96	0.8	0.5	2.4	35.0	32.1
40	50	2/11/96	1.1	0.4	2.4	16.2	13.4
40	50	2/12/96	0.8	0.3	2.4	14.6	11.9
40	50	2/13/96	0.0	0.2	2.4	12.9	10.3
40	50	2/16/96	2.0	0.5	2.4	11.6	8.7

Table of Centerline Exposure Data (continued)

Speed (mph)	Distance (ft)	Date	Wind (m/s)	Background CO (ppm)	Corrected Self Exposure CO (ppm)	Measured CO (ppm)	Corrected CO (ppm)
40	75	2/11/96	1.0	0.4	2.4	11.9	9.1
40	75	2/12/96	1.8	0.3	2.4	11.4	8.7
40	75	2/13/96	0.3	0.2	2.4	8.2	5.6
40	75	2/16/96	1.8	0.5	2.4	13.7	10.8
40	100	2/11/96	1.5	0.4	2.4	11.6	8.8
40	100	2/12/96	1.0	0.3	2.4	11.3	8.6
40	100	2/13/96	0.5	0.2	2.4	8.2	5.6
40	100	2/16/96	0.8	0.5	2.4	15.3	12.4
40	125	2/10/96	4.7	1.0	2.4	11.9	8.5
40	125	2/11/96	0.0	0.4	2.4	12.1	9.3
40	125	2/12/96	0.8	0.3	2.4	8.6	5.9
40	125	2/13/96	0.4	0.2	2.4	10.8	8.2
40	125	2/16/96	1.2	0.5	2.4	13.2	10.3

The Task 2 centerline exposure data is also plotted at each speed in the following four graphs.

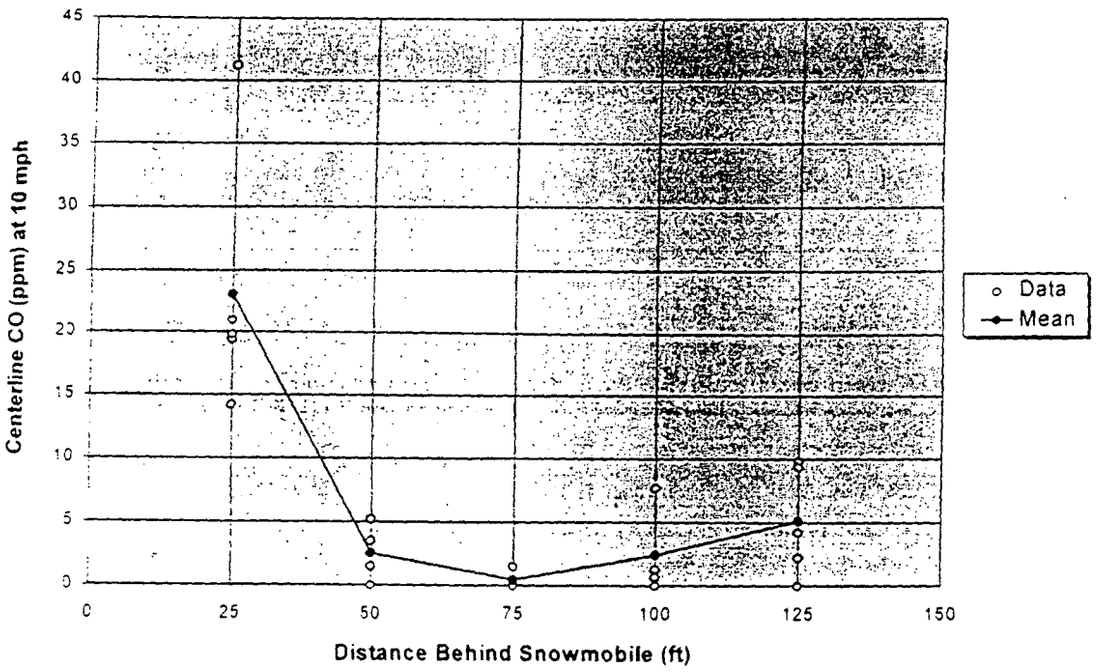

Graph of Centerline CO Vs. Distance at 10 mph

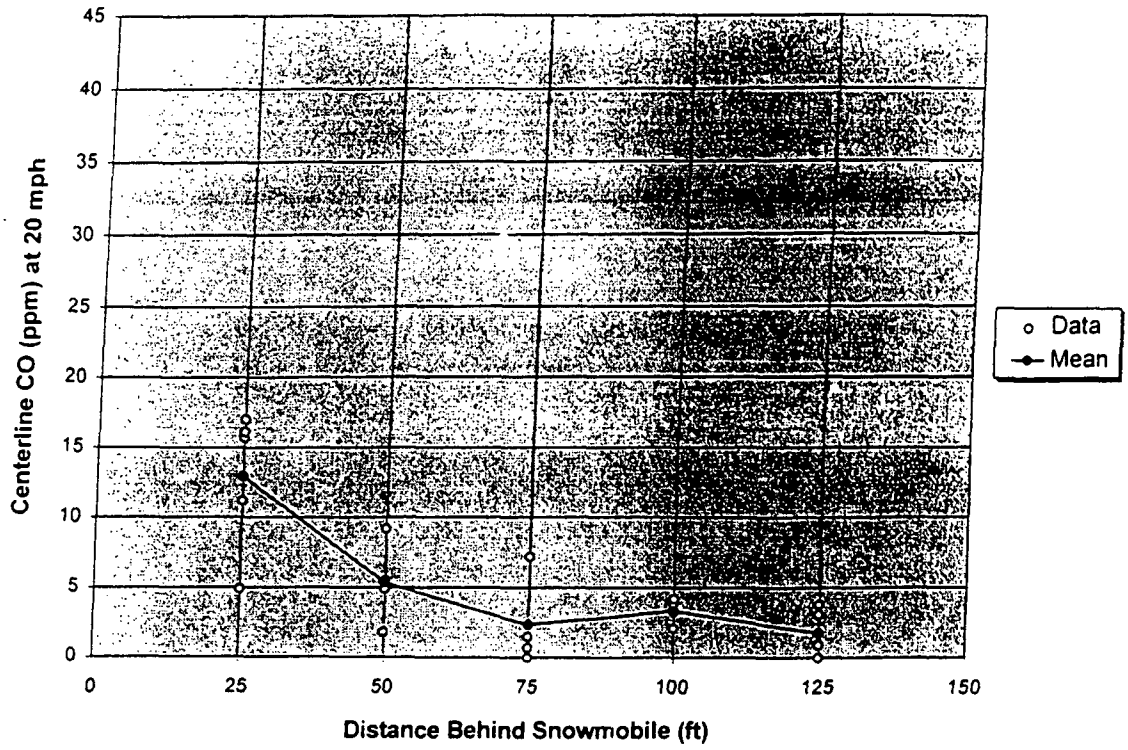

Graph of Centerline CO Vs. Distance at 20 mph

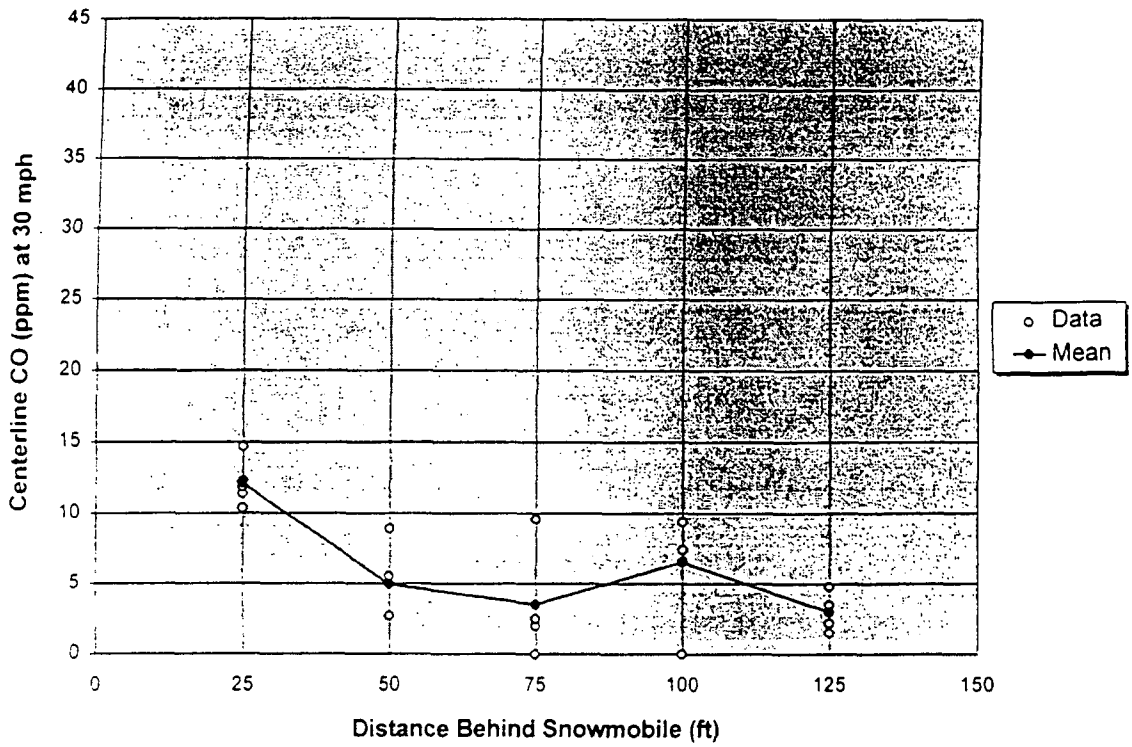

Graph of Centerline CO Vs. Distance at 30 mph

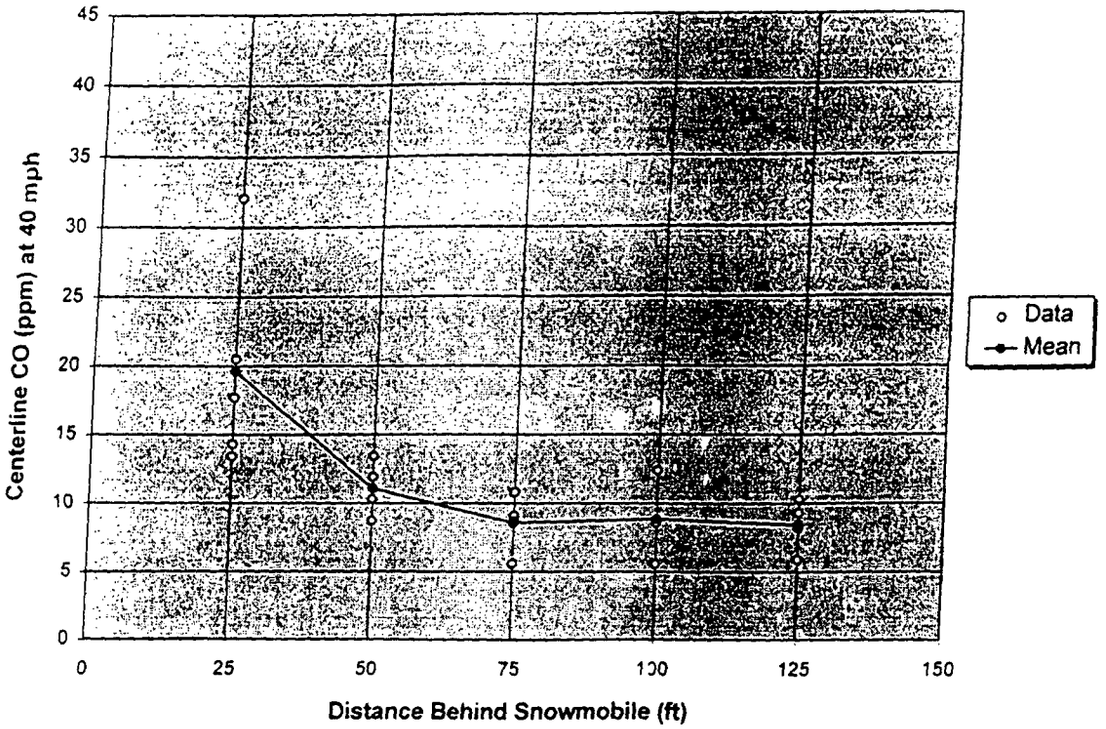

Graph of Centerline CO Vs. Distance at 40 mph

Off-Centerline Exposure Data

The following table contains all of the raw data collected during the off-centerline exposure measurements of Task 2. These include the snowmobile speed, the distance, the wind speed, the background CO, the CO from self-exposure (corrected for background CO), and the measured CO concentration. This table also contains the corrected off-centerline CO concentration (corrected for the background CO and self-exposure). Following the table are graphs of the off-centerline exposure data at each speed.

Table of Off-Centerline Exposure Data

Speed (mph)	Distance (ft)	Date	Wind (m/s)	Background CO (ppm)	Corrected Self Exposure CO (ppm)	Measured CO (ppm)	Corrected CO (ppm)
10	25	2/11/96	1.0	0.4	2.1	2.7	0.2
10	25	2/12/96	0.8	0.3	2.1	2.5	0.1
10	25	2/13/96	1.0	0.2	2.1	3.9	1.6
10	25	2/14/96	1.2	0.5	2.1	2.5	0.0
10	50	2/11/96	1.1	0.4	2.1	2.9	0.4
10	50	2/12/96	0.8	0.3	2.1	9.3	6.9
10	50	2/13/96	0.5	0.2	2.1	8.3	6.0
10	50	2/14/96	3.0	0.5	2.1	7.0	4.4
10	75	2/11/96	1.0	0.4	2.1	1.4	0.0
10	75	2/12/96	0.8	0.3	2.1	29.6	27.2
10	75	2/13/96	1.8	0.2	2.1	2.7	0.4
10	75	2/14/96	0.5	0.5	2.1	4.8	2.2
10	100	2/11/96	1.5	0.4	2.1	11.1	8.6
10	100	2/13/96	0.8	0.2	2.1	2.6	0.3
10	100	2/14/96	0.9	0.5	2.1	8.2	5.6
10	125	2/11/96	1.1	0.4	2.1	3.7	1.2
10	125	2/12/96	0.8	0.3	2.1	8.7	6.3
10	125	2/14/96	0.0	0.2	2.1	2.3	0.0
20	25	2/11/96	1.0	0.4	1.3	1.1	0.0
20	25	2/12/96	0.8	0.3	1.3	2.6	1.0
20	25	2/13/96	1.0	0.2	1.3	2.7	1.2
20	25	2/14/96	1.2	0.5	1.3	2.0	0.2
20	50	2/11/96	1.1	0.4	1.3	1.6	0.0
20	50	2/12/96	0.8	0.3	1.3	5.0	3.4
20	50	2/13/96	0.5	0.2	1.3	4.0	2.5
20	50	2/14/96	1.6	0.5	1.3	7.2	5.4
20	75	2/11/96	1.0	0.4	1.3	1.8	0.1
20	75	2/12/96	0.8	0.3	1.3	4.4	2.8
20	75	2/13/96	0.3	0.2	1.3	3.8	2.3
20	75	2/14/96	0.5	0.5	1.3	2.8	1.0
20	100	2/12/96	2.0	0.3	1.3	3.9	2.3
20	100	2/13/96	1.8	0.2	1.3	0.9	0.0
20	100	2/14/96	0.9	0.5	1.3	8.3	6.5
20	125	2/11/96	1.1	0.4	1.3	5.3	3.6
20	125	2/12/96	0.8	0.3	1.3	2.8	1.2
20	125	2/13/96	0.0	0.2	1.3	2.0	0.5
20	125	2/14/96	0.0	0.5	1.3	1.9	0.1
30	25	2/11/96	1.0	0.4	3.0	2.8	0.0
30	25	2/12/96	0.8	0.3	3.0	2.5	0.0
30	25	2/13/96	0.3	0.2	3.0	2.0	0.0
30	25	2/14/96	1.2	0.5	3.0	2.1	0.0
30	50	2/11/96	1.1	0.4	3.0	1.1	0.0
30	50	2/12/96	0.8	0.3	3.0	2.9	0.0
30	50	2/13/96	2.5	0.2	3.0	2.7	0.0
30	50	2/14/96	3.0	0.5	3.0	1.5	0.0

Table of Off-Centerline Exposure Data (continued)

Speed (mph)	Distance (ft)	Date	Wind (m/s)	Background CO (ppm)	Corrected Self Exposure CO (ppm)	Measured CO (ppm)	Corrected CO (ppm)
30	75	2/11/96	1.0	0.4	3.0	1.5	0.0
30	75	2/12/96	0.8	0.3	3.0	4.8	1.5
30	75	2/13/96	0.3	0.2	3.0	2.0	0.0
30	75	2/14/96	0.5	0.5	3.0	2.8	0.0
30	100	2/11/96	1.5	0.4	3.0	2.7	0.0
30	100	2/12/96	2.0	0.3	3.0	2.8	0.0
30	100	2/13/96	1.3	0.2	3.0	1.4	0.0
30	100	2/14/96	0.9	0.5	3.0	4.2	0.7
30	125	2/12/96	0.8	0.3	3.0	2.2	0.0
30	125	2/13/96	0.0	0.2	3.0	1.8	0.0
30	125	2/14/96	0.0	0.5	3.0	2.8	0.0
40	25	2/11/96	1.0	0.4	2.4	3.1	0.0
40	25	2/12/96	0.8	0.3	2.4	2.8	0.0
40	25	2/13/96	0.3	0.2	2.4	1.6	0.0
40	25	2/14/96	1.2	0.5	2.4	1.8	0.0
40	50	2/12/96	0.8	0.3	2.4	2.6	0.0
40	50	2/13/96	2.5	0.2	2.4	2.7	0.0
40	50	2/14/96	3.0	0.5	2.4	2.2	0.0
40	75	2/12/96	0.8	0.3	2.4	3.5	0.8
40	75	2/13/96	0.3	0.2	2.4	2.4	0.0
40	75	2/14/96	0.5	0.5	2.4	4.1	1.2
40	100	2/11/96	1.5	0.4	2.4	3.2	0.4
40	100	2/13/96	1.3	0.2	2.4	0.7	0.0
40	100	2/14/96	0.9	0.5	2.4	2.0	0.0
40	125	2/11/96	1.1	0.4	2.4	2.5	0.0
40	125	2/12/96	0.8	0.3	2.4	3.1	0.4
40	125	2/13/96	0.0	0.2	2.4	2.3	0.0
40	125	2/14/96	0.0	0.5	2.4	3.2	0.3

The Task 2 off-centerline exposure data is also plotted at each speed on the following pages.

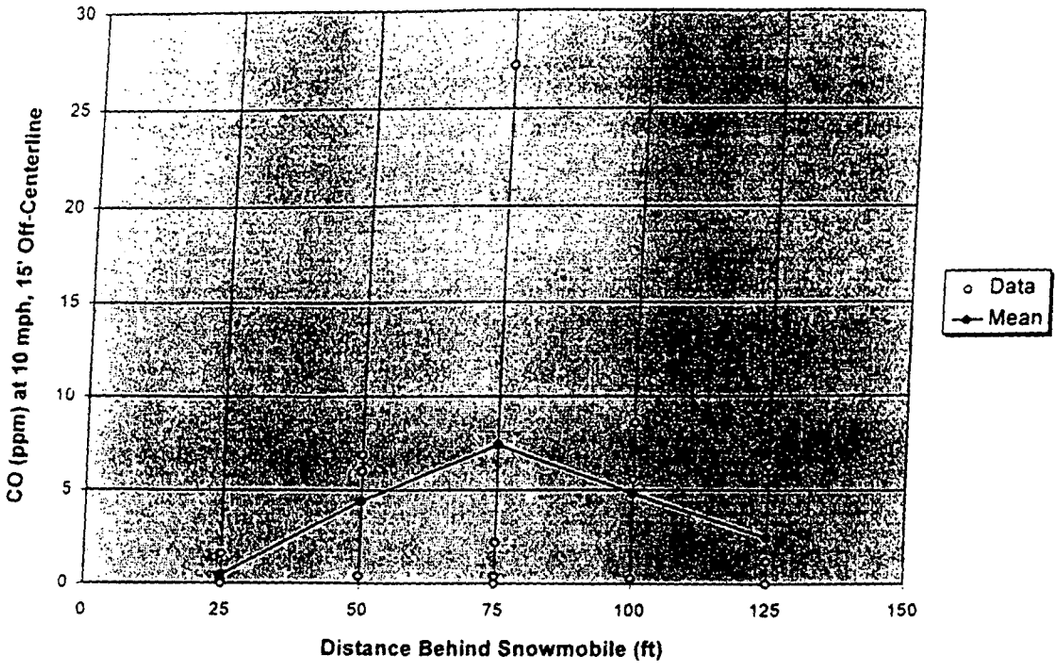

Graph of Off-Centerline CO Vs. Distance at 10 mph

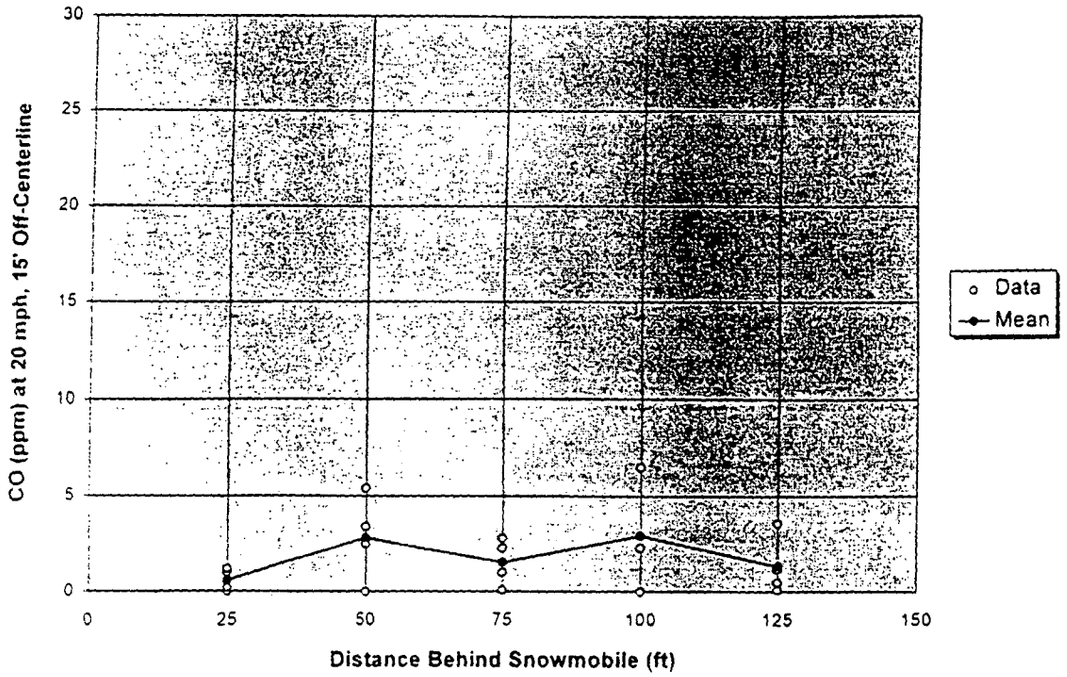

Graph of Off-Centerline CO Vs. Distance at 20 mph

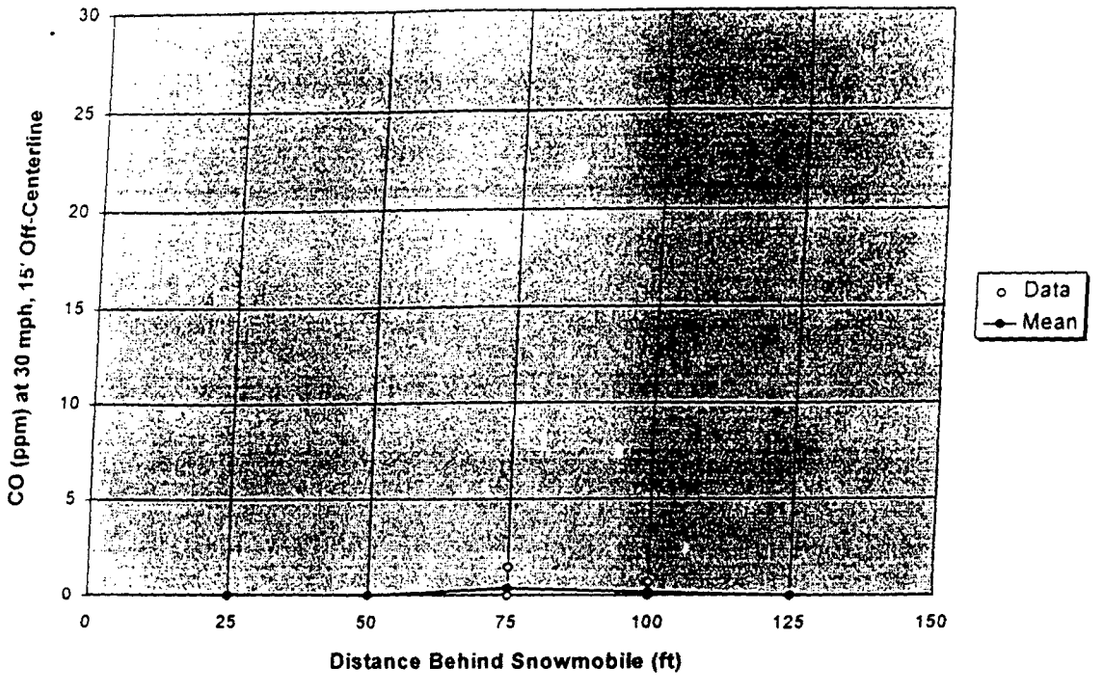

Graph of Off-Centerline CO Vs. Distance at 30 mph

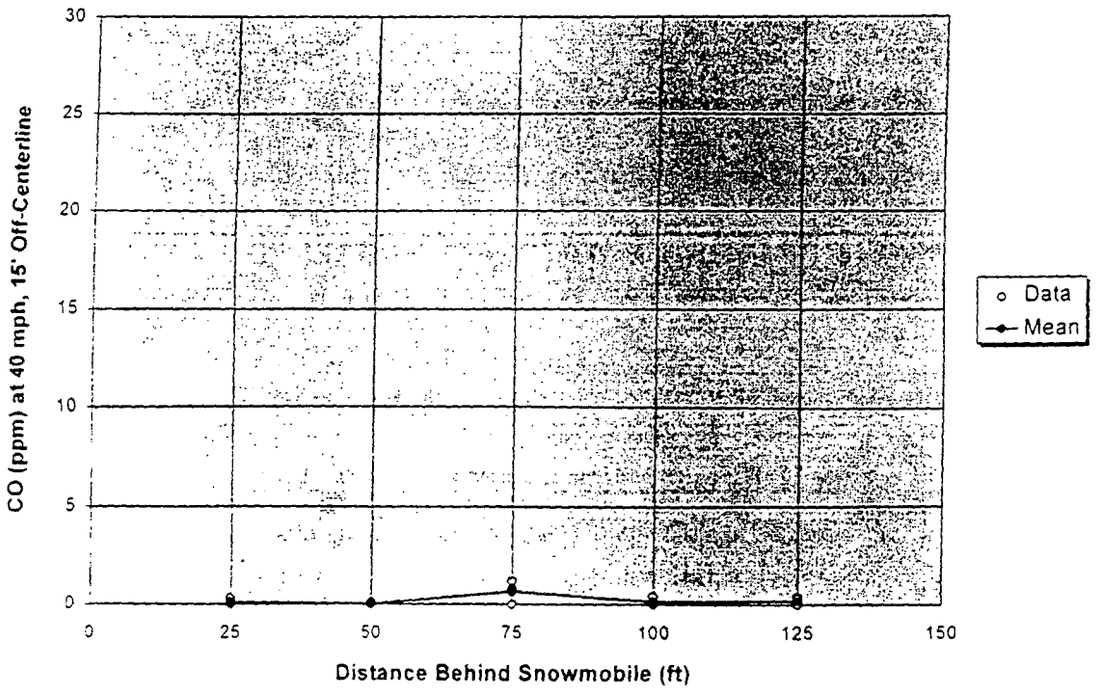

Graph of Off-Centerline CC Vs. Distance at 40 mph

VITA

Lori Marie Snook was born on March 3, 1970 in Portsmouth, Va. She resided in Virginia until the age of four, when her family moved to Bowie, Md. While in Maryland, she attended several different schools, and graduated from the Eleanor Roosevelt Science and Technology Center in 1988.

Ms. Snook entered the United States Air Force Academy in June 1988 to pursue a B.Sc. in aeronautical engineering. During her stay at the academy, she was on the dean's, commandant's, and superintendent's lists for outstanding academic and military performance. In the fall of 1989, Ms. Snook transferred to the University of Tennessee to pursue a B.Sc. in mechanical engineering.

While an undergraduate at the University of Tennessee, Ms. Snook was both the treasurer and chairman of the Society of Automotive Engineers, as well as an active member of Tau Beta Pi, ASME, Pi Tau Sigma, and the Natural Gas Vehicle Challenge Team. Upon graduation in May of 1992, she was named the Outstanding Senior in the College of Engineering, the Outstanding Senior in Mechanical and Aerospace Engineering, and was recognized for Outstanding Academic Performance in Mechanical and Aerospace Engineering.

In June of 1992, the receipt of both a DuPont Fellowship and a Hilton Smith Fellowship allowed Ms. Snook to begin work on her M.S. degree in mechanical engineering. During this time she was also the recipient of a Graduate Research Assistantship. While working on her M.S., she made several presentations on natural gas vehicles and air pollution and remained active on the Natural Gas Vehicle Challenge

Team. In April of 1993, she received a Chancellor's Citation for Extraordinary Professional Promise. She completed her M.S. in August of 1993.

In the fall of 1993, the receipt of a three-year NSF Fellowship allowed Ms. Snook to continue her higher education with the pursuit of a Ph.D. in Civil and Environmental Engineering. While working on her Ph.D., she served as the project manager for the University of Tennessee's Hybrid Electric Vehicle Team. Additionally, in November of 1995 Ms. Snook was selected as the Society of Automotive Engineers' international student representative at the International Pacific Conference on Automotive Engineering in Yokohama, Japan. She will receive her Ph.D. in August of 1996.

Picture of Lori Conducting Research in Grand Teton National Park